PROGRESS TOWARD THE SYNTHESIS OF A FAMILY OF ANTIMALARIAL DITERPENES: POTENTIAL UTILIZATION OF Co-SALEN-CATALYZED HYDROLYTIC KINETIC RESOLUTION (HKR) TO FORM CHIRAL INTERMEDIATES IN THE METABOLITES OF CALLOPHYCUS SERRATUS

A Thesis
Presented to
The Academic Faculty

by

Rebecca Elizabeth Key

In Partial Fulfillment
of the Requirements for the Degree
Doctor of Philosophy in the
School of Chemistry and Biochemistry

Georgia Institute of Technology
August 2015

PROGRESS TOWARD THE SYNTHESIS OF A FAMILY OF ANTIMALARIAL DITERPENES: POTENTIAL UTILIZATION OF Co-SALEN-CATALYZED HYDROLYTIC KINETIC RESOLUTION (HKR) TO FORM CHIRAL INTERMEDIATES IN THE METABOLITES OF CALLOPHYCUS SERRATUS

Approved by:

Professor Stefan France, Advisor
School of Chemistry and Biochemistry
Georgia Institute of Technology

Professor Christopher W. Jones
School of Chemical & Biomolecular Engineering
Georgia Institute of Technology

Professor Charles L. Liotta
School of Chemistry and Biochemistry
Georgia Institute of Technology

Professor Adegboyega K. Oyelere
School of Chemistry and Biochemistry
Georgia Institute of Technology

Professor Jake D. Soper
School of Chemistry and Biochemistry
Georgia Institute of Technology

Date Approved: 24 July 2015

In loving memory of my father,

Wyman J. Key, Jr.

1956-1987

ACKNOWLEDGEMENTS

I would like to begin my acknowledgements by saying a few words about the person that this dissertation is dedicated to: my father, the late Wyman Key. During his teenage and young adult years, whether it was on the baseball field, restocking the Coca-Cola vending machines around his hometown, or working at his final position as an office manager, he gave everything 110% and never shied away from hard work. From what I can recall, he was devoted to his career, as I can remember him practicing his presentations for work and/or his Toastmasters speeches at home; he also made time to spend with his family, whether it was playing baseball in the backyard with my brother, playing board games with me, or taking off of work to see me get my first award at kindergarten honors day. Despite his untimely death when I was six years old, I have learned a great deal from him though the stories of how hard-working, driven, and ambitious he was, and from my teenage years henceforth, these stories have inspired me to give everything I do in life my all. While I cannot thank him personally, I want to acknowledge him for the positive influence that he has had and will continue to have on me both professionally and personally.

During my time at Georgia Tech, I have encountered several people that have impacted me both professionally and personally that I would like to take a few moments to thank. First, I would like to thank both my former and current advisors, Professors Christopher Jones and Stefan France, respectively. In working in both of these groups, I have learned two different skill sets, and I would not be the scientist or person that I am today had I not worked for both of them. Specifically, I would like to thank Chris for taking me into his research group on a leap of faith that the project I was to work on got funded (it did), and not only did I learn a lot about molecular

catalysis, the insights he has given me on topics both inside and outside of the lab allowed me to see things from another perspective that I might not have considered before, which has been very helpful. As graduate school can be filled with several ups and downs, he helped me help myself at a time in my life when I really needed it: that will not be forgotten. I would like to thank Stefan for accepting me into his group as a fourth year graduate student. Through our many discussions about research, my knowledge about synthetic organic chemistry, as well as laboratory techniques, has increased exponentially. In addition, I have learned a great deal through the informal discussions that he has had with me and fellow co-workers through his daily trips to the lab. Also, his advice and help he has given me through my job search has been instrumental in securing a position after graduate school, which is very much appreciated.

I would like to thank my current committee members Professors Charles Liotta, Adegboyega "Yomi" Oyelere, and Jake Soper, as well as my former committee member, Professor Marcus Weck of New York University. The insights, as well as questions that they have proposed to me about my research, helped me to shape my research into what it is today.

I would also like to thank my boyfriend, Dr. Ben Greve. As someone I met on the first day of our graduate orientation, he later became my rock through the last half of graduate school, and his emotional support, as well as being my voice of reason, has helped me a great deal through the ups and downs of graduate school. I also thank him for his assistance in learning and utilizing LaTeX. I look forward to our new adventures and endeavors in life, and I could not imagine this journey with anyone else.

The time spent in both the Jones and France Groups allowed for me to encounter several influential co-workers along the way. From the Jones Group, Dr. Krishnan Venkatasubbaiah gave me many insights into my HKR project; these insights, as well

as our sometimes conflicting perspectives, made the project what it was, and I am proud of the final result. I would also like to acknowledge both Dr. Joey Kistler and Tobi Berto, also from the Jones Group, for their friendships in the lab amongst our research: my encounters with these gentlemen made the work day that much more fun. I would also like to thank Dr. Mike Kahn of the Weck Group at NYU: his advice regarding the synthesis of the supported Co-salens throughout the course of the HKR project was very valuable and greatly appreciated.

Changing research groups in the middle of one's Ph.D. can be a tough process. With that, I would like to thank the members of the France Group for quickly accepting me as one of their own and never making me feel like an outsider. Specifically, I would like to thank Drs. Dadasaheb Patil and Lien Phun for training me on laboratory techniques, as well as the unsolicited advice given about experiments and life/expectations in the France Group. I would also like to acknowledge my co-worker and friend Marchello Cavitt, whom I have bonded with over working the night shift in lab; our unconventional journeys through graduate school; and most recently, in our shared experiences in finishing our Ph.D.s. I will miss not having him on the other side of the lab when I move onto my next position.

In addition to the aforementioned graduate students in the France Group, there were two undergraduates that worked on the natural projects with me that were a joy to work with. First, Kedar Perkins, a summer REU student from the University of Maryland, Baltimore County, worked on the callophycolide A project. He always had a great attitude and came into lab ready to work and learn new things. The second undergraduate (from Georgia Tech) was Angel Cobos, who worked on bits of all of the natural product projects. Angel was also hard-working with a great attitude; not only did he get the experiments and (many) columns done that I had asked him to do, he would also replenish workup reagents, and even clean up our lab area without ever being asked to do so. The work from these two gentlemen was very much appreciated.

As a synthetic organic chemist, NMR and MS are the characterization techniques that I most commonly used. With that, I would like to thank Dr. Les Gelbaum, the director of the Georgia Tech NMR facility, for his training and help in using the NMRs. Finally, I would like to thank David Bostwick and Dr. Cameron Sullards of the Georgia Tech mass spectrometry facility for their advice, as well as the efficient analyses of my products.

TABLE OF CONTENTS

LIST OF TABLES

LIST OF FIGURES

LIST OF SYMBOLS OR ABBREVIATIONS

ACT Artemisinin-based combined therapy.

APIs Active pharmaceutical ingredients.

BDSB bromodiethylsulfonium bromopentachloroantimonate(V).

Co(III)-salen (*R,R*)-(*N,N'*)-bis(3,5-di-*tert*-butylsalicylidene)-1,2-cyclohexanediaminocobalt(III).

CQ Chloroquine.

CQDP Cloroquine diphosphate salt.

DBU 1,8-Diazabicyclo[5.4.0]undec-7-ene.

DCM Dichloromethane.

DDT Dichlorodiphenyltrichloroethane.

DIPEA *N,N*-diisopropylethylamine.

DVB Divinylbenzene.

EA Elemental analysis.

ECH Epichlorohydrin.

ee Enantiomeric excess.

EPR Electron paramagnetic resonance.

ERO Epoxide ring-opening.

Fe(III)PPIX Ferriprotoprophyrin IX.

Hb Hemoglobin.

HKR Hydrolytic kinetic resolution.

IAF Immunoaffinity fluorescent.

IRS Indoor residual spraying.

ITNs Insecticide-treated mosquito nets.

LLINs Long-lasting insecticide-treated mosquito nets.

MOA Mode of action.

MRSA Methicillin-resistant *Staphylococcus aureus*.

NBS *N*-bromosuccinimide.

PAA *para*-Anisaldehyde.

RBCs Red blood cells.

RBM Roll back malaria.

RR Resonance Raman.

salen (*R,R*)-(*N,N'*)-bis(3,5-di-*tert*-butylsalicylidene)-1,2-cyclohexanediamine.

SAR Structure-activity relationship.

TCTP Translationally controlled tumor protein.

TLC Thin-layer chromatography.

TOF Turnover frequency.

VREF Vancomycin-resistant *Enterococcus faecium*.

WHO World Health Organization.

SUMMARY

Callophycolide A is a meroditerpene isolated from *Callophycus serratus*, a Fijian red macroalgae. Callophycolide A has been shown to inhibit bacterial growth, and it exhibits moderate cytotoxicity against multiple human cancer cell lines. Most importantly, it exhibits moderate activity against *Plasmodium falciparum*, the deadliest malaria-causing parasite to humans. Due to its antimalarial action and the need for antimalarial drugs on the pharmaceutical market, efforts toward a modular approach to the total synthesis of callophycolide A are presented that incorporate inexpensive, commercially available starting materials, offer gram-level scalability, and utilize known chemistry, including copper-mediated aryl allylation, hydrolytic kinetic resolution, base-promoted epoxide ring-opening, and the Steglich esterification. Once completed, this synthetic pathway can be used as a template for the total synthesis of other related marine natural products, such as the callophycols, callophycoic acids, and the bromophycolides.

Callophycoic acids, also isolated from *C. serratus*, are the first examples of diterpene-benzoic acids observed in macroalgae. In addition, these acids, particularly callophycoic acids G and H, exhibit modest antibacterial activity. Although they are not strongly potent against malaria, they share a *trans*-decalin core identical to callophycols A and B, which are halogenated diterpene-phenols isolated from *C. serratus* that do exhibit modest antimalarial activity. Due to their identical core and their simpler structure (i.e., trisubstituted olefin tail), if a divergent total synthesis of callophycoic acids G and H can be established, it can serve as a template for synthesizing natural products that have been identified to be more potent against malaria, such

as the callophycols, which are more complex in structure. Herein, a total synthesis of callophycoic acids G and H is investigated, which consists of a Wittig reaction, nucleophilic addition, and a bromonium-induced cation-pi cascade cyclization, and the progress toward the target molecules in the current study will be disclosed.

To access chiral intermediates for the aforementioned metabolites, catalytic methods were sought. Hydrolytic kinetic resolution (HKR) resolves racemic epoxides using water as the nucleophile and is most often catalyzed by chiral Co(III)-salens. Previous studies have shown that the counter-ion of the Co(III)-salen has a direct effect on the rate of the HKR; when catalyzed by a 50:50 mix of (*R,R*)-Co(III)-salen-OH and (*R,R*)-Co(III)-salen-SbF_6, the fastest HKR rates occurred. It has further been shown that the enantioselectivity is primarily associated with the reaction of (*R,R*)-Co(III)-salen-OH on the activated epoxide. Based on the aforementioned origin of selectivity, a catalyst containing a 50:50 mix of (***R,R***)-Co(III)-salen-OH and (±)-***trans***-Co(III)-salen-SbF_6 could, in principle, give high activities and enantioselectivities for HKR comparable to a mixed counter-ion system containing both (***R,R***)-Co(III)-salens. In this dissertation, a series of experiments are described that demonstrate that highly selective catalysis is only achieved using 100% enantiopure ligand and that mixtures of (***R,R***)-Co(III)-salen and (±)-***trans***-Co(III)-salen yield lower activity and selectivity. Control experiments demonstrate that this is due to rapid counter-ion scrambling under the reaction conditions, precluding the possibility of effectively co-utilizing enantiopure (expensive) and racemic (inexpensive) catalysts with differing counter-ions. The mechanistic investigations resolving the counter-ion scrambling are consistent with the currently accepted mechanism for catalysis, involving cooperative activity of the two Co(III)-salen species that activate the epoxide and water in the reaction. Moreover, the application of HKR in the progress toward the total synthesis of callophycolide A will be highlighted and discussed.

CHAPTER I

INTRODUCTION

1.1 Overview of malaria

Malaria is an extremely serious infectious disease; it is also one of the most ancient diseases on Earth, with the first documentation of the disease's symptoms dating back to 3000 B.C. in ancient China. The disease, however, originated in Central and West Africa over 10,000 years ago and was spread via the migration of man to other countries, such as Northern Europe, Southeast Asia, the Mediterranean, and the Americas [1, 2]. A total of 300-500 million malaria cases are reported annually, with 1-2 million of these cases being fatal [3].

1.2 Causation and symptoms of malaria

The causation of malaria is through a protozoan parasite of the genus *Plasmodium*. Specifically, five of the known 300 species cause malaria in humans: *P. ovale, P. malaria, P. vivax, P. knowlesi*, and the most lethal malaria-causing parasite, *P. falciparum* [4, 5, 6] (Figure 1) [7].

P. falciparum is carried to the human host via the female *Anopheles* mosquito (Figure 2): when one of these parasite-infected mosquitoes bites an uninfected human, it transfers sporozoites of the *Plasmodium* into the human bloodstream via saliva. These sporozoites concentrate in the liver, where they grow into schizonts and multiply. The infected liver cells will eventually rupture, thus releasing merozoites. These merozoites infect the red blood cells (RBCs) of the human host, where they reproduce asexually; it is here where symptoms of uncomplicated malaria, such as vomiting, diarrhea, anemia, fever, and headaches, develop [4]. Once the schizonts

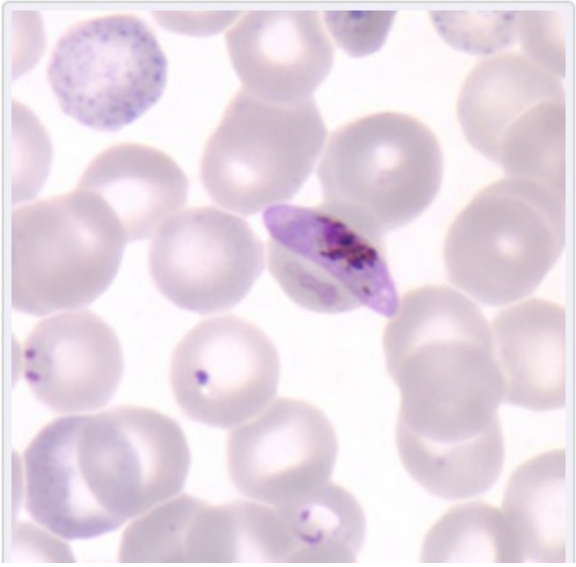

Figure 1: Thin blood smear of *P. falciparum* gametocyte (reproduced from reference [7]).

form in the RBCs, the RBCs rupture, releasing merozoites, which will either infect new RBCs or will be converted into either male or female gametocytes [7, 4, 8, 9, 10]. Furthermore, note that in the more severe stages of malaria, RBCs containing these mature schizonts can cause cerebral death and vascular occlusion via adhesion to the walls of the capillary veins [4]. These gametocytes can be transferred to an uninfected *Anopheles* via biting a parasite-infected human host; once the gametocytes are taken up by the *Anopheles*, they will reproduce sexually, eventually forming sporozoites, which concentrate in the mosquito's salivary glands; the aforementioned cycle repeats upon biting an uninfected human host [7, 4, 8, 9, 10].

1.3 Treatments for malaria

Several methods have been used to eradicate malaria. In the 1950s, vector control using pesticides, such as dichlorodiphenyltrichloroethane (DDT), eradicated malaria from North America and the majority of Europe. As a result of the success of DDT,

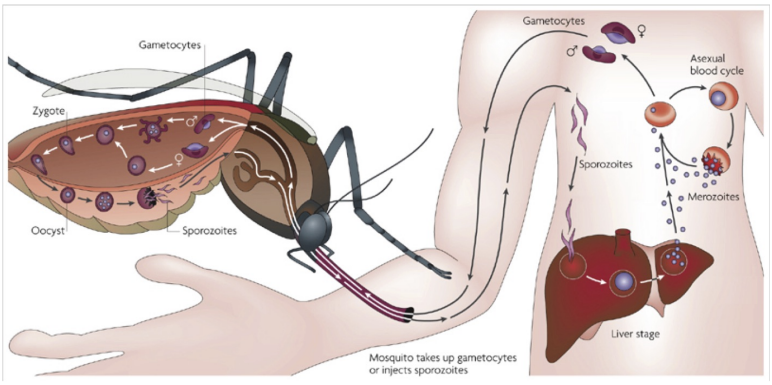

Figure 2: Depiction of how the *Plasmodium* infects a human host with malaria (reproduced from reference [8]).

several programs were launched that focused on eradicating malaria globally [1]. Antimalarial drugs and widespread spraying of DDT were implemented globally [11]. As a result of this global campaign, mortality rates significantly decreased, and by the early-to-mid 20th century, only 10% of the global population was at risk of contracting malaria [1].

Despite the aforementioned progress against malaria, the global eradication campaign steadily declined due to events such as the ban on DDT, the evolution of drug-resistant *Plasmodium* strains, and the emergence of mosquitoes that were resistant to insecticides [12]. By the 1980s, 300-500 million cases of malaria were reported annually, and in 2004, worldwide malaria fatalities peaked at 1,814,000 [13, 14, 15]. Through partnerships such as the World Health Organization (WHO) and Roll Back Malaria (RBM) collaboration, malaria-related casualties have decreased by 32% since 2004, with 1,238,000 malaria-related fatalities in 2010 [15].

Although progress has been made in decreasing the number of malaria-related casualties, this progress is delicate, as the *Plasmodium* adapts very well to inclement conditions [4]. Moreover, drug-resistant *Plasmodium* strains are a continual threat that could cause a malaria resurgence, even in epidemically controlled countries [4]. Therefore, continual funding and research in the prevention and treatment of this

disease are paramount to preventing a pandemic [4].

As mentioned previously, vector control is a method used to prevent the spread of malaria. Two of the most prominent methods are indoor residual spraying (IRS), which are insecticides applied onto a dwelling's inner surface, and long-lasting insecticide-treated mosquito nets (LLINs or ITNs) or "bed nets" [16]. With increased global funding for the control of malaria, ITNs have been provided to areas that are at a high risk for malaria infection, such as sub-Saharan Africa; consequently, approximately 75% of the at-risk population are protected against contracting malaria [17].

1.3.1 Quinoline derivatives

In addition to vector control, natural products, along with their synthetic derivatives, have been the primary source for seeking malarial treatments [18]. Quinoline-containing derivatives are commonly known as schizontocides, as they target and kill schizonts, which are the predominant form of the *Plasmodium* in the intraerythrotic infection stage [19]. The oldest group of antimalarials contain a quinoline group within their structure (Figure 3).

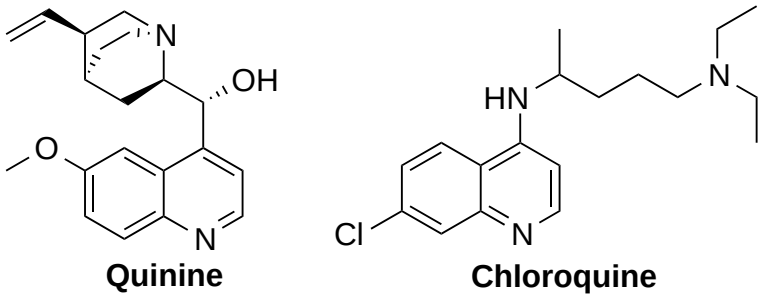

Figure 3: Examples of historic antimalarial treatments that are quinoline derivatives.

All of the antimalarials derived from quinoline offer advantages and disadvantages, which are due to their toxic side effects or the development of resistance [4]. These disadvantages are commonly counterbalanced by pairing the quinoline derivative with artemisinin or artemisinin derivatives [4].

1.3.1.1 Quinine

The *Cinchona* tree bark component quinine, a quinoline methanol, was the first antimalarial treatment (Figure 3) [20, 11], identified and isolated in 1820 [21]. For nearly 200 years, quinine was the sole readily available treatment for malaria [21]. Although it has a somewhat low tolerability and efficacy, quinine is currently used to treat multi-drug resistant strains of malaria [22, 23] and is one of the few drugs recommended for the treatment of the most severe forms of malaria [22]. Moreover, it can be administered to patients via an intravenous solution if they cannot tolerate the oral formulation [22].

1.3.1.2 Chloroquine

As mentioned previously, quinine was used for nearly 200 years to treat malaria [21]. First synthesized in 1934, the 4-amino quinoline drug chloroquine (Figure 3) then replaced quinine in the 1940s, becoming commercially available in 1946 [4, 20]. Chloroquine was widely used following World War II, and it was the first line treatment for malaria worldwide for 50 years [21]. Chloroquine, during its peak in popularity, was highly effective against many of the *Plasmodium* strains. Moreover, its pharmaceutical properties, including high patient tolerance, as well as greater effectiveness and lower toxicity relative to quinine, contributed to the drug's popularity, as well as its low production costs [24, 22, 23].

Chloroquine was commonly delivered in the form of its diphosphate salt (CQDP), whose side effects include dizziness, nausea, headaches, and double vision [23]. In the effort to eradicate malaria worldwide, chloroquine was widely distributed, included in table salt stocks around the world as a prophylactic [24]. This world distribution in table salt most likely contributed to the parasite's resistance to the drug in the late 1950s, effectively destroying its therapeutic efficacy [4].

1.3.2 Mode of action (MOA) of quinoline-containing antimalarials

As mentioned previously, quinoline-containing antimalarials are solely active against the intraerythrocytic parasite stage of infection, thus clearing the *Plasmodium* from the bloodstream [25]. Once the *Plasmodium* enters the RBCs, it is surrounded by human hemoglobin (Hb), which is ingested by the parasite, thus engulfing it into its digestive vacuole, with a pH ranging from 5.0-5.4 [26, 27]. Once Hb is ingested by the parasite, it is exposed to many diverse proteases that specialize in degrading the Hb tetramer [9], thus supplying the parasite with the essential amino acids for its growth and its maturation and is therefore crucial for *Plasmodium* survival [26, 27]. As a result, this essential Hb catabolism is a logical target for treatments against malaria.

Hb proteolysis results in free heme being released as waste; once this free heme is released, the Fe^{2+} center is oxidized to Fe^{3+}, forming ferriprotoporphyrin IX (Fe(III)PPIX, Figure 4) [4], which is toxic to the *Plasmodium*, resulting in enzyme inhibition, membrane peroxidation, the formation of radicals that are free of oxygen and reduced leukocyte function, as the *P. falciparum* has little to no heme oxygenase to effectively catabolize the free heme [28]. However, the parasite circumvents the effects of this toxicity by crystallizing the heme, thus converting it to hemozoin (Figure 4) [4], a five-coordinated $(Fe(III)PPIX)_2$ dimer in a crystalline arrangement that are linked via the propionate side-chains of the adjacent monomers; these Fe(III)PPIX dimers connect to other Fe(III)PPIX dimers via hydrogen bonds [29, 30, 31]. Thus, it is logical that the mode of action (MOA) for antimalarials is to interrupt this hemozoin formation, which should lead to a buildup of heme that will ultimately kill the parasite.

The MOA of antimalarials derived from quinoline targets the interruption of hemazoin formation [25, 32]. Taking the weakly basic chloroquine (CQ) as an example ($pKa_1 = 8.1$, $pKa_2 = 10.2$), in its fully deprotonated form at neutral pH, it will

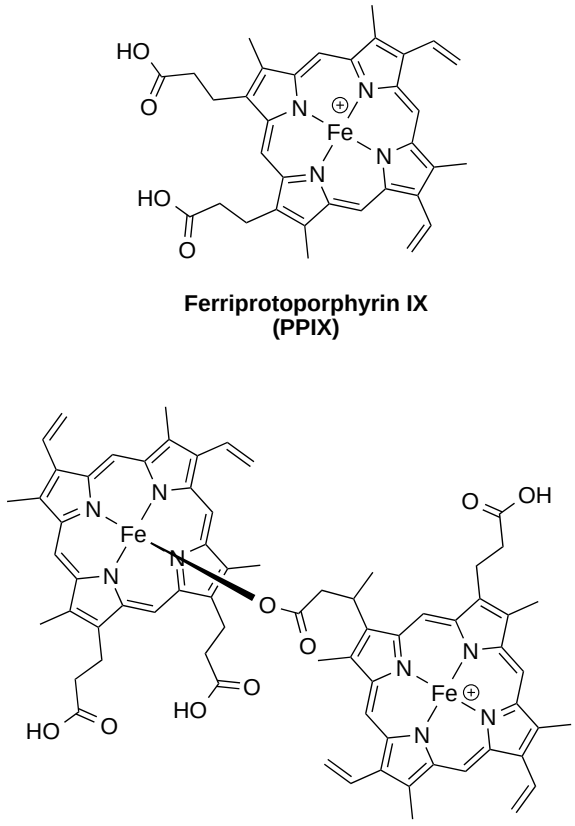

Figure 4: Figure depicting the structures of Fe(III)PPIX and a hemozoin dimeric unit [4].

diffuse across the membrane of the food vacuole (Figure 5) [4]. Once inside the *Plasmodium* food vacuole, which is acidic, the amount of protonated CQ increases and thus becomes trapped within the vacuole, as it is now ionic [19]. Consequently, the protonated CQ can either bind the Fe(III)PPIX or the crystallized hemozoin. Both of these pathways result in the interruption of the hemozoin crystallization process; consequently, free heme begins to build up in large concentrations. This buildup of heme results in destruction of the membrane of the digestive vacuole and consequently in the death of the *Plasmodium* [4, 19, 33, 34, 35]. Over time, however, the food vacuole of the *Plasmodium* evolves such that the transmembrane proteins undergo a mutation that allows the quinoline derivative to be pumped out of the food vacuole, thus

resulting in the drug being inactive [4, 19, 33, 34, 35, 36].

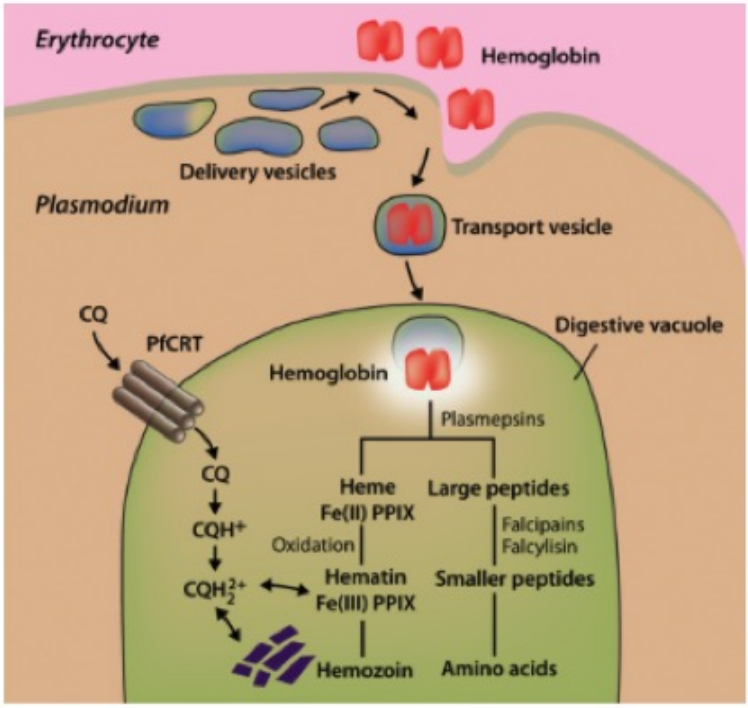

Figure 5: Figure depicting the MOA of quinolines on the *Plasmodium* (reproduced from reference [4]).

1.3.3 Artemisinin

Artemisinin is a natural product that was isolated from the Chinese sweet wormwood *Artemisia annua* in the early 1970s [14] and was first synthesized in 1983 [37]. Structurally, it is a sesquiterpene lactone with an endoperoxide bridge within a seven-membered ring system (Figure 6) [38, 39]. Although once deemed too expensive for commercial pharmaceutical production [37], artemisinin has been significant in treating malaria over the past 20 years. Artemisinin is currently the most fast-acting, potent drug available, with an IC_{50} value of >7nM [38, 39], and thus, it is the recommended treatment for malaria caused by *P. falciparum* [40]. The efficiency of artemisinin against *P. falciparum* can be attributed to the fact that it is rapidly eliminated from the bloodstream of the host ($t_{1/2}$ = <1 h) [41]; this rapid elimination helps to minimize the chance of building resistance [4]. Consequently, artemisinin-based drugs must be taken frequently to maximize their effects and thus they are commonly used together with other antimalarial drugs with a different MOA, better known as arteisinin-based combined therapy (ACT), to improve efficacy [42].

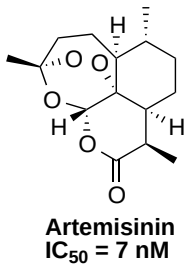

Figure 6: Artemisinin, the most fast-acting, potent drug available to-date against malaria [38, 39].

1.3.3.1 MOA of artemisinin and derivatives

Unlike the quinoline-based antimalarials, which act on the erythrotic state of parasite infection, artemisinin displays antiplasmodial effects at multiple stages of the infection by the *Plasmodium* (which contributes to its potency), including the liver, erythrotic,

and the sexual stages; it is in the sexual stage where the gametocytocidal agents kill gametes of the parasite inside the gut of the mosquito, thereby decreasing the rate of transmission [43]. Structure-activity relationship (SAR) studies, however, have attributed the endoperoxide bridge as being essential to its antimalarial activity [37, 41]. Furthermore, in contrast to the quinolines, artemisinin does not bind to the hemozoin crystals, thus inhibiting its formation; rather, it forms adducts with the hemozoin, as well as additional biological macromolecules, such as the translationally controlled tumor protein (TCTP) [44]. This binding serves as a catalyst for the breakdown of the labile endoperoxide bridge. The breakdown of this bridge results in the formation of free radicals, the alkylation of parasitic proteins, and fatal damage to the membrane systems of the parasite [45].

1.3.3.2 Drawbacks to the use of artemisinin

Although artemisinin is currently the most potent-acting drug available to treat *P. falciparum*-related malaria, there are several drawbacks to this drug, in addition to its fast clearance from the body [41]. The shortage of the Chinese sweet wormwood, low yield of production, and costly semi-synthetically produced artemisinin and derivatives cause the drug to not be readily available [46]. Moreover, because its MOA involves a free-radical mechanism, the potential of artemisinin to be neuro- and cumulatively toxic is likely [4]. With artemisinin resistance on the rise, there is an urgent need to pursue alternative antimalarial treatments.

Currently, for patients with uncomplicated malaria (stemming from *P. falciparum*), the recommended first-line treatment consists of ACT [40], which combines artemisinin or its derivatives with a second drug that has a differing MOA to amplify efficacy while minimizing the potential of the parasite developing resistance [42]. However, artemisinin and its derivatives are at risk for parasite resistance, as there

have been reports of *P. falciparum* resistance toward artemisinin in Vietnam, Thailand, Myanmar, and Cambodia [47]. Although the efficacies of these ACTs have yet to be compromised, should they fail, there are currently no alternatives to treat malaria because the present options in the pipeline are also derivatives of artemisinin, which would potentially give rise to similar resistance [4].

1.4 Potential alternatives to treat malaria

1.4.1 Antimalarial diterpenes

In investigating alternatives for treating malaria, several diterpenes have been isolated and tested for antimalarial activity. Specifically, diterpene lactones, such as the compounds isolated from *Parinari capensis* (**1** - **3**, Figure 7) [48, 49], displayed promising activity against malaria, with IC_{50} values of 0.54, 0.67, and 1.57 μM, respectively. However, due to their toxicity, further investigations regarding their biological activity were ceased [48].

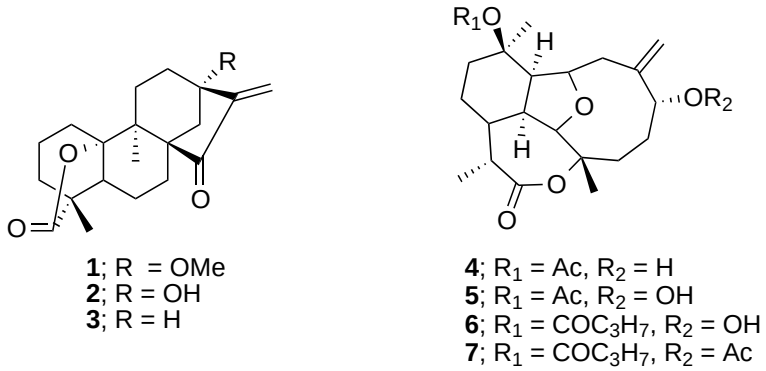

Figure 7: Examples of diterpene lactones isolated from *Parinari capensis* and briarellins [48, 49].

Other diterpene lactones from the eunicellin class, briarellins (**4** - **7**, Figure 7) [48, 49], displayed activity against malaria (IC_{50} = 15.0, 9.0, 9.0, and 8.0 μM, respectively); this activity was attributed to the presence of the -OR group at the C-6 position [49]. Thus, activity against malaria can be attributed to the diterpene

lactone structures.

1.4.1.1 Diterpenes isolated from Callophycus serratus

In 2005, Kubanek et al. discovered a class of compounds from *Callophycus serratus*, a Fijian red macroalgae [50]. Through several liquid-liquid partitioning steps, followed by normal and reverse-phased HPLC fractionation [51, 52, 53], they were able to isolate several novel compounds called the bromophycolides (Figure 8) [50, 51, 52, 53, 54].

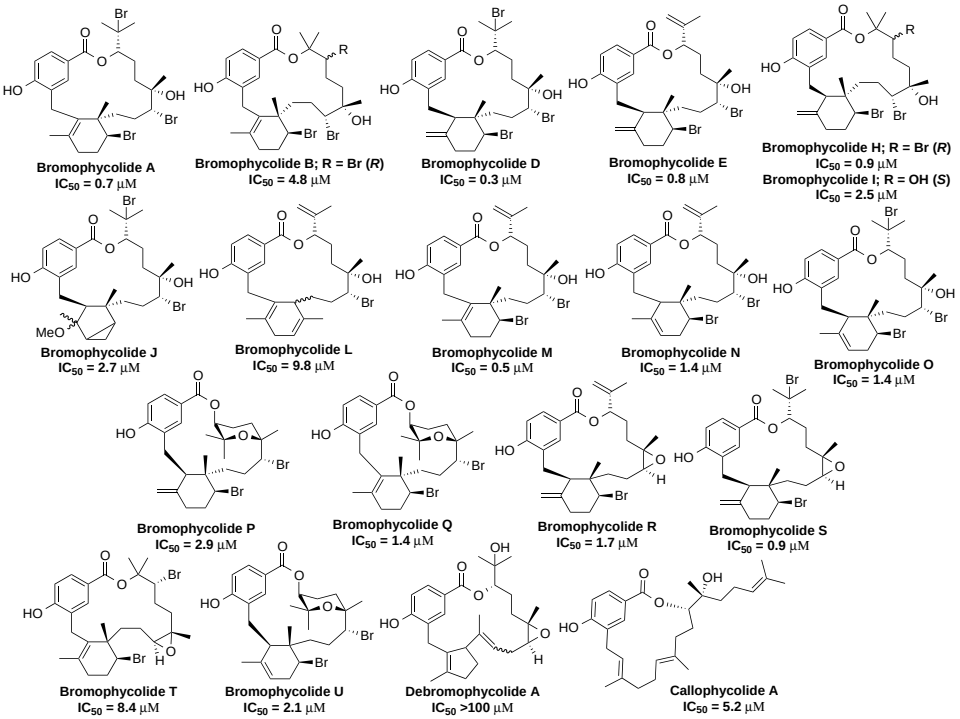

Figure 8: Benzoate diterpenoids isolated from *C serratus* [50, 51, 52, 53, 54].

Characterization of the compounds using X-ray crystallography, NMR, and MS revealed that each of these compounds contained a novel diterpene-benzoate structure [50]. The group has since isolated multiple benzene diterpenoids, including 21 bromophycolides [50, 51, 52, 53], debromophycolide A [50], eight callophycoic acids [55], five bromphycoic acids [56], two callophycols [55], and callophycolide A (Figures 8 and 9) [50, 51, 52, 53, 54, 55, 56].

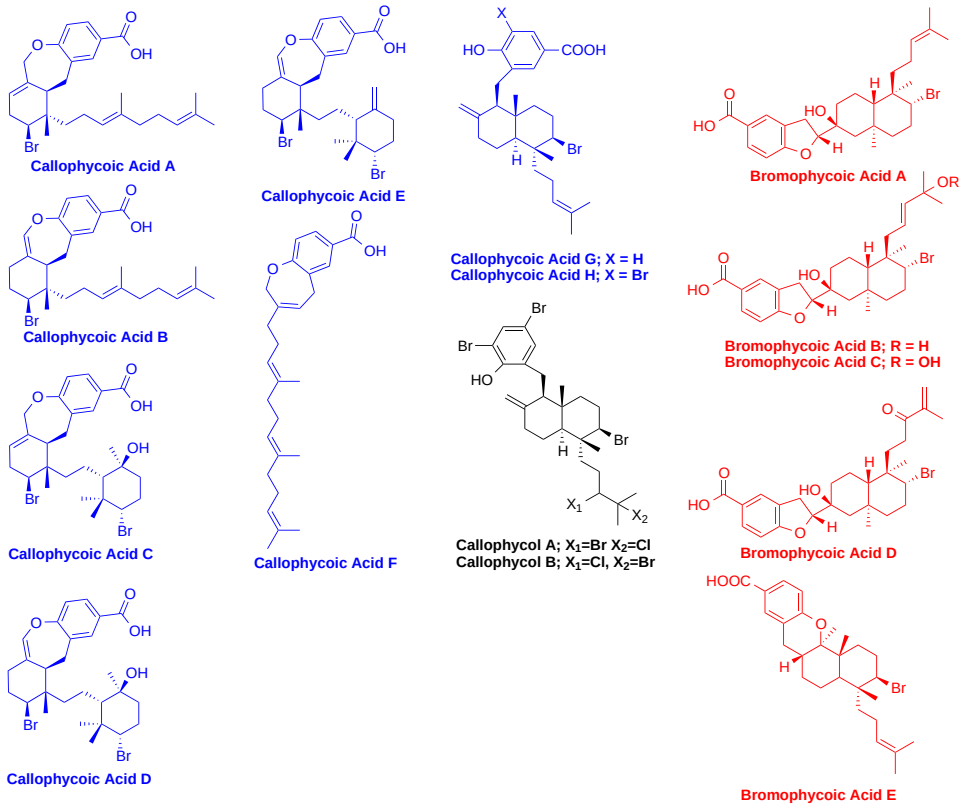

Figure 9: Diterpene-benzoic acids and diterpene-phenols isolated from *C. serratus* [55, 56].

All of the bromophycolides display varying activity against *P. falciparum*; the most potent ones being the bromophycolides, with IC_{50} values ranging from 0.3 to 0.9 μM; therefore, with respect to antimalarial activity, the lactone macrocycle is a critical component of the SAR between the aforementioned natural products and their activities against *P. falciparum* (Figure 8) [50, 51, 52, 53]. Consequently, the aforementioned natural products isolated from *C. serratus* could potentially serve as alternative antimalarial treatments, as resistance to artemisinin is increasing.

Of the bromophycolides isolated, bromophycolide A was found in the greatest abundance (0.8% plant dry mass) [50]. Thus, bromophycolide A was the most logical starting point for biological activity studies. Bromophycolide A was determined to have an IC_{50} value of 0.7 μM against *P. falciparum* [5]. To investigate the MOA

of bromphycolide A, the macrolide was modified with the addition of immunoaffinity fluorescent (IAF) tags (Figure 10) [5] via a Steglich esterification, and the IAF-tagged bromophycolide A molecules were used to determine the intracellular distribution of this probe in erythrocytes infected by *P. falciparum* [5]; it was observed that fluorescence was seen only in the parasite-infected erythrocytes.

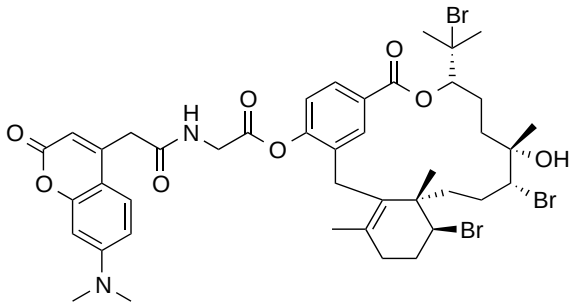

IAF Probe

Figure 10: Bromophycolide A molecule tagged with an IAF [5].

This probe was also used in co-incubation studies and multichannel fluorescence confocal microscopy. It was determined that the probe associated with intracellular neutral lipids [5]. As hemozoin formation occurs inside lipid nanospheres, it was suggested that bromophycolide A could be targeting the crystallization of heme. When tested for the inhibition of heme crystallization, bromophycolide A inhibited this process, with an IC_{50} of 2.5 molar equivalents of bromophycolide to heme. Absorbance spectroscopy of Fe(III)PPIX in the presence of bromophycoide A resulted in a decrease in the Soret band of Fe(III)PPIX by 45%, which further suggests that bromophycolide A targets heme crystallization. Moreover, bromophycolide A was found to be active against the chloroquine-resistant strain Dd2, with an IC_{50} value of 0.377 μM, thus unrecognizable with respect to the parasite efflux system [5].

1.4.1.2 Drawbacks to using C. serratus-isolated compounds as antimalarials

Currently, the likelihood of these natural products becoming active pharmaceutical ingredients (APIs) for antimalarial drugs is limited. The vast majority of these compounds from *C. serratus* comprise less than 0.01% of the plant dry mass, leading to only milligrams of isolated pure product; several grams are required to fully investigate biological activity. Thus, the current protocol for obtaining these pure benzene diterpenoids is not practical or efficient. Therefore, other avenues must be explored to obtain these compounds in usable quantities. Although there have been investigations into the syntheses of the bromophycolide A and D skeleta [57], there are, to our knowledge, no known divergent total syntheses of bromophycolide A.

1.4.1.3 Addressing the drawbacks of the aforementioned antimalarials

As shown in Figure 8 [50, 51, 52, 53, 54], the bromophycolide macrocycles are either 15- or 16-membered and all contain a *para*-hydroxybenzoate moiety. However, despite these similarities, these structures are also very diverse in that some contain varying bromocyclohexene moieties, tetrahydropyran rings, oxirane rings, and *tert*-butyl moieties. Due to this structural complexity, a rational approach toward the synthesis of the macrolides, such as bromophycolide A, would be to investigate the synthesis of an alternative diterpene-benzoate that is simpler in structure, as this will allow for similar, if not the same, synthetic steps to be determined and optimized before focusing on the more structurally complex meroditerpenes. Callophycolide A is also a 15-membered macrolide isolated from *C. serratus*; although not as potent as bromophycolide A ($IC_{50} = 5.2\ \mu M$) [54], it has a more simplistic macrolide skeleton, with only two stereocenters and no bromine atoms, cyclohexenes, or cyclic ether moieties present (Figure 11) [50, 54].

Thus, if a total synthesis of callophycolide A could be accomplished, some of the chemical transformations used for this synthesis could be used to synthesize the more

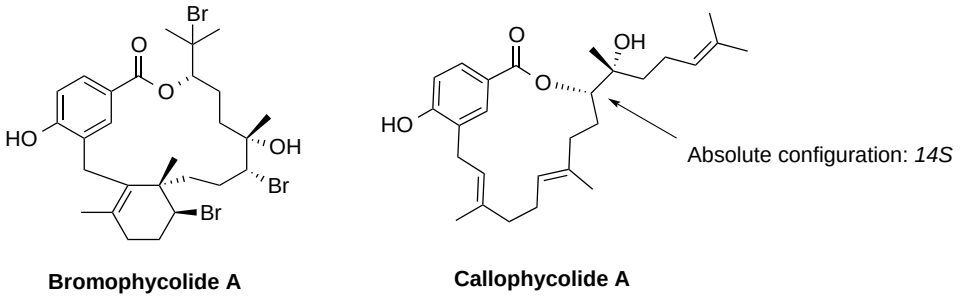

Figure 11: Structural comparison of the macrolides bromo- and callophycolide A [50, 54].

structurally complex bromophycolides that are more potent against malaria.

1.4.1.4 Callophycoic acids G and H and callophycols A and B

With respect to diterpenes with simpler structures, callophycoic acids are another class of diterpenes isolated from *C. serratus* (Figure 8) [50, 51, 52, 53, 54]. These were the first examples of diterpene-benzoic acids that were observed in macroalgae [55]. They do not express significant potency against malaria (IC_{50} >100 μM) [55]; however, they do display modest antibacterial activity, namely, callophycoic acids G and H (>10-63.9 μM and 27.4- >50 μM, respectively, against *Staphylococcus aereus*, *Enterococcus faecium*, and tubuclar bacteria) [55]. They also share a similar *trans*-decalin core to callophycols A and B, which are halogenated diterpene-phenols that are potent against malaria (relative to callophycoic acids G and H), with IC_{50} values of 35.7 and 40.7 μM, respectively [55]. Due to this similar core and simpler trisubstituted olefin tail, a divergent total synthesis of callophycoic acids G and H can serve as a template to synthesize callophycols A and B. Regarding a biosynthetic pathway for the synthesis of the *trans*-decalin core of the diterpene-benzoic acids and phenols, it was proposed that it was formed via halogenation of the compounds at their electrophilic sites, which can be achieved by vanadium haloperoxidase. However, a drawback of catalysis via vanadium haloperoxidase is the low specificity in the formation of the

bromine-carbon bond [58]. Snyder's group has synthesized and utilized bromodiethylsulfonium bromopentachloroantimonate(V) (BDSB), an electrophilic bromine source, to form bromonium ions and thus promote stereoselective bromonium-induced cation-pi polyene cyclizations of electron-deficient terpenes derived from geraniol, nerol, and farnesol (Figure 12) [59], forming the respective cyclohexanes/enes and *cis*- and *trans*-decalin compounds [60, 59].

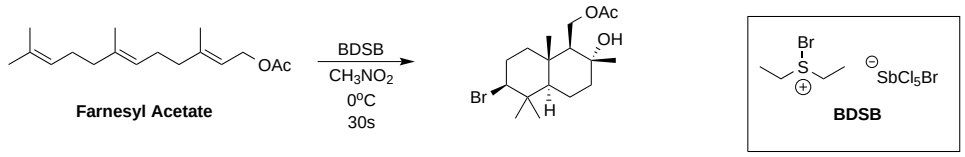

Figure 12: Example of a stereoselective bromonium-induced cation-pi cyclization using BDSB [59].

If the reaction conditions concerning the *trans*-decalin formation can be determined for callophycoic acids G and H using BDSB, then this would serve as a more stereospecific alternative to the syntheses of this family of metabolites.

1.5 Overall thesis goals

To access the chiral intermediates for the aforementioned *C. serratus* metabolites, catalytic methods were sought. Hydrolytic kinetic resolution (HKR) is a method for resolving racemic, terminal epoxides using water as the nucleophile; it is most often catalyzed by chiral Co(III)-salens and can be used to synthesize chiral intermediates for active pharmaceutical ingredients (APIs) [61, 62, 63]. Because a chiral, terminal epoxide can be utilized in the total synthesis of some of the above natural products, the application of HKR will be presented. Thus, this thesis consists of two parts: the first part regards metallosalens and the Co(III)-salen-catalyzed hydrolytic kinetic resolution (HKR), and the other regards the progress toward the syntheses of five different diterpenes isolated from the Fijian red macroalgae *Callophycus serratus*.

Chapter two presents the evaluation of enantiopure and non-enantiopure Co(III)-salen catalysts and their counter-ion effects in the HKR of racemic epichlorohydrin. Catalysis of HKR via chiral Co(III)-salens occurs via a bimetallic mechanism, where Co(III)-salen-X activates the electrophilic epoxide and Co(III)-salen-OH serves as the nucleophile-delivering complex to the activated epoxide. Because each epoxide enantiomer binds to Co(III)-salen-X with equal affinity, studies were conducted to determine whether the salen ligand for Co(III)-salen-X must be enantiopure. The results showed that the HKR with 50% racemic Co(III)-salen-SbF_6 did not lead to highly active and enantioselective catalysis, which was due to the counter-ion scrambling between the Co centers. Chapter three describes the progress toward the synthesis of callophycolide A. Regarding callophycolide A, the chapter will show the specifics of the successful syntheses of various intermediates. Specifically, it will showcase the potential use of Co(III)-salen-catalyzed HKR to access a chiral epoxylinalool moiety that is otherwise difficult to access in high yields. In addition, the troubleshooting behind the base-promoted epoxide ring-opening step will also be discussed. Chapter four will discuss the progress toward the syntheses of callophycoic acids G and H and callophycols A and B. Specifically, access to the *trans*-decalin core that is common to these four compounds will be described, as well as investigations of a model system to determine and optimize their endgames (final stages of the syntheses). Finally, chapter five summarizes the findings of both the HKR and natural product total syntheses and suggests multiple paths forward for the aforementioned projects.

CHAPTER II

EVALUATION OF ENANTIOPURE AND NON-ENANTIOPURE Co(III)-SALEN CATALYSTS AND THEIR COUNTER-ION EFFECTS IN THE HYDROLYTIC KINETIC RESOLUTION (HKR) OF RACEMIC EPICHLOROHYDRIN

The research presented in this chapter is published data from Key, R. E.; Venkatasubbaiah, K.; Jones, C. W. *J. Mol. Catal. A: Chemical*, **2013**, *366*, 1.

2.1 Introduction

Kinetic resolution separates a racemic mixture into its enantiomers based on the differential reaction rates of each enantiomer. This reaction requires an enantiomerically pure reagent to effectively resolve the enantiomeric pair [64]. Hydrolytic kinetic resolution (HKR) is a well-established technique used to resolve racemic epoxides, specifically terminal epoxides, into a single enantiomer via a ring-opening reaction using water as the nucleophile (Figure 13) [61].

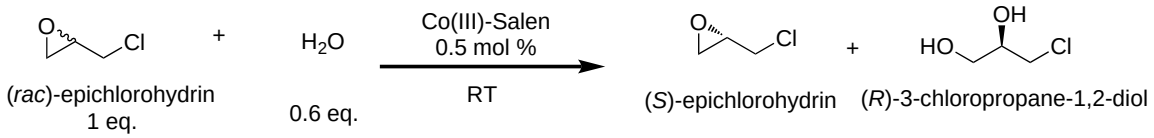

Figure 13: HKR of racemic epichlorohydrin using a Co(III)-salen catalyst **1-4** [61].

HKR was discovered serendipitously by the Jacobsen group while investigating Co-salen-catalyzed enantioselective *meso*-epoxide ring-opening reactions using carboxylic acid nucleophiles (see Figure 14) [65]. During these investigations, they observed both

1) contamination from water, thus forming a 1,2-diol byproduct in high enantiomeric excess (ee), and 2) acetic acid contamination in commercial grade 1-hexene oxide used in the experiments [66] oxidized the Co(II) complex to the active Co(III) complex. Expanding on their HKR discovery, an optimal method for the syntheses of enantioenriched terminal epoxides was sought, as at that time, there were no useful methods that existed for the direct formation of these types of epoxides [66]. Tokunaga et al. determined that their newly discovered HKR reaction was suitable for the synthesis of a variety of enantioenriched terminal epoxides, such as propylene oxide, 1-octene oxide, epichlorohydrin (ECH), and 1-hexene oxide, with high yields and moderate-to-high enantioselectivities and low catalyst loadings [61].

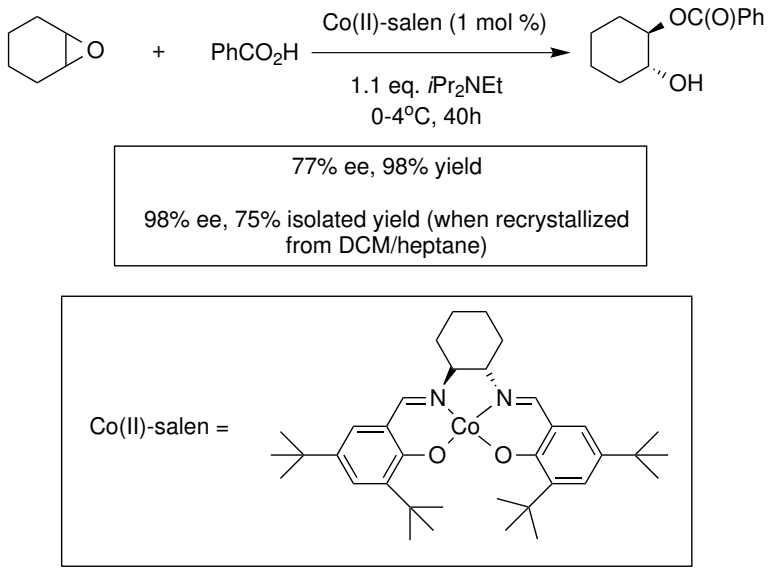

Figure 14: Co(II)-salen-catalyzed enantioselective ring-opening of cyclohexene oxide using benzoic acid [65].

The HKR of terminal epoxides has attracted widespread interest for a number of reasons. From a synthetic chemistry perspective, the strained, reactive, and three-membered ring functionality makes enantiopure epoxides a useful chiral building block for a multitude of reactions [62]. In addition, the coproduct of the reaction, a chiral diol, can be a useful building block as well, being used, for example, in the synthesis

Table 1: Initial study, performed by Jacobsen's group, of the Co(III)-salen-OAc-catalyzed HKR of racemic terminal epoxides demonstrating moderate yields, high enantioselectivity, and reaction scope [61].

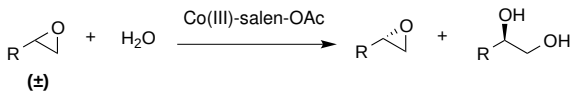

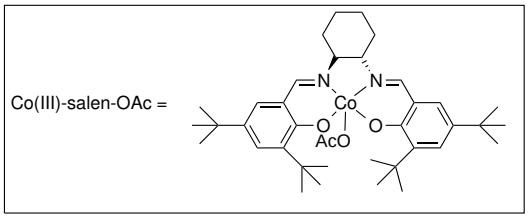

Entry	R	Loading (mol %)	Water (equiv.)	Time (h)	Epoxide ee (%)	Epoxide yield (%)	Diol ee (%)	Diol yield	k_{rel}[a]
1	CH_3	0.20	0.55	12	>98	44	98	50	>400
2	CH_2Cl	0.30	0.55	8	98	44	86	38	50
3	$(CH_2)_3CH_3$	0.42	0.55	5	98	46	98	48	290
4	$(CH_2)_5CH_3$	0.42	0.55	6	99	45	97	47	260
5	Ph	0.80	0.70	44	98	38	98[b]	39[b]	20
6	$CH{=}CH_2$	0.64	0.50	20	84	44	94	49	30
7	$CH{=}CH_2$	0.85	0.70	68	99	29	88	64	30

[a] k_{rel} (selectivity factor) is determined by the equation ln[(1-C)(1-ee)]/ln[(1-C)(1+ee)], where C = conversion and ee = enantiomeric excess[67].
[b] Denotes ee and isolated yield after recrystallization.

of active pharmaceutical ingredients (APIs), such as muconin, an anticancer agent, as shown in Figure 15 [68, 69, 62, 63].

Moreover, with respect to pharmaceutical significance, a macrocyclic Co(III)-salen-PF_6 has been used as a catalyst in HKR to produce the enantiopure terminal epoxides (S)-1-naphthyl glycidyl ether and (S)-propene oxide to be used in the syntheses of the chiral drugs (R)-mexiletine and (S)-propranolol, respectively (Figures 16 and 17, respectively) [70]. HKR is a simple, straightforward method for preparing a variety of highly enantioenriched terminal epoxides from inexpensive materials that would otherwise be difficult to access [62]. Many epoxides are commercially available as racemic mixtures, making a kinetic resolution for a single epoxide enantiomer appealing. The only reagent required for HKR is water, which is safe and inexpensive [61]. From a catalysis science perspective, the Co(III)-salen-catalyzed HKR reaction has become a useful test-bed for the development of supported catalysts that enhance cooperative catalysis, as the HKR reaction is now the prototypical cooperative bimolecular reaction catalyzed by a metal-ligand complex (vide infra) [71].

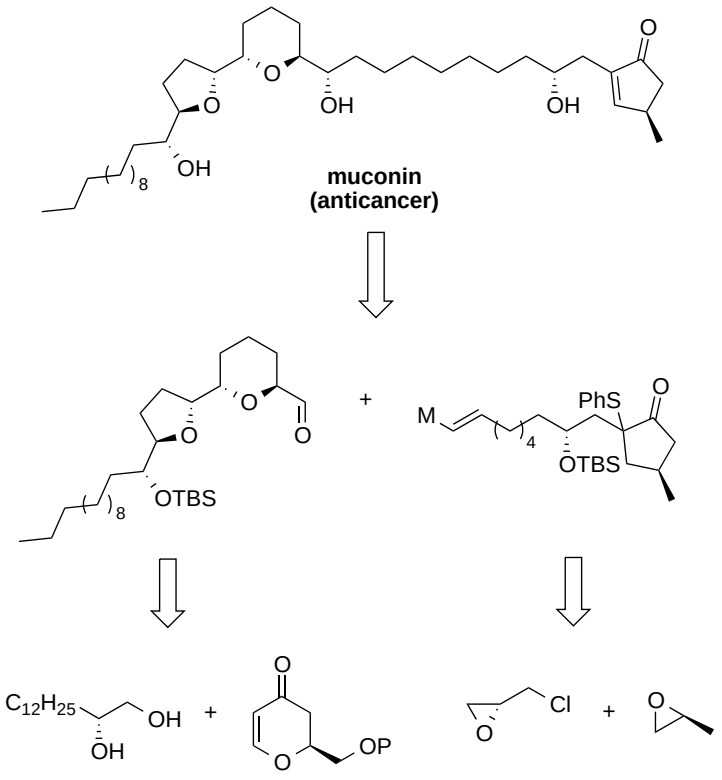

Figure 15: Synthesis of the anticancer agent muconin [68, 69].

2.1.1 Co(III)-salen catalysis of HKR occurs via a bimetallic/cooperative mechanism

Using chiral Co(III)-salen-X (X = nucleophilic counter-ions, such as Cl, OAc) complexes, Jacobsen and Blackmond showed that the reaction typically follows a second-order, cooperative bimetallic pathway (where two cobalt centers participate in the rate-determining step of the reaction) [72, 73, 74, 75]. In this proposed mechanism, one Co(III)-salen (presumed to have the original counter-ion, X) activates the electrophilic epoxide, while the other Co(III)-salen (presumed to have an OH^- counter-ion) activates the nucleophilic water (Figure 18, red pathway) [72, 74, 75].

The Co(III)-salen-OH is a hypothetical species, first proposed by Nielsen et al. [72]. This active species has yet to be isolated or conclusively characterized. Kemper et al. used *in situ* solution NMR and quantum chemical calculations to study

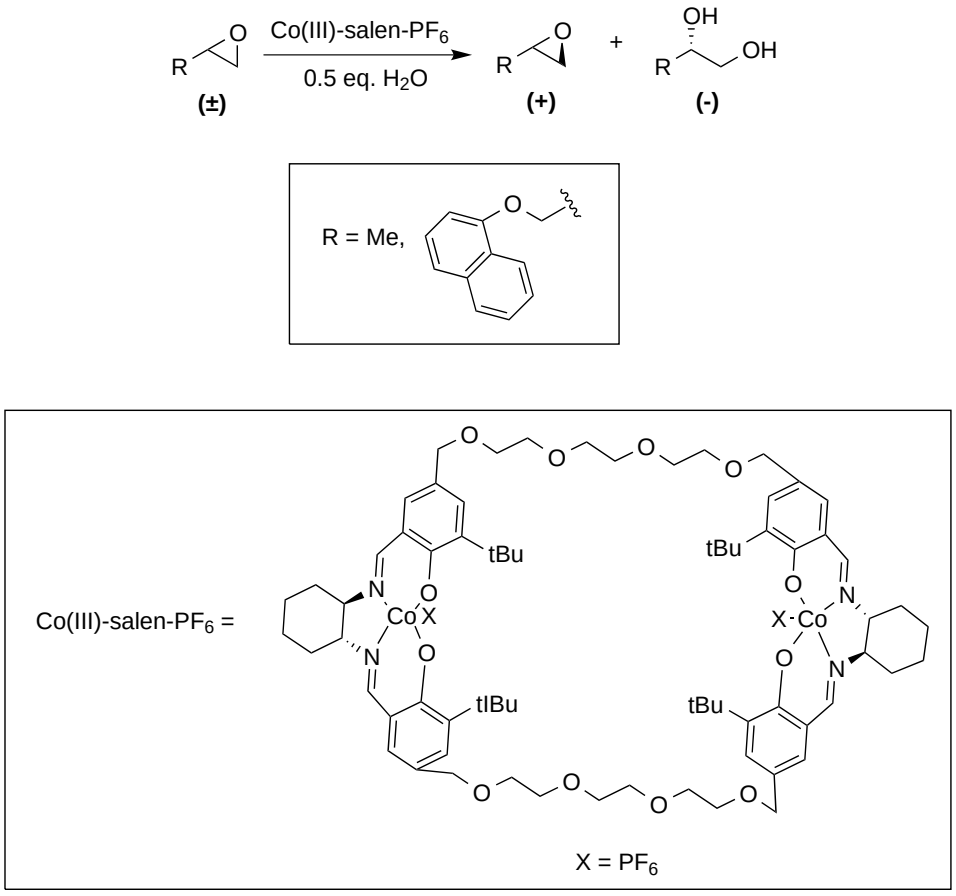

Figure 16: HKR of (S)-1-naphthyl glycidyl ether and (S)-propene oxide using macrocyclic Co(III)-salen-PF_6 [70].

the coordination, conformational, and electronic properties of Co(III)-salens to better understand the enantioselectivity of HKR [76]. They determined that for the bimetallic transition state exemplified by the two Co(III)-salens in HKR, the nucleophilic Co(III)-salen-OH exists as a pentacoordinated, high spin, paramagnetic complex, and the Co(III)-salen-X (X $\neq$ OH) that activates the epoxide exists as a hexacoordinated, low spin, diamagnetic complex [76]. The two Co(III)-salens are aligned in a "head-to-tail" orientation [66]. Due to this orientation, the Co(III)-salen-OH can attack one epoxide enantiomer over the other [76]. Recently, Vinck et al. proposed that a small fraction of the Co(III)-salen-OAc species in HKR is a Co(III)-bound phenoxyl radical that is formed via air oxidation of Co(II) with acetic

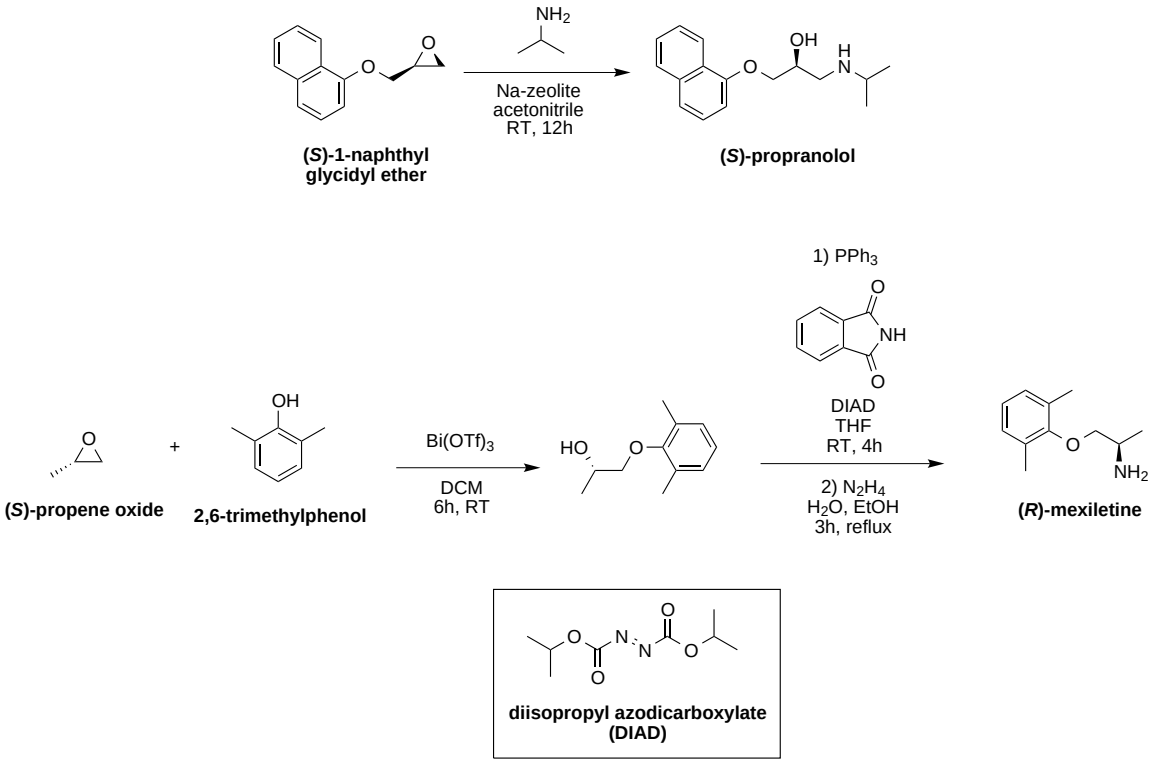

Figure 17: Applications of HKR-synthesized enantiopure terminal epoxides used for the syntheses of chiral drugs (*R*)-mesitylene and (*S*)-propranolol [70].

acid present (Figure 19) [77]. This radical, which has one to two acetates ligated to the complex, is proposed to have formed via a two-electron, two-proton reduction of oxygen to hydrogen peroxide, thus producing a delocalized phenoxyl radical that is stabilized by the bulky *tert*-butyl groups located at the *ortho*- and *para*-positions of the phenolate [77]. The radical was characterized by pulsed and continuous-wave electron paramagnetic resonance (EPR), as well as resonance Raman (RR) [77].

2.1.2 Rate of HKR: dependent upon the Co(III)-salen counter-ion

Nielsen et al. demonstrated that the nucleophilicity of the Co(III)-salen counter-ion had a direct and important effect on the rate of HKR [72]. At low catalyst loadings, it has been reported that there is a less selective, monometallic pathway that competes with the bimetallic pathway [78]. Taking the nature of the Co(III)-salen counter-ion into consideration, Jain et al. suggested that a less selective, monometallic

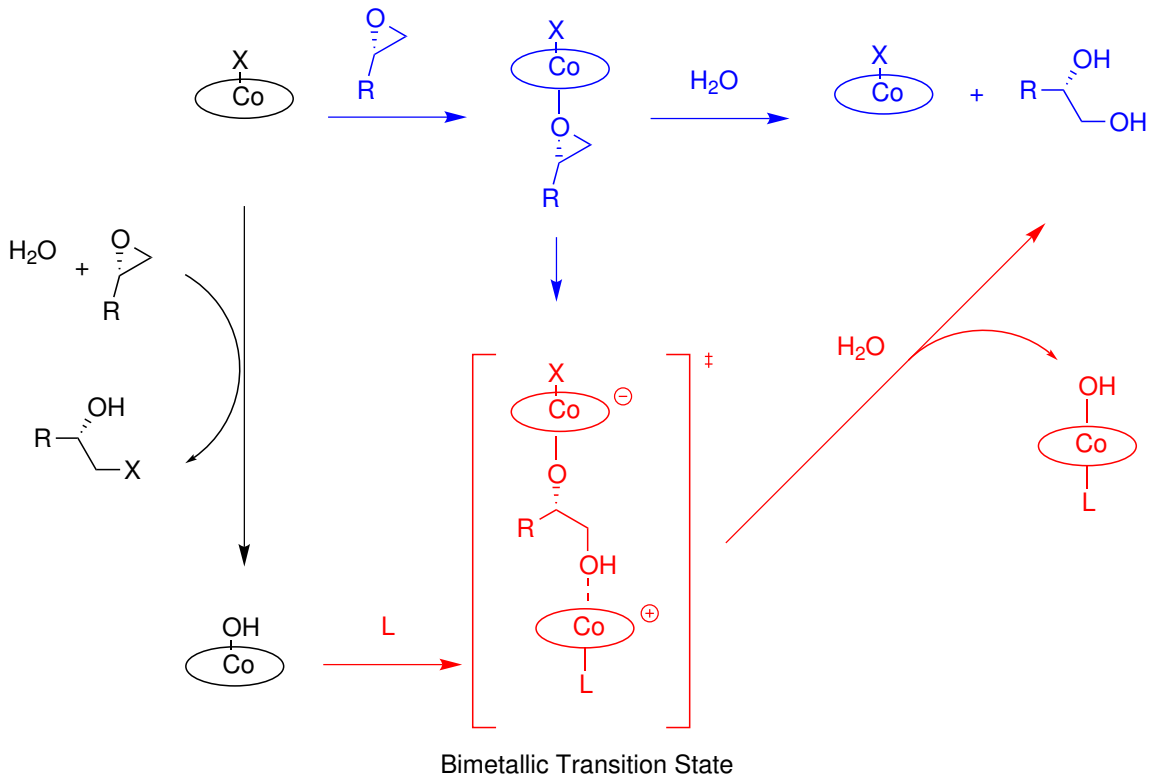

Figure 18: Scheme of the mechanism that shows the presence of the proposed monometallic (blue) and bimetallic (blue coupled with red) pathways in HKR [72, 73].

pathway (Figure 18, blue pathway) [73] couples with the bimetallic pathway (Figure 18, red pathway) [72] when Co(III)-salens with highly non-nucleophilic counter-ions are present in the reaction. For the bimetallic pathway, the hypothetical Co(III)-salen-OH is formed *in situ* from Co(III)-salen-X (X $\neq$ OH) via a nucleophilic attack (by the counter-ion X) on the epoxide (Figure 18, black pathway) [72].

If X^- is a good nucleophile, such as Cl^-, the counter-ion will rapidly add to the epoxide in the black pathway, and water is suggested to produce the hypothetical Co(III)-salen-OH. With an accumulation of Co(III)-salen-OH occurring in the HKR reaction, the catalytic activity decreases because Co(III)-salen-OH is a poorer Lewis acid than Co(III)-salen-X (X $\neq$ OH) [72]. If X = OTs, HKR catalysis is highly efficient, as counter-ion addition is reversible because Co(III)-salen-OTs is not suggested to completely convert to Co(III)-salen-OH [79]. If X is non-nucleophilic, such as

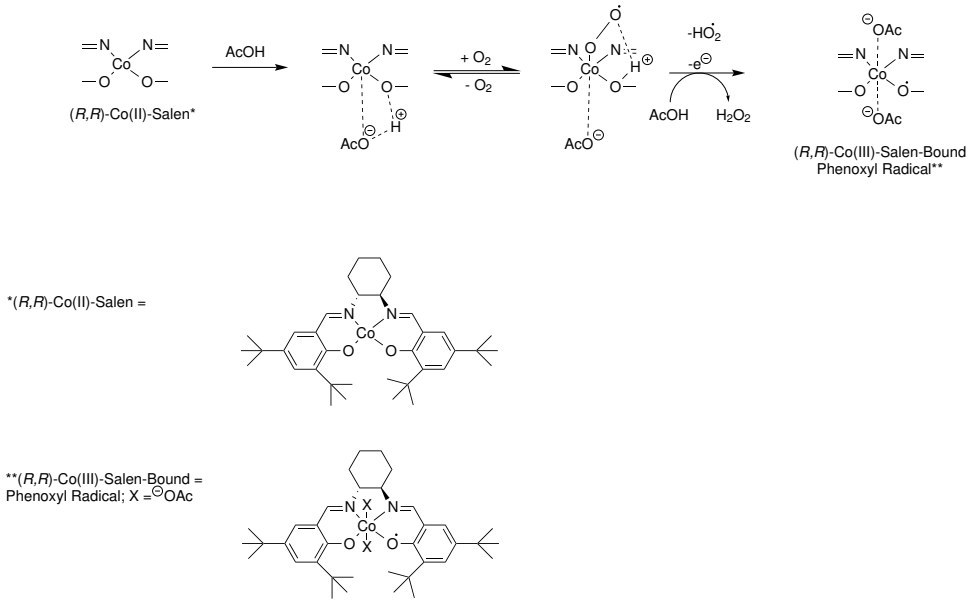

Figure 19: Scheme of the formation of the proposed Co(III)-bound phenoxyl radical that is formed in small amounts via air oxidation of Co(II)-salen in the presence of acetic acid [77].

SbF_6^-, there should be no nucleophilic attack of the counter-ion on the epoxide, and thus, no generation of Co(III)-salen-OH [72]. As a result, the cooperative, bimetallic pathway is not suggested to take place to a significant extent (Figure 18, red pathway) [72], and the HKR reaction is suggested to be catalyzed primarily via a less selective, monometallic pathway (Figure 18, blue pathway) [73]. Based on the above mechanistic picture, it has been demonstrated that with a 1:1 ratio of Co(III)-salen-OH and Co(III)-salen-SbF_6, the fastest rates for the HKR occur, with the rapid formation of the bimetallic transition state, allowing the enantioselective, bimetallic pathway to dominate [72, 73].

2.1.3 Origin of the high selectivity of Co(III)-salen-catalyzed HKR

As mentioned previously, the salen catalysts used for HKR are typically enantiopure, which is required to successfully produce a highly enantiopure product. However, Nielsen et al. suggested that each epoxide enantiomer bound to Co(III)-salen-X with the same affinity ($K_{E:matchedepoxide}/K_{E:mismatchedepoxide} = 1.0 \pm 0.2\ M^{-1}$) [72]. This suggests that the binding of an epoxide to Co(III)-salen-X is not a strongly enantiodiscriminating step, and thus, they concluded that the high enantioselectivity of the HKR is predominantly due to the selective reaction resulting from the nucleophilic Co(III)-salen-OH attacking one of the Co(III)-salen-X-epoxide complexes [72]. This is consistent with the suggestion that the monometallic pathway (Figure 18, blue pathway) [73] is less enantioselective (31% ee at 36% conversion, Table 2 [73]) than the cooperative pathway (59% ee at 36% conversion, Table 2 [73]) (Figure 18, blue + red pathway) [72, 73], although the still moderate enantioselectivity achieved using only non-coordinating counter-ions suggests that (i) there is some selectivity associated with epoxide binding or (ii) the bimetallic pathway still operates when only trace amounts of the Co(III)-salen-OH species are produced [72].

Table 2: Catalyst selectivity as a result of the bimetallic or monometallic catalytic pathway of Co(III)-salen-catalyzed HKR [73].

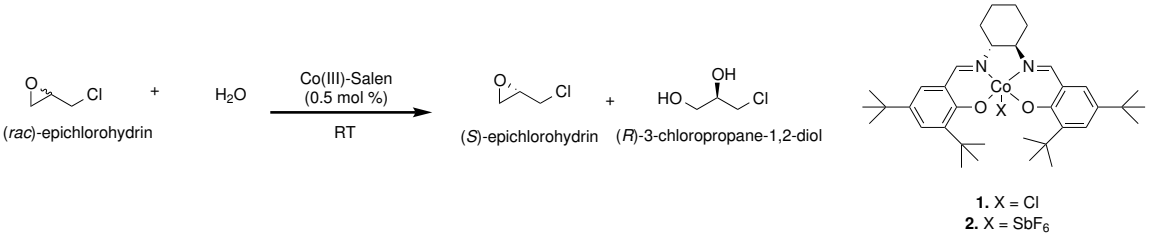

Entry	Catalyst	Reaction time (h)	Epoxide conversion (%)	Epoxide ee (%)	Catalytic pathway
1	**1**	0.5	36	59	Bimetallic
2	**2**	4	36	31	Monometallic

Based on these findings, it might be inferred that the chirality of the Co(III)-salen-X (X = non-nucleophilic counter-ion) is less important or even unimportant in

determining the enantioselectivity of the HKR reaction. To probe this hypothesis, the HKR of epoxides was evaluated using salen complexes constructed from a variety of counter-ions (Cl^-, OH^-, $SbF_6{}^-$, and ^-OAc) using both enantiopure and racemic salen ligands (Figure 20) [72].

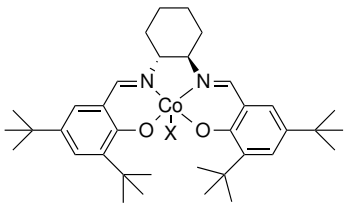

(*R,R*)-(*N,N'*)-bis(3,5-di-*tert*-butylsalicylidene)-1,2-cyclohexanediaminocobalt(III) X
1. X = Cl
2. X = SbF_6

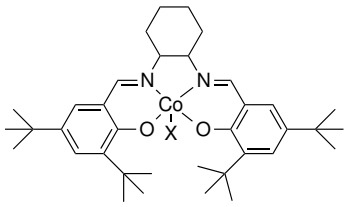

(±)-*trans*-(*N,N'*)-bis(3,5-di-*tert*-butylsalicylidene)-1,2-cyclohexanediaminocobalt(III) X
3. X = Cl
4. X = SbF_6

Figure 20: Co(III)-salen pre-catalysts used in this work, built from enantiopure (**1,2**) and racemic (**3,4**) ligands [72].

If each complex is stable under the reaction conditions, a catalyst containing a 50:50 mix of (***R,R***)-Co(III)-salen-OH and (±)-***trans***-Co(III)-salen-SbF_6 might provide good activity and enantioselectivity for the HKR of epoxides that is comparable to a catalyst containing a 50:50 mix of (***R,R***)-Co(III)-salen-OH and (***R,R***)-Co(III)-salen-SbF_6. This 50% decrease in use of the more expensive chiral ligand [80] could provide significant practical advantages for Co(III)-salen-catalyzed HKR reactions. To this end, mixed (***R,R***)-Co(III)-salen-OH and (±)-***trans***-Co(III)-salen-SbF_6 catalyst systems are explored here for the HKR of racemic epichlorohydrin. This approach is not found to yield highly enantioselective catalysis, and the causes for the reduced selectivity are enumerated in this study, providing further insights into the nature of the HKR reaction pathways.

2.2 Experimental procedures

2.2.1 Chemicals

Reagents were purchased from commercial vendors and used as received unless otherwise stated. All solid starting materials were dried under high vacuum before use, and anhydrous solvents were obtained either from a solvent purification system or from a bottle sealed under nitrogen (from commercial vendors). Prior to use, divinylbenzene (DVB) was washed with 5% NaOH (2x) and deionized water (2x) to remove the polymerization inhibitors, and then it was dried with anhydrous $MgSO_4$.

2.2.2 Instrumentation

^{1}H NMR spectra were obtained using a Varian Mercury spectrometer (400 MHz); the chemical shifts were expressed in ppm and are referenced to the corresponding residual nuclei in the deuterated solvents. FT-IR spectra were obtained using a Bruker Vertex 80v (Ram II) by dispersing the samples in a KBr pellet. Elemental analyses (EA) of the samples were performed by Columbia Analytical Services, Tuscon Laboratory (Tuscon, AZ, USA). The conversion of racemic epichlorohydrin and the ee of (*S*)-epichlorohydrin were determined using a Shimadzu 17A GC equipped with an FID and Chiraldex γ-TA column (40 m x 25 mm x 0.25 μm). Either *para*-dichlorobenzene or mesitylene was used as an internal standard.

2.2.3 Catalyst preparation

*2.2.3.1 Synthesis of (R,R)- and (±)-trans-Co(III)-salen-Cl (**1** and **3**, respectively)*

Catalysts **1** and **3** were prepared according to previously published procedures, and the characterization data matched the data previously reported [72].

*2.2.3.2 Synthesis of (R,R)- and (±)-trans-Co(III)-salen-SbF_6 (**2** and **4**, respectively)*

Catalysts **2** and **4** were prepared according to previously published procedures, and the characterization data matched the data previously reported [72] [73].

*2.2.3.3 Synthesis of polymer resin-supported (R,R)-Co(III)-salen-OAc (**8**)*

Catalyst **8** was prepared according to previously published procedures, and the characterization data matched the data previously reported [81, 82, 83].

2.2.4 Synthesis of styrene/DVB resin

Styrene/DVB resin was synthesized according to previously published procedures [82]. A two-neck round-bottom flask equipped with a stirbar and a reflux condenser was purged with nitrogen. Then, 1 equivalent of styrene and 5 equivalents of DVB were added to the flask, and the reaction mixture was heated under nitrogen for 36 h at 80°C. After cooling to room temperature, the white solid was then washed several times with methanol and dichloromethane. After filtration, the resin was allowed to dry overnight under high vacuum.

2.2.5 HKR of racemic epichlorohydrin

A pear-shaped flask equipped with a stirbar was charged with the respective catalyst at the appropriate loadings (0.25 or 0.5 mol%). The flask was then immersed in a water bath to keep the reaction temperature constant. Next, 1 equivalent of racemic epichlorohydrin was added to the flask, followed by the internal standard (mesitylene or *para*-dichlorobenzene). After stirring briefly, 2.5 μL of the mixture was passed through a silica plug and washed with diethyl ether prior to the catalytic reaction. Deionized water (0.6 equivalents) was then added to initiate the reaction. For homogeneous catalytic studies, 2.5 μL samples were taken until 99% ee or a constant,

maximum % ee was reached. For reactions using the polymer resin-supported catalysts, 2.5 μL samples were taken for 4 h.[1] Samples from all of the reactions were passed through a plug of silica gel (to remove the catalyst) and washed with diethyl ether prior to GC/FID analysis.

2.2.6 Catalyst recovery

Upon completion of the HKR reactions using the polymer resin-supported catalysts, the reaction mixture was filtered through a fritted funnel to isolate the solid catalyst, and this catalyst was washed with dichloromethane until the liquid filtrate became clear and colorless. The solid catalyst was dried under high vacuum overnight and then analyzed via EA and FT-IR. The recovered filtrate was concentrated under reduced pressure ($T < 60$°C) to recover the homogeneous catalyst from the reaction. This catalyst was also dried overnight under high vacuum and analyzed via EA.

2.3 Results and Discussion

As noted above, previous work has suggested that only the (***R,R***)-Co(III)-salen-OH complex generated from (***R,R***)-Co(III)-salen-X containing a nucleophilic counter-ion plays a key role in the enantiodiscriminating step of HKR [72]. To this end, an array of reactions was first explored to evaluate the ligand chirality and the role of the counter-ion in the HKR of racemic epichlorohydrin (Tables 3 and 4, respectively). Specifically, both the (±)-***trans***-salen and (***R,R***)-salen ligands were used in combination with the non-nucleophilic SbF_6^- counter-ion and the nucleophilic Cl^- counter-ion, which has been suggested to rapidly convert to the OH^- counter-ion under the reaction conditions [72] (Table 3).

[1]The time elapsed to determine that 99% ee of the HKR reaction with catalyst mix **2** + **8** was reached.

Table 3: HKR[a] of racemic epichlorohydrin evaluating ligand chirality and the role of the counter-ion. Data from Ref. [84].

Entry	Catalyst	Total loading (mol%)	Overall initial TOF (min^1)	Time at ≥99% ee (m)	Total conversion at ≥99% ee (%)	k_{rel}[b]
1	**1**	0.25	1.78	240	52.1	>99
2	**2**	0.25	0.89	1740[c] (97%)[d]	71.6	8.2
3	**1** + **2** (50:50 mix)	0.50	3.23	180	56.8	36.0
4	**1** + **4** (50:50 mix)	0.50	2.73	180[c] (77%)[d]	69.3	4.3
5	**2** + **3** (50:50 mix)	0.50	2.79	187.5[c] (82%)[d]	71.9	4.5

[a]HKRs were run with 1 equiv. (*rac*)-epichlorohydrin (782.1 μL, 10 mmol) and 0.6 equiv. water (108.1 μL, 6 mmol). *para*-Dichlorobenzene (120.3 μL) was used as an internal standard.

[b]k_{rel} (selectivity factor) is determined by the equation ln[(1-C)(1-ee)]/ln[(1-C)(1+ee)], where C = conversion and ee = enantiomeric excess[67].

[c]Time at which the %ee reaches a maximum.

[d]Denotes maximum %ee reached by the reaction.

2.3.1 HKR of racemic epichlorohydrin

The conversion of racemic epichlorohydrin and the resulting enantiomeric excess (ee) of (*S*)-epichlorohydrin were monitored by GC/FID using a chiral capillary column. The results are collected in Table 3. In the first entry, the use of (***R,R***)-Co(III)-salen-Cl (**1**) at 0.25 mol% catalyst loading is demonstrated to be an active and selective catalyst over one use, providing a high turnover frequency (TOF) and good enantioselectivity of the unreacted epichlorohydrin, achieving 99% ee at 52.1% conversion (perfect selectivity would give a conversion of 50%) [84]. Catalyst **1** gave an initial TOF of 1.78 min^{-1} [84] and displayed a selectivity marked by a very high k_{rel}[2] of >99. By comparison, at the same catalyst loading, the (***R,R***)-Co(III)-salen-SbF_6 catalyst (**2**) gave a much lower initial rate (0.89 min^{-1}) and was also less enantioselective, with a k_{rel} of 8.2 (Table 3, entry 2) [84]. These results are consistent with the reaction pathways described above, with the catalyst in entry 1 rapidly proceeding down the selective pathway shown in Figure 18 (red + blue pathway) [72] and the catalyst in entry 2 being shuttled through the less selective blue pathway (Figure 18) [73]. In entry 3, a 50:50 mixture of the two counter-ions on the enantiopure ligand (catalysts **1** and **2**) was employed at 0.5 mol% catalyst loading. This combination also gave a

[2]See Table 1 for the definition of k_{rel} [67].

selective catalyst and was the most active of all runs, as exemplified in the literature [72, 73].

Next, reactions were run with a 50:50 mixture of enantiopure and racemic salen ligand. First, in entry 4, the reactions resulting from the use of (***R,R***)-Co(III)-salen-Cl (**1**) and (±)-***trans***-Co(III)-salen-SbF_6 (**4**) are described. If the enantiospecificity of the reaction was largely determined by the chirality of the complex with the nucleophilic counter-ion, in this case complex **1**, then this reaction should proceed with identical selectivity as entry 1 in the absence of counter-ion exchange. However, as shown in the table, this catalyst combination was less selective relative to the reactions described in entries 1-3, suggesting that either the mechanistic hypothesis above is incorrect or that other factors are important. In entry 5, catalysts **2** and **3** [(***R,R***)-Co(III)-salen-SbF_6 and (±)-***trans***-Co(III)-salen-Cl, respectively] were used, with the opposite pairing of ligands and counter-ions as seen in the previous case (entry 4). Based on the mechanistic hypothesis described above, this catalyst should be the least selective of the combinations in the absence of counter-ion exchange. However, as shown in Table 3, this catalyst combination (entry 5), while also unselective, gave nearly identical results to entry 4. These last two runs, in combination, are consistent with the occurrence of a rapid scrambling of counter-ions under the reaction conditions, as such scrambling should produce the same average combination of catalysts in both entries 4 and 5. If this scrambling were to occur, the above results would then remain fully consistent with the overall mechanistic picture described in Figure 18 [72, 73, 74, 75] and remove the possibility of lowering the cost of the reactions by using a combination of enantiopure and racemic ligands. Therefore, the counter-ion exchange hypothesis was explored in more detail to support or refute this hypothesis.

2.3.2 Co(III)-salen-X counter-ion exchange

One approach for determining whether the counter-ion exchange is present in a mixed counter-ion Co(III)-salen system is to separate and isolate one Co(III)-salen-X species from the other for direct characterization; this can best be explored by immobilizing one of the Co(III)-salens on a support. Previously, Co(III)-salen-OTf complexes have been immobilized on gold colloids [85], and the Jones and Weck groups have immobilized metallosalens on silica [86], soluble polymers [81, 87], polymer resins [82, 86], and oxide-supported polymer brushes [88]. (*R,R*)-Co-salen-OAc (**8**) was supported on a polymer resin with a flexible ethylene glycol linker, as these salens have previously been used to give good catalytic rates and selectivities, as reported by the Jones and Weck groups (Figure 21) [81, 82, 83]. This catalyst was combined with (*R,R*)-Co(III)-salen-SbF_6 as a soluble homogeneous catalyst (Figure 20, catalyst **2**) [73]. Catalysts **2** (Figure 20)[72] and **8** (Figure 21) [81, 82, 83] were prepared according to previously published procedures [73, 81, 82, 83] and characterized by EA (Table 4, entries 1, 3, and 4).

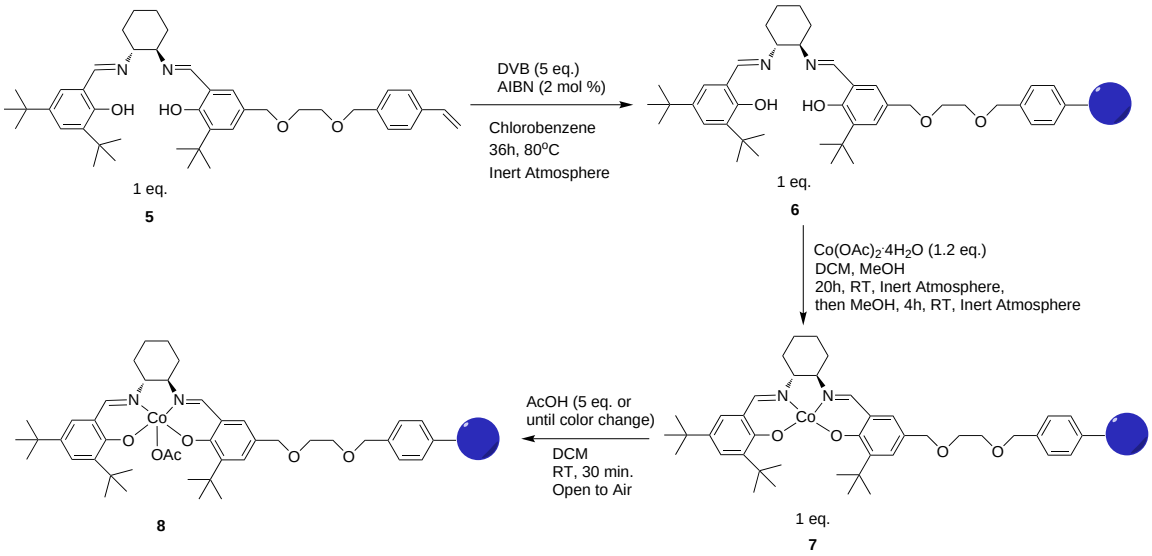

Figure 21: Scheme of the reaction pathways for the formation of the resin-supported Co(II)- and Co(III)-salens for the HKR reactions [81, 82, 83].

Table 4: Elemental analysis data from the catalysts used for HKR[a] evaluating the counter-ion exchange. Data from Ref. [84].

Entry	Catalyst	C (wt.%)	H (wt.%)	N (wt.%)	Sb (wt.%)	Co (wt.%)	mol Co/mol N	mol Sb/mol Co
1	**2**, Fresh	48.63	6.19	3.04	12.92	6.11	0.48	1.02
2	**7**, Fresh	80.81	8.96	1.88	<0.04	3.23	0.50	<0.01
3	**8**, Fresh	78.31	7.52	1.89	<0.30	3.17	0.40	<0.05
4	**8**[b]	74.24	7.70	1.50	<0.20	2.74	0.43	<0.04
5	**2** + **8**[c]	68.38	6.90	1.39	1.39	2.58	0.45	0.26
6	Filtrate of **2** + **8** reaction[c]	33.81	5.81	0.19	0.31	0.25	0.32	0.60
7	**2** + **7**[c]	72.43	6.87	1.54	2.05	2.88	0.44	0.34
8	Filtrate of **2** + **7** reaction[c]	35.03	6.17	0.14	0.24	0.20	0.34	0.58
9	Styrene/DVB Resin,[d] Fresh	90.51	7.83	0.94	<0.03	<0.03	<0.01	N/A
10	**2** + Styrene/DVB resin[c]	90.09	7.83	0.72	<0.08	<0.03	<0.01	N/A
11	Filtrate of **2** + styrene/DVB resin reaction[c]	37.22	5.69	0.54	2.11	1.12	0.49	0.91

[a]HKRs were run with 1 equiv. (*rac*)-epichlorohydrin and 0.6 equiv. water. Mesitylene was used as an internal standard.

[b]Recovered after one HKR cycle.

[c]Solid catalyst, **8**, or Co(II)-salen-functionalized resin, **7**, recovered from the catalyst mixes denoted above after one HKR cycle.

[d]Blank polymer resin composed of styrene crosslinked 1:5 with DVB.

HKR reactions were run with the combination of resin-supported (*R,R*)-Co(III)-salen-OAc (**8**) and homogeneous (*R,R*)-Co(III)-salen-SbF_6 (**2**), along with the appropriate control reactions (Table 4, entries 1-4). Following the HKR, the resin-supported salens were recovered via vacuum filtration for analysis via EA and FT-IR. If counter-ion exchange occurred during the reactions, the spent supported catalysts should exhibit an increased Sb/Co ratio, and an Sb-F stretch near 660 cm^{-1} should be apparent in the FT-IR spectrum of the recovered solid, which was initially Sb-free [89].

For the HKR reaction with a catalyst mix of **2** (Co(III)-salen-SbF_6) and **8** (supported Co(III)-salen-OAc), the supported spent catalyst **8**, when analyzed by EA, had an Sb/Co ratio of 0.26 (Table 4, entry 5). Although the Sb/Co ratio ratio observed for this catalyst mix is less than the Sb/Co ratio of fresh catalyst **2** that is fully oxidized to Co(III)-SbF_6 (1.02, Table 4, entry 1), it is greater than the Sb/Co ratio of the fresh and spent catalyst **8**, which has no SbF_6^- counter-ion (<0.05 and <0.04, Table 4, entries 3 and 4, respectively). This suggests that some of the SbF_6^- counter-ion from the homogeneous catalyst **2** has exchanged with the counter-ion from the supported catalyst **8**. To verify the presence of SbF_6^- in the spent catalyst

8, the solid was examined by FT-IR [84].

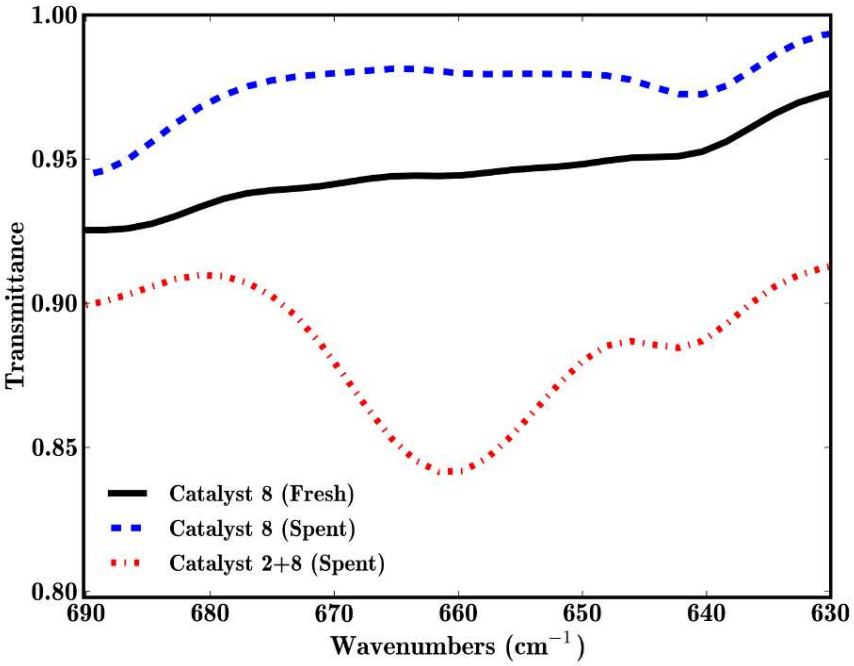

Figure 22: FT-IR spectra of the fresh (solid line) and spent resin-supported (*R,R*)-Co(III)-salen-OAc (**8**) (after one HKR cycle, dotted line) and the recovered solid catalyst **8** (dot-dashed line) from the HKR using homogeneous (*R,R*)-Co(III)-salen-SbF_6 + resin-supported (*R,R*)-Co(III)-salen-OAc (**2** + **8**). The appearance of the Sb-F stretch at 661 cm^{-1} is indicative of the SbF_6^- likely coordinating to the Co center of the resin-supported (*R,R*)-Co(III)-salen. Data from Ref. [84].

A peak at 661 cm^{-1} associated with an Sb-F stretch (Figure 22, dot-dashed line) clearly suggests the presence of SbF_6^- in the spent solid **8**, whereas both the fresh and spent catalyst **8** from regular reactions without catalyst **2** do not have this peak (Figure 22, solid and dotted lines, respectively). Analysis of the filtrate of the HKR reaction using catalyst mix **2** and **8** (which includes homogeneous (*R,R*)-Co(III)-salen-SbF_6) gave an Sb/Co ratio of 0.60 (Table 4, entry 6), indicating that there is a decrease in SbF_6^- relative to the fresh catalyst **2** (Table 4, entry 1). Based on the data presented in Table 4 and Figure 22, it can be concluded that there is a degree of counter-ion exchange occurring, where SbF_6^- is transferred from the homogeneous

(*R,R*)-Co(III)-salen **2** to the resin-supported (*R,R*)-Co(III)-salen **8**, which originally included $^{-}$OAc [84].

This exchange is further exemplified when an HKR reaction is run with the homogeneous (*R,R*)-Co(III)-salen-SbF_6 and the resin-supported (*R,R*)-Co(II)-salen, which is orange in color (catalyst mix **2** and **7**, respectively). A brown solid catalyst was recovered from this reaction, indicative of a Co(III)-salen species supported on the resin. The Sb/Co ratio for this catalyst was 0.34 (Table 4, entry 7), which is greater than the ratio that would be expected for catalyst **7**, which has no counter-ion coordinated to the Co center (<0.01, Table 4, entry 2). This suggests that either the SbF_6^- species is transferred onto the supported Co(II) species, converting it to Co(III)-SbF_6, or that the homogeneous Co(III)-salen-SbF_6 species are trapped within the resin. In this case, the spent resin material, **7**, also shows an Sb-F stretch at 661 cm^{-1} in its FT-IR spectrum (Figure 23, dotted line), whereas the spectrum of the fresh catalyst **7** does not show this peak (Figure 23, solid line). The light brown filtrate from the HKR reaction using catalysts **2** and **7** gives an Sb/Co ratio of 0.58 (Table 4, entry 8), indicative of a partial SbF_6^- transfer from the homogeneous (*R,R*)-Co(III)-salen to the resin-supported (*R,R*)-Co(II)-salen [84].

To determine whether significant amounts of SbF_6^- become trapped within the polymer resin without reacting with a Co-salen center, HKR reactions were run using catalyst **2** and a polymer resin composed of a 1:5 cross linked styrene/DVB, which does not include any salen species. In evaluating the EA data, the Sb content in both the fresh and spent styrene/DVB resins were found to be negligible (Table 4, entries 9 and 10). Moreover, there was no Sb-F stretch observed at 661 cm^{-1} in the FT-IR spectra (Figure 23, dot-dashed line). In addition, the dark green filtrate of the HKR reaction with the salen-free styrene resin and **2** had a Co/N ratio of 0.49 and an Sb/Co ratio of 0.91 (Table 4, entry 11), indicating that nearly all of complex **2** was recovered (Table 4, entry 1). Because an increase in the Sb/Co ratio and

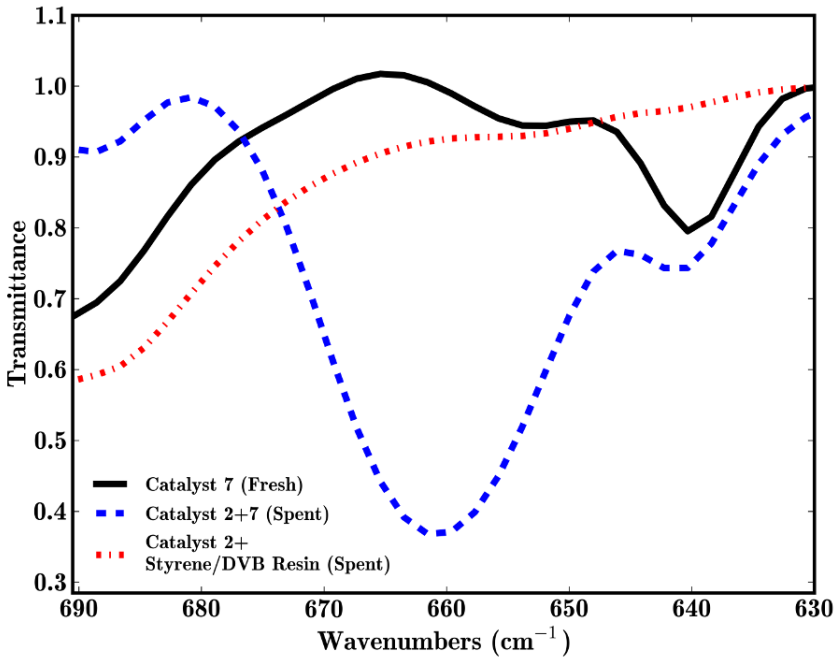

Figure 23: FT-IR spectra of the fresh (solid line) resin-supported (*R,R*)-Co(II)-salen (**7**), the recovered solid catalyst (dotted line) from the HKR reaction using homogeneous (*R,R*)-Co(III)-salen-SbF_6 + resin-supported (*R,R*)-Co(II)-salen (**2** + **7**), and the recovered solid catalyst from the HKR reaction using homogeneous (*R,R*)-Co(III)-salen-SbF_6 (**2**) + styrene/DVB resin (dot-dashed line). The appearance of an Sb-F stretch at 661 cm^{-1} is indicative of the SbF_6^- likely coordinating to the Co center of the resin-supported (*R,R*)-Co-salen. Data from Ref. [84].

the presence of the Sb-F stretch are observed in the spent catalysts upon exposure to catalyst **2** and minimal to no amount of catalyst **2** becomes trapped within the salen-free polymer resin, it can be concluded that the Sb species found in the spent catalysts from entries 5 and 7 of Table 4 are indicative of the prevalence of a counter-ion exchange occurring between SbF_6^- and ^-OAc. Thus, the similar reactivity seen in Table 3, entries 4 and 5, demonstrates that rapid counter-ion exchange occurs between the Co(III)-salen species during catalysis, and therefore, mixed chiral-racemic ligand systems cannot be used to reduce the cost of HKR reactions [84]. It should further be noted that the counter-ion scrambling is consistent with the mechanism of Nielsen et al., which describes the Lewis acidic Co(III)-salen-X activating the epoxide, while

the nucleophile-delivering Co(III)-salen-OH selectively attacks this activated epoxide [79].

2.4 Conclusions

The potential of combining chiral and racemic ligands in the enantioselective HKR of epoxides based on the mechanistic hypotheses of Nielsen et al. was explored [72]. Based on the currently accepted mechanism, high activity and enantioselectivity might be achieved in reactions catalyzed using 50% enantiopure ligand with a counter-ion designed to make the salen complex a nucleophile-delivering complex (e.g., OH^-) and 50% racemic ligand with a counter-ion designed to make the salen complex a Lewis acidic, electrophilic complex (e.g., SbF_6^-). In this work, it was shown that such experiments do not lead to highly selective catalysis due to counter-ion scrambling between the Co centers. The counter-ion scrambling hypothesis was supported by control experiments using a polymer-supported Co-salen species and the associated kinetic evidence, FT-IR spectra, and EA results. This study also showed that the oxidation of a Co(II) species on a polymer support can be promoted via contact with a homogeneous Co(III) species, which suggests a method for catalyst regeneration after deactivation by counter-ion loss, a there is a need for supported catalyst regeneration, as it is currently a drawback in commercial-scale catalysis [83, 90].

2.5 Acknowledgements

This study was funded by the U.S. Department of Energy, Basic Energy Sciences for financial support via Catalysis Science Grant No. DE-FG01-03R15459. Drs. Marcus Weck and Michael Kahn (both from New York University) are also acknowledged for helpful discussions, as well as Dr. Yan Feng (Georgia Tech) for experimental assistance.

CHAPTER III

PROGRESS TOWARD THE SYNTHESIS OF CALLOPHYCOLIDE A, AN ANTIMALARIAL BENZENE DITERPENOID

Malaria is an extremely serious infectious disease caused by the parasite *Plasmodium falciparum*, the deadliest malaria-carrying parasite to humans [5, 6]. A total of 300-500 million cases of malaria are reported annually, with 1-2 million of these cases being fatal [3]. Historically, natural products, along with their synthetic derivatives, have been the primary source for seeking antimalarial treatments (Figure 24) [4, 18].

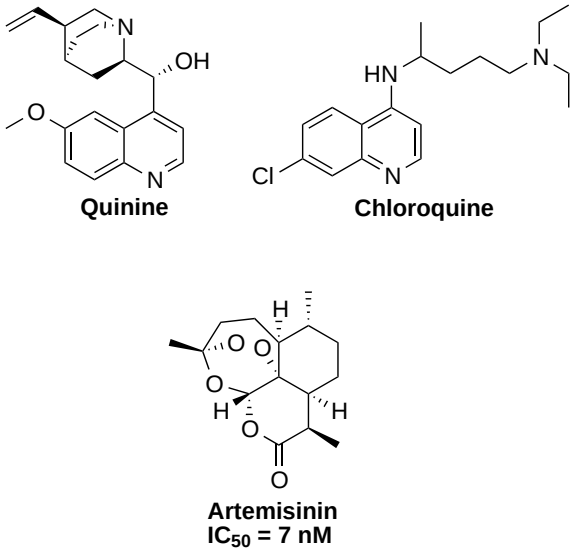

Figure 24: Former and current natural products used to treat malaria [4].

The cinchona tree bark component quinine (Figure 24) [4] was used as an antimalarial treatment for centuries until its synthetic derivative, chloroquine (Figure 24) [4], replaced it in the 1940s [20]. Chloroquine was the treatment of choice for nearly 50 years until resistance to the drug emerged [91, 92]. Artemisinin (Figure

24) [4], which is isolated from the plant *Artemisia annua*, subsequently emerged as a treatment for malaria and is currently the most fast-acting, potent drug available to date, with an $IC_{50} > 7$ nM [38, 39]. Unfortunately, malaria strains that are resistant to artemisinin have been reported [93, 94]. With artemisinin resistance on the rise, there is an urgent need to pursue alternative antimalarial treatments.

3.1 Introduction

In 2005, Kubanek et al. discovered a novel class of macrolides from *Callophycus serratus* [50]. Characterization of these macrolides using X-ray crystallography, NMR, and MS revealed that each macrolide consisted of a diterpene-benzoate structure (Figure 25) [50, 51, 52, 53, 54]. It was later determined via an adapted SYBR Green parasite proliferation assay [52, 95, 96] that bromophycolides A, D, E, H, and M expressed potent activity against *P. falciparum*, with IC_{50} values ranging from 0.3 to 0.9 μM [52]. All of the above compounds contain a macrolide motif, as depicted in Figure 25 [50, 51, 52, 53, 54]. In contrast, other natural products isolated from *C. serratus* lacking the macrolide motif, such as the callophycoic acids, callophycols, and bromophycoic acids, are not as potent as the bromophycolides against *P. falciparum*, with IC_{50} values ranging from 8.7 to > 100 μM; therefore, with respect to antimalarial activity, the lactone macrocycle is a critical component of the structure-activity relationship (SAR) between the aforementioned natural products and their activities against *P. falciparum* (Figure 26) [55, 54, 56, 52].

Now that multiple antimalarial benzoate-diterpenes and their SARs have been identified, the next step is to increase the likelihood of these antimalarials becoming APIs. In addition to being a potent antimalarial agent, bromophycolide A was found in the greatest abundance by Kubanek et al. [50]. Therefore, bromophycolide A (Figure 27) [50, 52, 51] is the most practical starting point concerning key antimalarial agents. However, there are disadvantages associated with bromophycolide A, as well

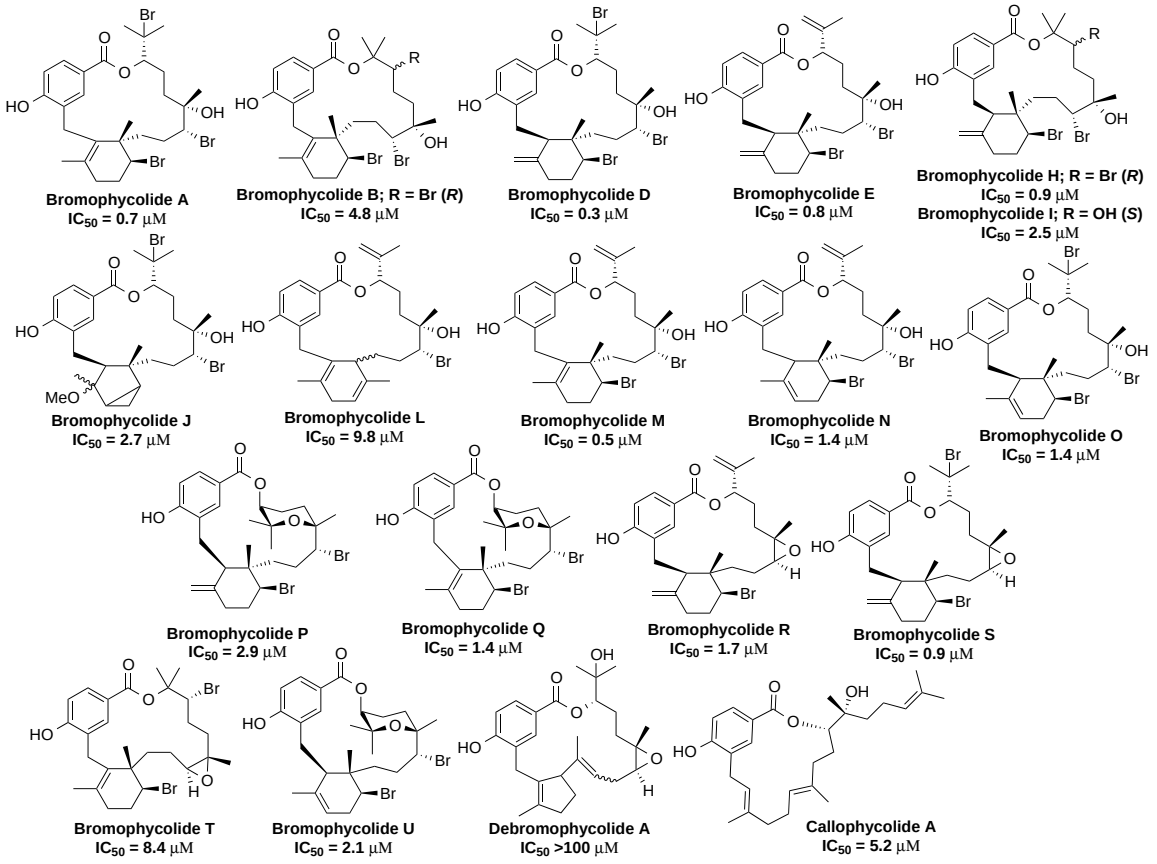

Figure 25: Benzoate diterpenoids isolated from *C. serratus* [50, 51, 52, 53, 54].

as with the other aforementioned macrolides, that could decrease their probability of becoming commercially available drugs. Primarily, the method for isolating these natural products involves several liquid-liquid partitioning steps followed by normal and/or reversed phase HPLC fractionation [52, 51, 54, 53] to obtain, for example, 4 mg of pure natural product [51]. Despite the fact that bromophycolide A is the most abundant natural product isolated from *C. serratus* [5], obtaining large-scale quantities of this material via extraction is not practical or realistic, as multiple grams of bromophycolide A are needed for further studies regarding its antimalarial activity [97]. Although efforts toward a concise, seven-step approach have been made in synthesizing the bromophycolide D skeleta [57], there is currently no known divergent total synthesis of bromophycolide A.

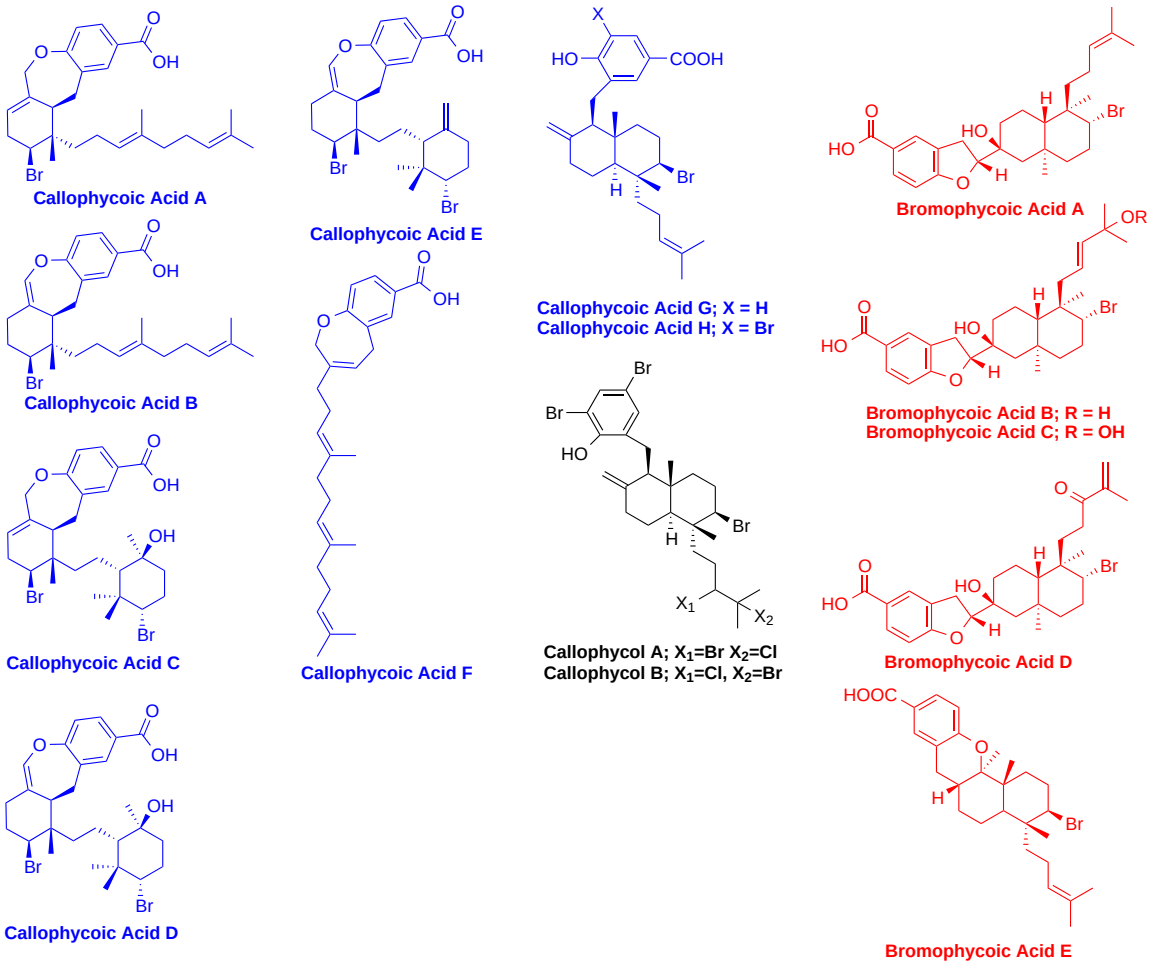

Figure 26: Diterpene-benzoic acids and diterpene phenols isolated from *C. serratus* [55, 56].

A practical approach toward the synthesis of bromophycolide A is to first synthesize alternative diterpene-benzoates, such as callophycolide A (Figure 27) [50, 54]. Although callophycolide A (IC_{50} of 5.2 μM) [54] is not as potent as bromophycolide A, it was shown to inhibit bacterial growth (IC_{50} of 9.1 μM for both VREF and MRSA), and it exhibits moderate anticancer activity (mean IC_{50} of 18 μM) [54]. Most importantly, it exhibits activity against *P. falciparum* (IC_{50} of 5.2 μM) [54]. Similar to the bromophycolides, it consists of a 15-membered macrolide. The macrolide structure of callophycolide A is simple, with only two stereocenters and no bromine atoms present (Figure 27) [50, 54]. Due to this simplified macrolide backbone, callophycolide A can

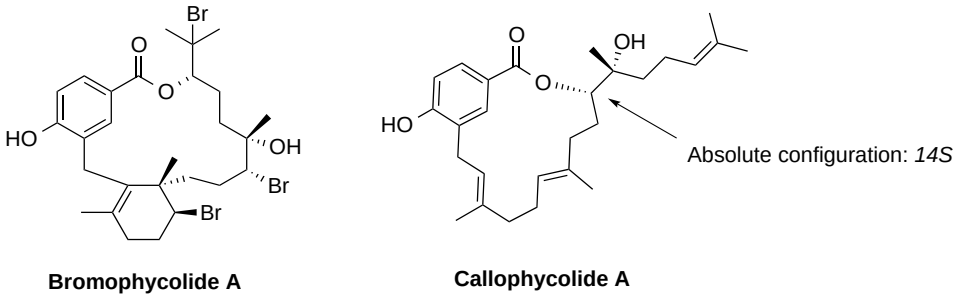

Figure 27: Structural comparison of the macrolides bromo- and callophycolide A [50, 54].

serve as a template for obtaining more potent derivatives. In addition, when Stout et al. isolated and characterized callophycolide A, they were able to only confirm the absolute configuration of C-14 as *S* (Figure 27) [50, 54]. If a total synthesis can be established for callophycolide A, the remaining three stereoisomers can also be synthesized and tested for biological activity, thus confirming absolute configurations and, therefore, the exact meroditerpene isolated previously [54]. Herein, efforts toward a divergent total synthesis of callophycolide A (**1**) are sought that incorporate inexpensive, commercially available starting materials, such as methyl 4-hydroxybenzoate (**4**) and geraniol (**7**), and that utilize known chemistry, including copper-mediated aryl allylation, hydrolytic kinetic resolution (HKR), base-promoted epoxide ring-opening, and the Steglich esterification. If the synthesis is successful, then it can serve as a template for the synthesis of more potent, as well as more structurally complex, antimalarials.

3.2 Retrosynthetic analysis of compound (1)

Evaluating the retrosynthesis shown in Figure 28, the target molecule **1** can be synthesized via a Steglich esterification of compound **28**. Alkylation product **28** can be formed through a base-promoted epoxide ring-opening reaction using (2*S*,3*R*)-MOM-epoxylinalool (**21**, formed via Co-salen-catalyzed HKR) and phenylsulfonylaliphatic

arene **18**. Compound **18** can be synthesized through a copper-mediated aryl allylation using methyl 3-iodo-4-MOM-benzoate (**6**) and phenylsulfonylgeranyl bromide (**13**).

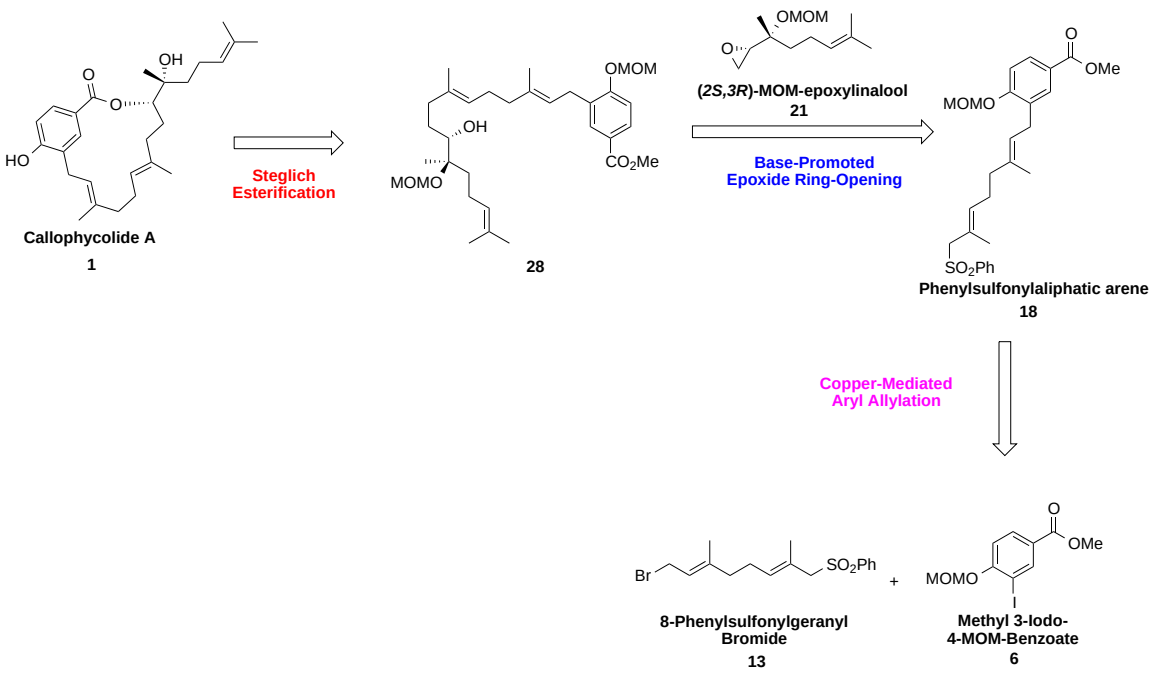

Figure 28: Retrosynthetic analysis of callophycolide A (**1**).

3.3 Results and Discussion

3.3.1 Copper-mediated aryl allylation

Compound **6** was formed in two steps from 36 g of commercially available methyl 4-hydroxybenzoate (**4**, Figure 29), followed by MOM-protection of methyl 4-hydroxy-3-iodobenzoate (**5**) [98, 99]. 8-phenylsulfonylgeraniol (**12**) can be synthesized in five steps beginning with the commercially available geraniol (**7**, Figure 30) (note that allylic bromides, such as 8-phenylsulfonylgeranyl bromide (**13**) do not have a long shelf-life and are thus made on an as-needed basis) [98, 100, 60, 101, 102, 103, 104].

With compounds **6** and **13** in hand, efforts can be made toward the endgame of callophycolide A. Several routes were investigated toward synthesizing compound

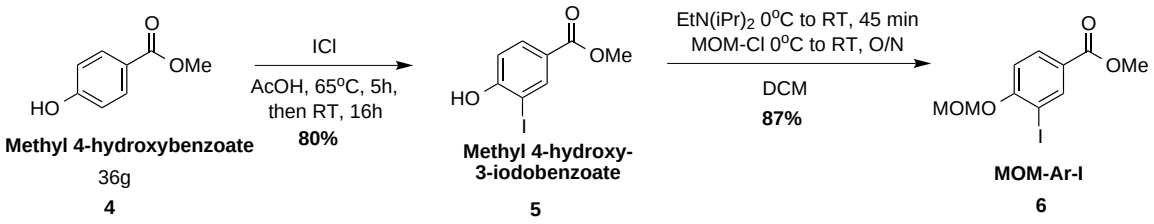

Figure 29: Scheme of the formation of MOM-Ar-I (**6**) used for the synthesis of (**1**) [98, 99].

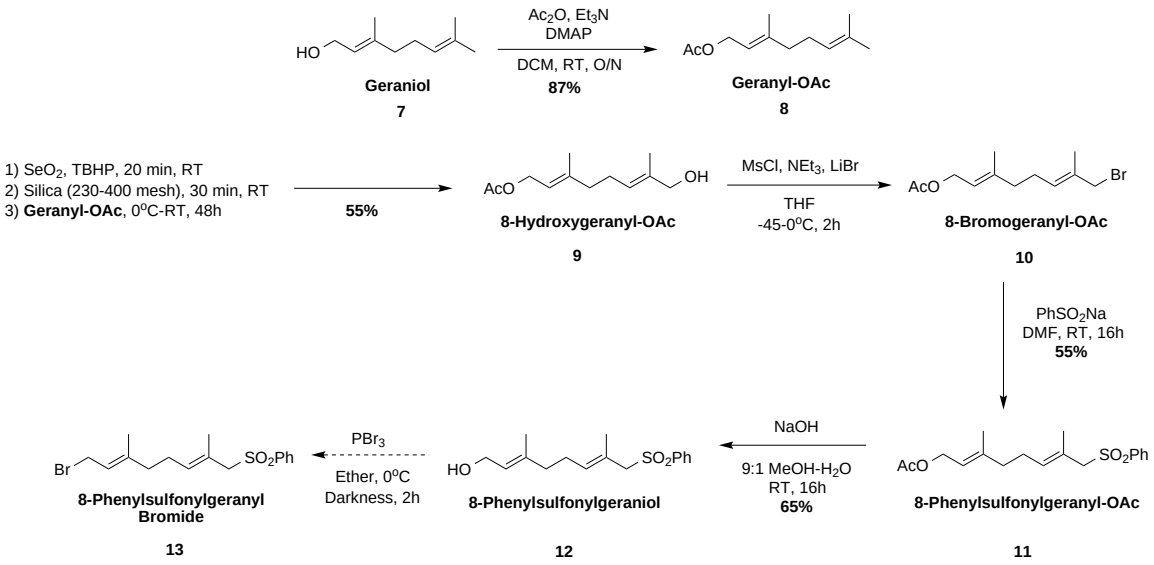

Figure 30: Scheme of the formation of 8-phenylsulfonylgeranyl bromide **13** from geraniol [98, 100, 60, 101, 102, 103, 104].

18. Efforts regarding the use of compound **6** and geranyl bromide (**14**) for copper-mediated aryl allylation [100] resulted in the formation of the desired aliphatic arene (**15**) in 44% yield (Figure 31) [100, 102, 103].

Allylic oxidation of **15** (to form **16**), followed by allylic bromination (forming **17**) and then sulfonation at the allylic position resulted in the formation of compound **18** [100, 102, 103]. However, due to the low yields, primarily due to the allylic oxidation step (forming **16** in 24% yield), the coupling of MOM-Ar-I (**6**) and 8-phenylsulfonyl bromide (**13**) was proposed, as the route to form **13** (Figure 30) [98, 100, 60, 101, 102, 103, 104] allows for the allylic oxidation step to occur earlier in the synthetic pathway, thus potentially resulting in a low-yielding step to lessen its impact on the

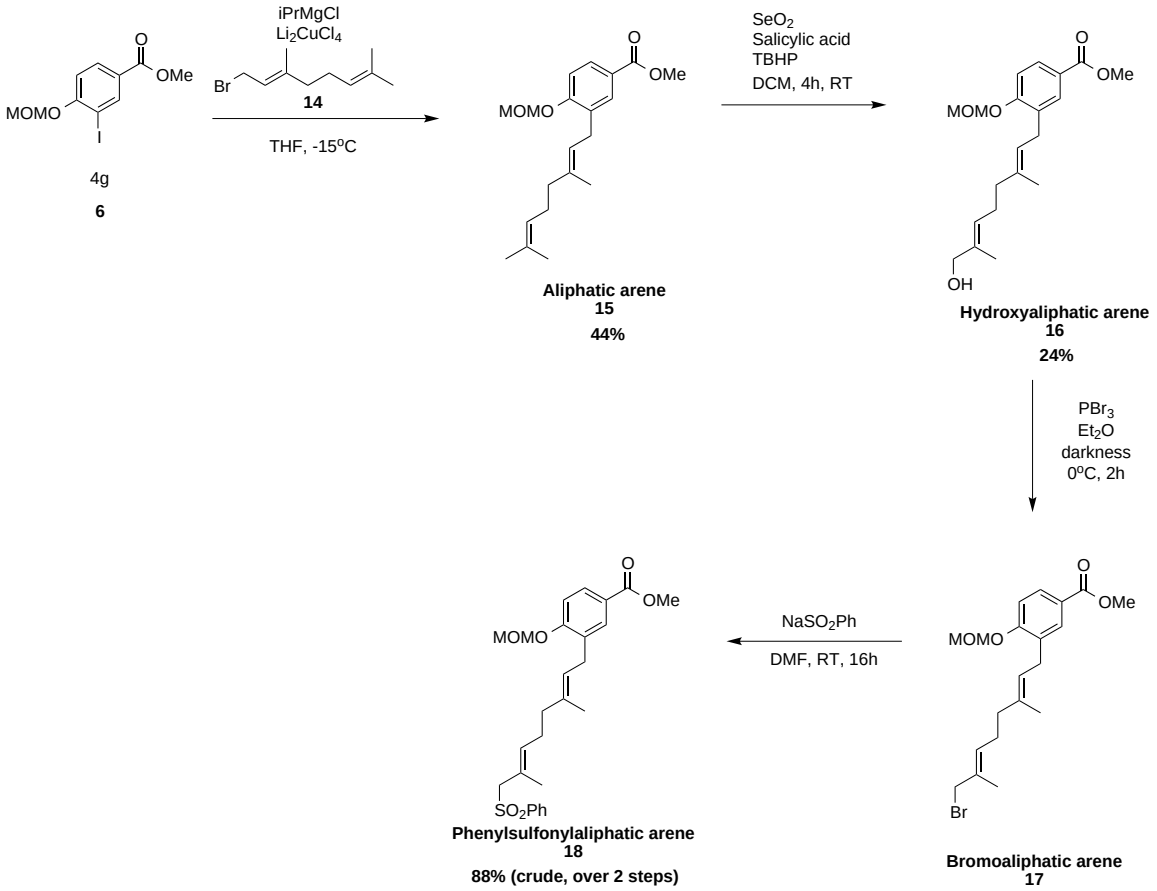

Figure 31: Scheme of the initial proposed synthesis for phenylsulfonylaliphatic arene **18** [100, 102, 103].

overall yield of the target molecule.

3.3.2 Base-promoted epoxide ring-opening (ERO)

Toward synthesizing compound **28**, (2*S*,3*R*)-MOM-epoxylinalool (**21**) was initially synthesized via the Sharpless asymmetric epoxidation of commercially available (*R*)-linalool (**19**), followed by MOM protection of (2*S*,3*R*)-epoxylinalool (**20**) (Figure 32) [105, 99, 106, 107].

Due to the trace quantities obtained from the synthesis of **20**, an alternative route to synthesizing compound **21** was sought. As mentioned in the previous chapter, HKR is a method for synthesizing enantiopure terminal epoxides, which can be used as chiral building blocks in a multitude of reactions [62]. Regarding the synthesis of the

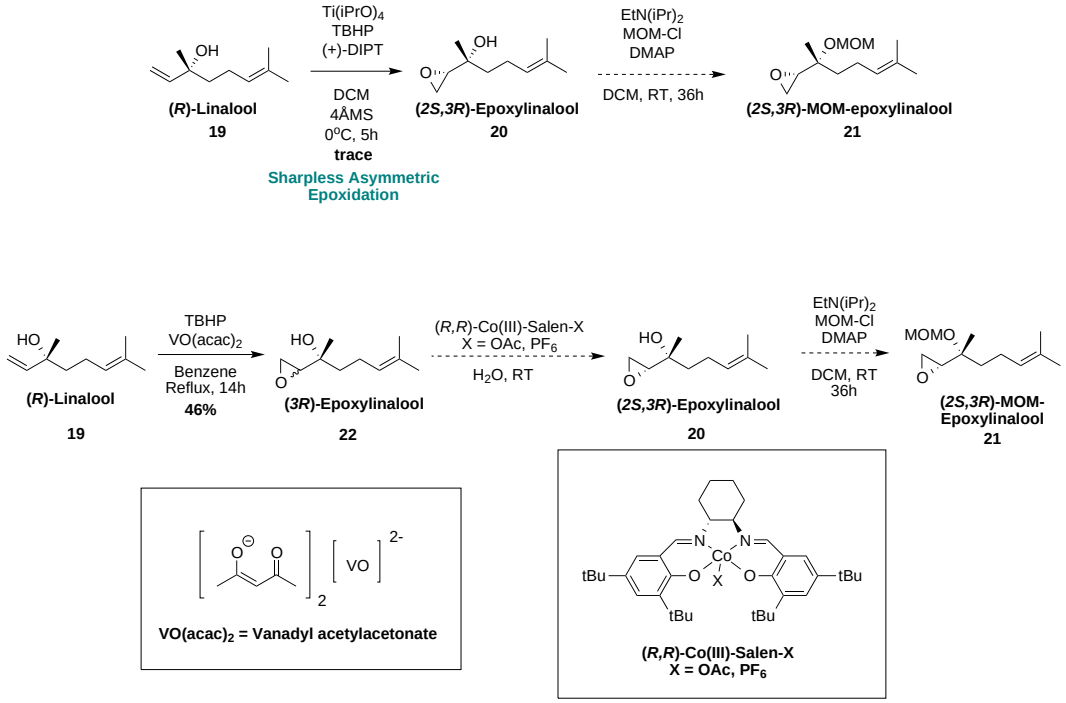

Figure 32: Scheme of the synthesis of (2*S*,3*R*)-MOM-epoxylinalool (**21**) [105, 99, 106, 107].

chiral terminal epoxide **21**, Singh et al. utilized (*R*,*R*)-Co(III)-salen-OAc-catalyzed (Figure 32) [105, 99, 106, 107] HKR for the formation of (*S*)-2-(oxiran-2-yl)propan-2-ol, a 2,3-epoxyalcohol, in 30% yield and 96% ee [107]. Thus, it was proposed that HKR could be used to produce the compound **20**, also a 2,3-epoxyalcohol, with significantly greater yields than with using the Sharpless asymmetric epoxidation. Therefore, the alternative synthesis for **21** was to involve epoxidation of **19** to form racemic **22**, followed by HKR of **22** to form **20**, and then MOM protection would provide **21** (Figure 32) [105, 99, 106, 107]. Prior to synthesizing chiral compound **21**, a model system for the synthesis of compound **26** was investigated to optimize the ERO, as well as the desulfonylation (to form **27**) using ((2-methylallyl)sulfonyl)benzene (**24**) and commercially available racemic styrene oxide (**25**) (Figure 33) [108, 109, 110].

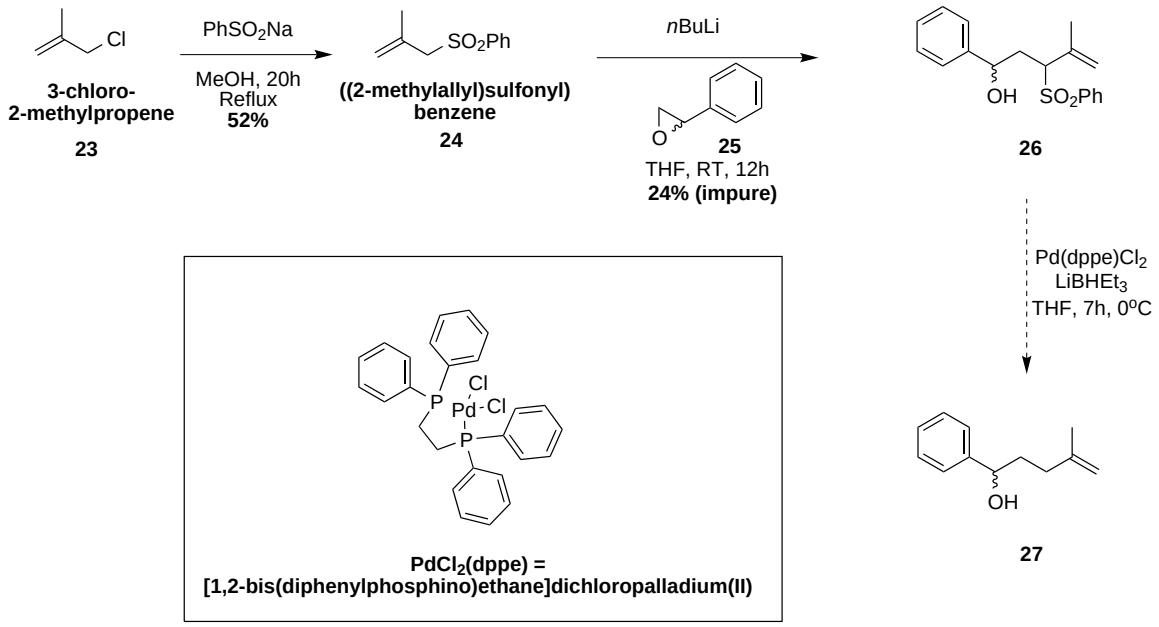

Figure 33: Scheme of the ERO model system, which should result in the formation of compound **27** [108, 109, 110].

Compound **24** was synthesized in moderate yield from commercially available 3-chloro-2-methylpropene (**23**). Then, the ERO reaction was investigated; the reaction conditions are listed in Table 5 [109, 110]. In testing various reaction conditions, it was determined that the reaction conditions [109, 110] displayed in entries 3 and 4 of Table 5 afforded product. However, the yields were low (24%), and the products isolated were determined to be impure by both ^{1}H NMR and ESI-MS. Despite all precautionary measures to prevent exposure of the reaction to air and moisture, reaction yields did not improve. Therefore, further investigations are needed to optimize alkylation via base-promoted ERO to continue to determine the synthetic routes for callophycolide A.

3.4 Conclusions

Routes toward a divergent, modular, multi-gram scalable total synthesis of callophycolide A were sought in an effort to confirm the absolute configuration of the compound previously reported [54], perform a thorough determination of biological

Table 5: Reaction conditions for the ERO model system for the synthesis of callophycolide A [109, 110].

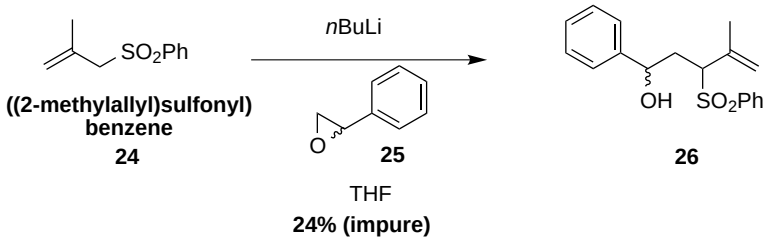

Entry	equiv. **24**	Conc. **24** in THF (M)	equiv. **25**	equiv. *n*BuLi	Conc. THF (M)	Reaction time and temperature	Yield (%)
1	1	neat	1	2.02	0.25	0°C, 1h, then -78°C-RT, 12h	No reaction
2	1	neat	1	1	0.25	0°C, 1h, then -78°C-RT, 12h	No reaction
3	1.21	0.16	1	1.3	0.45	-78°C, 4h	24 (impure)
4	1	neat	1	1	0.25	-78°C, 10m, then RT, O/N	24 (impure)

activity, and determine synthetic steps, as well as intermediates that could be used to synthesize more potent antimalarials isolated from *C. serratus*, such as bromophycolide A. While progress toward this goal was achieved, a thorough, extensive investigation of the optimal conditions for the base-promoted ERO is essential to the success of the total synthesis of callophycolide A. Therefore, our attention was turned toward the total syntheses of alternative diterpenes isolated from *C. serratus* and will later return to optimization of the ERO. Once this step is successful, the focus can be returned to applying HKR to form the enantiopure epoxide **20**; once capped with MOM (forming **21**), it can be utilized for ERO to form compound **28**.

3.5 Experimental

3.5.1 General

Reagents were purchased from commercial vendors and were used as received unless otherwise stated. All starting materials were dried under vacuum prior to use. Anhydrous DCM was distilled from CaH_2, and anhydrous THF was distilled from Na and benzophenone. *n*BuLi (2.5 M in hexanes) was purchased from Sigma-Aldrich

(St. Louis, MO USA) and titrated against *N*-(3-benzylphenyl)pivalamide (recrystallized in hexanes) prior to use. Grignard reagents were titrated against (*E*)-2-((2-phenylhydrazono)methyl)phenol. All glassware was flame dried and placed under a nitrogen atmosphere prior to use. Purification via flash chromatography was performed using silica gel from Dynamic Adsorbents (32-65 μm) and technical grade eluents. Thin-layer chromatography (TLC) was conducted using EMD silica gel 60 F_{254} glass-backed plates. Plate visualization was accomplished using UV light and/or iodine staining. ^{1}H NMR spectra were obtained using either a Varian Mercury Vx spectrometer (300 or 400 MHz) or a Bruker AVII (400 or 500 MHz) spectrometer; the chemical shifts were expressed in ppm and are referenced to the corresponding residual nuclei in the deuterated solvents. ESI-MS and accurate mass was performed using a ThermoFisher Scientific LTQ Orbitrap XL ETD.

3.5.2 Synthesis of compounds to construct callophycolide A

Compounds **5**, **6**, **8-12**, **20-22** and **24** were prepared according to previously published procedures, and the characterization data matched the data previously reported [98, 100, 60, 101, 102, 103, 104, 105, 99, 106, 107, 108].

3.5.3 Synthesis of methyl (*E*)-3-(3,7-dimethylocta-2,6-dien-1-yl)-4-(methoxymethoxy)benzoate (15)

To a solution of compound **6** (4 g, 12.4 mmol) in anhydrous THF (62 mL) was added iPrMgCl (12.6 mL, 1.48 M in THF) dropwise at -15°C. The reaction was then allowed to stir for 1 h. Li_2CuCl_4 (40.9 mL, 0.1M in THF) was then added dropwise, and the reaction was stirred for 30 min. A solution of geranyl bromide (**14**) (2.4 mL, 12.3 mmol) in anhydrous THF was added over a period of 30 min, and the reaction was allowed to stir for an additional 1.5 h. The reaction was then quenched with saturated aqueous NH_4Cl and was allowed to stir until the reaction mixture turned blue. The mixture was then extracted with ether (3X), and the organic layer was washed with

brine, dried using anhydrous Na_2SO_4, and concentrated under reduced pressure [100]. Purification (silica gel and 0-1-2% EtOAc:hexanes) afforded the aliphatic arene **15** as a clear, colorless oil in 44% yield. ^{1}H NMR ($CDCl_3$, 400 MHz) δ 7.87-7.83 (m, 2H), δ 7.11-7.06 (d, 1H), δ 5.32-5.29 (tq, 1H), δ 5.26 (s, 2H), δ 5.12-5.08 (tq, 1H), δ 3.87 (s, 3H), δ 3.47 (s, 3H), δ 3.37-3.35 (d, 2H) δ 2.14-2.03 (m, 4H), δ 1.72 (s, 3H), δ 1.66 (s, 3H), δ 1.59 (s, 3H).

3.5.4 Synthesis of methyl 3-((2*E*,6*E*)-8-hydroxy-3,7-dimethylocta-2,6-dien-1-yl)-4-(methoxymethoxy)benzoate (16)

To a round-bottom flask equipped with a stirbar was added SeO_2 (5.5 mg, 0.05 mmol), salicylic acid (15.2 mg, 0.11 mmol), TBHP (0.6 mL, 5.5M in nonane), and anhydrous DCM (1.25 mL). The above compounds were allowed to stir for 40 min at room temperature. The reaction mixture was then cooled to 0°C; a solution of **15** (332.1 mg, 1.0 mmol) in anhydrous DCM (0.72 mL) was added in one shot, and the reaction mixture was allowed to stir at 0°C for 5 h. The mixture was then washed with saturated aqueous $NaHCO_3$, dried using anhydrous Na_2SO_4, and concentrated under reduced pressure. The crude oil was then dissolved in a 4% MeOH:THF solution and cooled to 0°C. $NaBH_4$ was added in portions, and the reaction mixture was allowed to stir at 0°C for 1 h before being quenched with ice-cold saturated aqueous NH_4Cl. After warming to room temperature, the mixture was extracted with ether (3X), and the organic layer was washed with brine, dried using anhydrous Na_2SO_4, and concentrated under reduced pressure [102]. Purification (silica gel and 2-5-7-10-15-20% EtOAc:hexanes) provided **16** in 24% yield. ^{1}H NMR ($CDCl_3$, 300 MHz) δ 7.88-7.82 (m, 2H), δ 7.09-7.05 (d, 1H), δ 5.45-5.38 (tm, 1H), δ 5.37-2.59 (tm, 1H), δ 5.27 (s, 2H), δ 3.98 (s, 2H), δ 3.88 (s, 3H), δ 3.48 (s, 3H), δ 3.39-3.34 (d, 2H) δ 2.24-2.06 (m, 4H), δ 1.71 (s, 3H), δ 1.65 (s, 3H).

3.5.5 Synthesis of methyl 3-((2*E*,6*E*)-8-bromo-3,7-dimethylocta-2,6-dien-1-yl)-4-(methoxymethoxy)benzoate (17)

In a round-bottom flask equipped with a stirbar, the hydroxyaliphatic arene (**16**) (79.6 mg, 0.23 mmol) was dissolved in anhydrous ether (0.71 mL) and cooled to 0°C. PBr_3 was added dropwise (0.01 mL, 0.091 mmol), and the reaction was stirred for 2 h in the dark. After warming to room temperature, the reaction mixture was poured slowly into saturated aqueous $NaHCO_3$ and then washed with saturated aqueous $NaHCO_3$, dried using anhydrous $MgSO_4$, concentrated under reduced pressure, dried under vacuum and carried forward to the next step without further purification [100].

3.5.6 Synthesis of methyl 3-((*2E,6E*)-3,7-dimethyl-8-(phenylsulfonyl)octa-2,6-dien-1-yl)-4-(methoxymethoxy)benzoate (phenylsulfonylaliphatic arene, (18))

A solution of bromoaliphatic arene (**17**) (14.2 mg, 0.035 mmol) in anhydrous DMF (0.07 mL) was added to $NaSO_2Ph$ (5.7 mg, 0.035 mmol) at room temperature, and then the solution was stirred for 16 h at room temperature. The organic compounds were extracted with EtOAc (2X); the organic layer was then washed with H_2O and brine, dried over anhydrous $MgSO_4$, and concentrated under reduced pressure [103] to afford the crude compound **18** in 88% yield (over 2 steps).

3.5.7 Synthesis of 4-methyl-1-phenyl-3-(phenylsulfonyl)pent-4-en-1-ol (26)

3.5.7.1 Method A

Compound **24** (198.0 mg, 1.0 mmol) was dissolved in anhydrous THF (6.3 mL) and cooled to -78°C. *n*BuLi (0.46 mL, 2.35 M in hexanes) was added dropwise, and the reaction was allowed to stir for 2.5 h. A solution of racemic styrene oxide **25** (0.1 mL, 0.83 mmol) in anhydrous THF (1.8 mL) was added, and the reaction was allowed to stir for an additional 1.5 h. The reaction was then quenched with a 1:1 mixture of MeOH:ether. After warming to room temperature, the reaction mixture was extracted with ether (3X), and then the organic layer was washed with brine,

dried using anhydrous Na_2SO_4, and concentrated under reduced pressure [110]. Purification (silica gel and 10-15-20% EtOAc:hexanes) afforded impure compound **26** as a clear, colorless oil in 24% yield. ^{1}H NMR ($CDCl_3$, 400 MHz) δ 7.94-7.76 (m, 2H) δ 7.66-7.60 (m, 1H), δ 7.56-7.49 (m, 2H), δ 7.38-7.27 (m, 5H), δ 5.15 (s, 1H), δ 4.87 (s, 1H), δ 4.64-4.60 (dd, 1H), δ 4.09-4.04 (dd, 1H) δ 2.57-2.43 (m, 1H), δ 2.23-2.09 (m, 1H), δ 2.05 (s, 1H), δ 1.77 (s, 3H). HRMS (ESI) $[M + Na]^+$ Calc for $C_{18}H_{20}O_3SNa$, 339.1025, found 339.1023.

3.5.7.2 Method B

Compound **24** (167.3 mg, 0.83 mmol) was dissolved in anhydrous THF (3.3 mL) and cooled to -78°C. *n*BuLi (0.31 mL, 2.71 M in hexanes) was added dropwise, and the reaction was allowed to stir for 10 min. Racemic styrene oxide **25** (0.1 mL, 0.83 mmol) was added, and the reaction was allowed warm to room temperature and stir overnight. The reaction was then quenched with a 1:1 mixture of MeOH:ether. After warming to room temperature, the reaction mixture was extracted with ether (3X), and then the organic layer was washed with brine, dried using anhydrous Na_2SO_4, and concentrated under reduced pressure [110]. Purification (silica gel and 0-0.5-1-2-5-7% MeOH:DCM) afforded impure compound **26** as a clear, colorless oil in 24% yield. ^{1}H NMR ($CDCl_3$, 400 MHz) δ 7.93-7.76 (m, 2H) δ 7.66-7.60 (m, 1H), δ 7.57-7.48 (m, 2H), δ 7.38-7.27 (m, 5H), δ 5.15 (s, 1H), δ 4.87 (s, 1H), δ 4.64-4.59 (dd, 1H), δ 4.09-4.03 (dd, 1H) δ 2.58-2.42 (m, 1H), δ 2.25-2.14 (m, 1H), δ 2.05 (s, 1H), δ 1.77 (s, 3H).

3.6 Acknowledgements

This study was funded by the Blanchard Assistant Professor Fellowship and by the Graduate Assistance in Areas of National Need (GAANN) fellowship. Mr. Kedar Perkins, Ms. Kymberlee Osborne, and Mr. Angel Cobos are also acknowledged for experimental assistance.

CHAPTER IV

PROGRESS TOWARD THE SYNTHESES OF CALLOPHYCOIC ACIDS G AND H, ANTIBACTERIAL DITERPENE-BENZOIC ACIDS

4.1 Introduction

Callophycoic acids are diterpene-benzoic acids that were also isolated from *C. serratus*, a Fijian red macroalgae (Figure 34) [55, 56]. These compounds were characterized via X-ray crystallography, MS, and NMR by Lane et al. and are the first examples of diterpene-benzoic acids observed in macroalgae [55]. In addition, they display modest antibacterial activity, namely, callophycoic acids G and H (IC_{50} for callophycoic acid G = 31.9 μM against *S. aureus*; 63.9 μM against *E. faecium*; for callophycoic acid H = 27.4 μM against both *S. aureus* and *E. faecium* >10-63.9 μM) [55].

Structurally, although all callophycoic acids share the benzoic acid moiety, G and H significantly differ in that they do not contain a fused tricyclic diterpene-benzoic acid (Figure 34, in red) [55]. Instead, callophycoic acids G and H consist of a *trans*-decalin moiety (Figure 34, in blue) [55]. With regard to the terpene head, callophycoic acids G and H also differ from callophycoic acids A-F in that G and H contain an isoprene tail, whereas the other callophycoic acids consist of either a monoterpene (A and B), a bromocyclohexanol (C and D), a methylenebromocyclohexane (E), or a sesquiterpene (F) unit (Figure 34, in purple) [55]. However, callophycolides G and H do consist of the same *trans*-decalin core as callophycols A and B (Figure 34, in blue) [55]. Due to this common *trans*-decalin core, a divergent total synthesis can be envisioned for callophycoic acids G and H and callophycols A and B. Using the common *trans*-decalin precursor **40** (Figure 35), as the acetate and acetal moieties

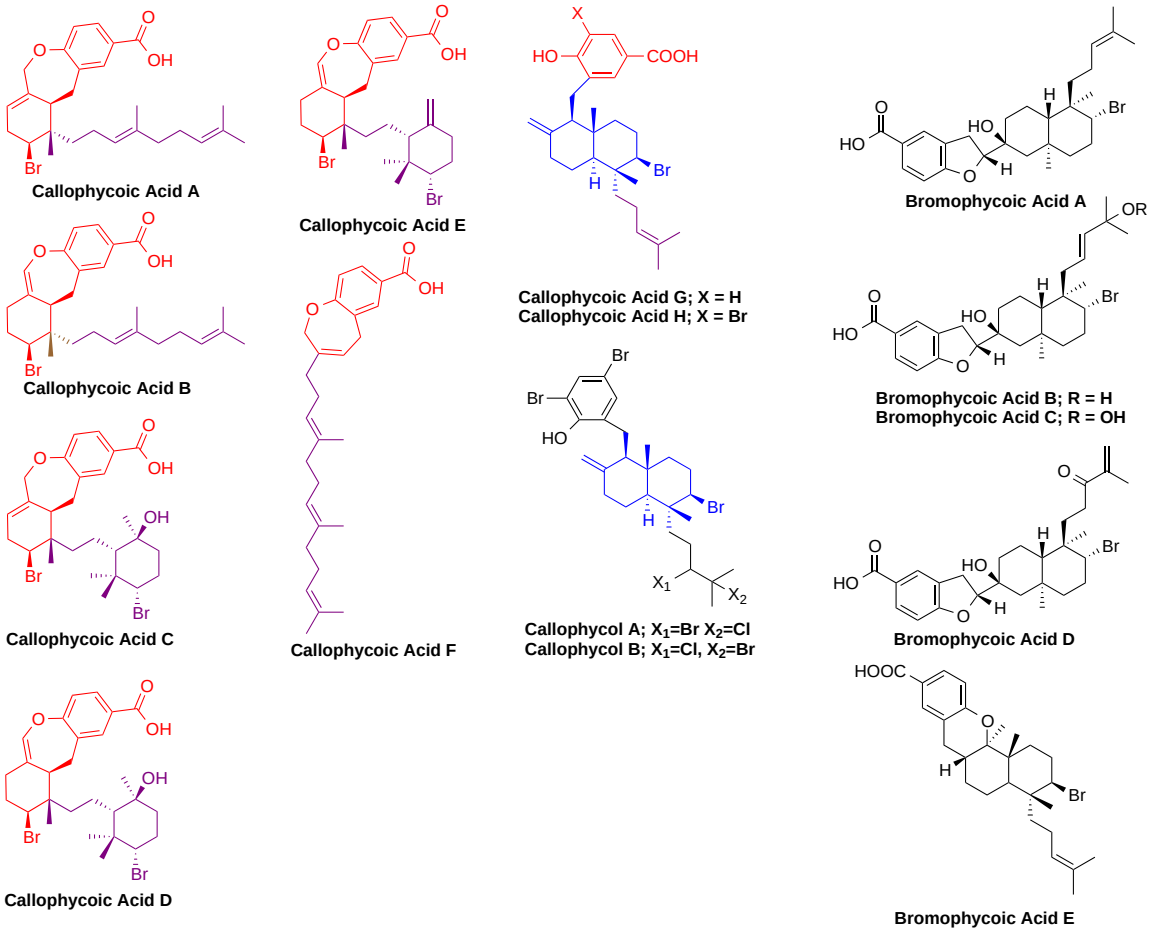

Figure 34: Structural comparisons of callophycoic acids and callophycols isolated from *C. serratus* [55, 56].

would lead to functionalization to introduce the appropriate aryl groups for all four metabolites, as well as to introduce the trisubstituted olefin (callophycoic acids G and H) or vicinal dihalide (callophycols A and B) moieties, this synthetic approach is modular in nature (Figure 35). As a result of these synthetic pathways, they could also provide access to novel antibacterial agents, as bromophycoic acids A and E also display modest activity against bacteria (IC_{50} = 1.6 μg/mL for Methicillin-resistant *Staphylococcus aureus* (MRSA) for bromophycoic acid A; 1.6 μg/mL for Vancomycin-resistant *Enterococcus faecium* (VREF)) in addition to accessing other compounds that display modest activity against malaria, such as callophycols A and

B and bromophycoic acid D (IC_{50} = 35.7 μM, 40.4 μM, and 8.7 μM, respectively) [55, 56]. Herein, postulated pathways to synthesize callophycoic acids G and H and callophycols A and B are presented here, taking advantage of accessing a common *trans*-decalin moiety (Figure 35), which will be discussed below.

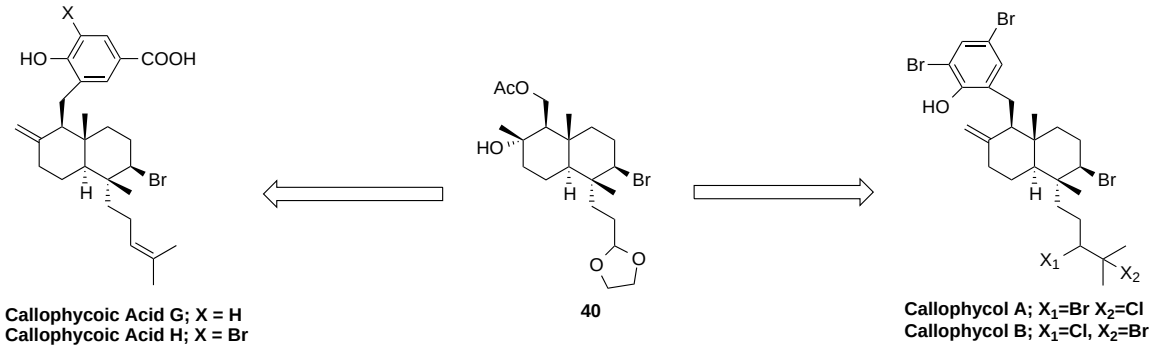

Figure 35: Depiction of the common *trans*-decalin core to access callophycoic acids G and H and callophycols A and B.

4.2 Retrosynthetic analyses of callophycoic acids G (2) and H (3)

A retrosynthetic route to callophycoic acids G (**2**) and H (**3**), is shown in Figure 36. These target molecules can be synthesized via a Wittig reaction between triphenyl(propan-2-ylidene)-λ^5-phosphane and either aldehyde **41** or **42**. Aldehyde **41** or **42** can be formed by a cross-coupling reaction of arene **7** or **10**, respectively, to compound **40**. Compound **40**, which is a common intermediate to access callophycols A and B, can be synthesized through a bromonium-induced cation-pi cyclization of compound **39**. Compound **39** can be formed by an oxidative cleavage reaction of epoxide **27**, which is formed via a bromohydrin reaction of geranylgeranyl acetate (**25**), followed by epoxidation. Finally, geranylgeranyl acetate can be formed via the Pd-catalyzed isomerization of commercially available, inexpensive geranyllinalool (**23**).

4.3 Results and Discussion

4.3.1 Synthesis of 3-bromo-4-(methoxymethoxy)benzoic acid (7) and 3,5-dibromo-4-(methoxymethoxy)benzoic acid (10)

Compound **7** was formed in three steps using the commercially available 3-bromo-4-hydroxybenzoic acid **4** (Figure 37) [111, 112, 113]. Specifically, transesterification of **4** formed compound **5**; MOM protection of the phenol group formed compound **6**, all in high yields. Saponification of **6** formed **7** in moderate yield (42%) [111, 112, 113], which will later be used in the endgame of the synthesis of callophycoic acid G. Similarly, compound **10** can also be formed via bromination of compound **5**, followed by protection of the phenol (to form **9**) and then saponification to give compound **10**, which can be used for the synthesis of callophycoic acid H (Figure 37) [111, 112, 113].

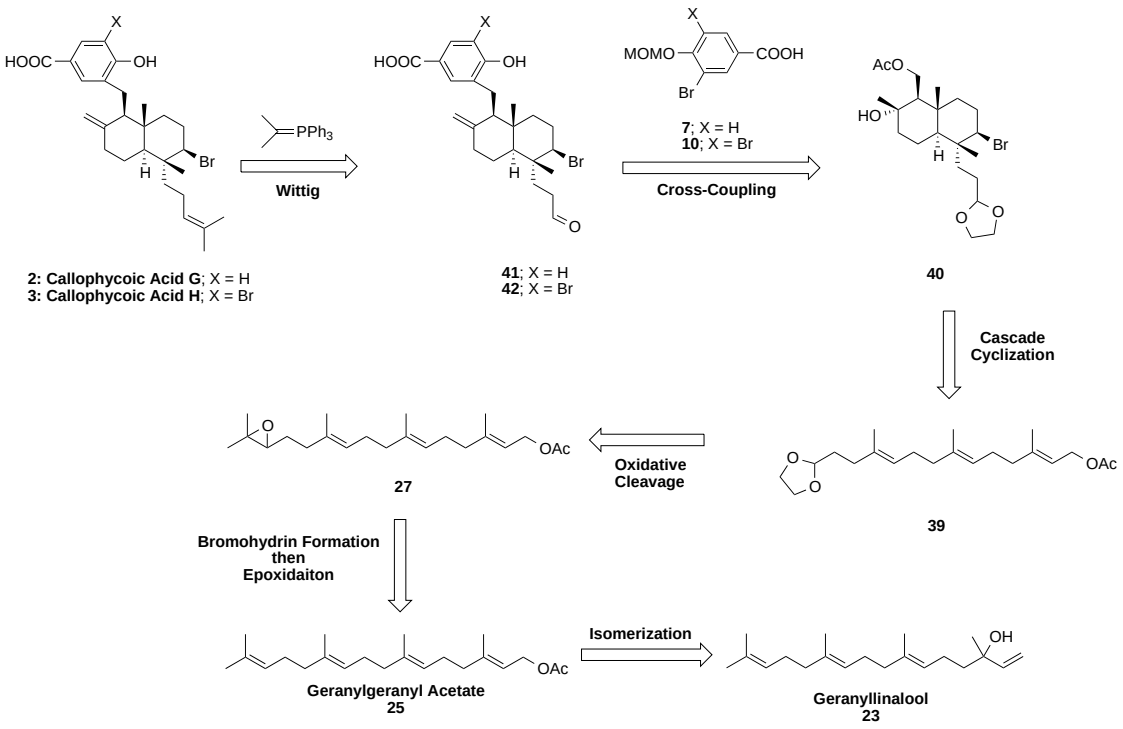

Figure 36: Initial retrosynthetic analysis of callophycoic acids G (**2**) and H (**3**).

4.3.2 Synthesis of (2*E*,6*E*,10*E*)-14-((*tert*-butyldiphenylsilyl)oxy)-3,7,11-trimethyltetradeca-2,6,10-trien-1-yl acetate (54): the precursor to the *trans*-decalin core

Initial attempts at forming the precursor to the *trans*-decalin core of callophycoic acids G and H and callophycols A and B involved the use of dioxolane **39** (Figure 38) [114, 115, 59, 116, 117, 118]. Attempts to form compound **39** using a Horner-Wadsworth-Emmons reaction involving phosphonate **13** and aldehyde **14** (synthesized in three steps from commercially available farnesyl acetate (**19**) (Figure 39) [119, 120] were investigated. Many reaction conditions were examined using various bases, such as *n*BuLi, LDA, NaOH, NaOEt, and $NaNH_2$; the use of *n*BuLi with additive appeared to be promising (Figure 40) [121]; however, ^{1}H NMR showed a product that was the

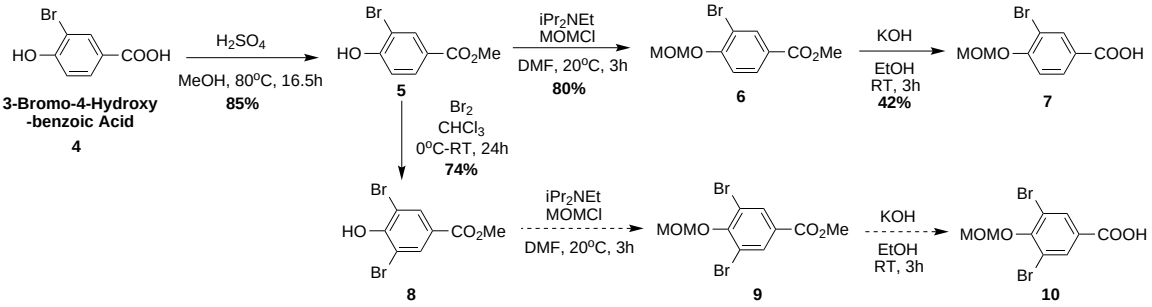

Figure 37: Synthesis of 3-bromo-4-(methoxymethoxy)benzoic acid **7** and 3,5-dibromo-4-(methoxymethoxy)benzoic acid (**10**) [111, 112, 113].

result of nucleophilic addition to the carbonyl groups on the molecule.

After evaluating a simpler model system using phosphonate **13** and benzaldehyde **21**, as shown in Figure 40 [121], it was concluded that the benzaldehyde was indeed undergoing nucleophilic addition via *n*BuLi (thus not forming compound **22**); therefore, other avenues were investigated toward obtaining compound **39**.

Rather than synthesizing the farnesyl acetate trisnoraldehyde **14** and priming it for nucleophilic attack to form the desired farnesyl derivative (dioxolane **39**), a more straightforward approach was proposed that initially involved starting with the commercially available (2*E*,6*E*,10*E*)-geranylgeraniol. However, due to the cost of geranylgeraniol ($519 per 1 g [122]), the less expensive geranyllinalool (**23**, $8.68 per 1 g [123]) was used as the starting material instead. Evaluating the forward synthesis (Figure 41) [124, 125, 119, 126, 127, 128, 129], the hydroxyl group of commercially available geranyllinalool (**23**) was protected with an acetyl group, thus forming geranyllinalyl acetate (**24**) in moderate yield (67%) [124].

Pd-catalyzed isomerization of **24** produced geranylgeranyl acetate **25** in high yield [124]. Subjecting compound **25** to *N*-bromosuccinimide (NBS) in aqueous solution formed bromohydrin **26**, which was then treated with 1,8-diazabicyclo[5.4.0]undec-7-ene (DBU) to form epoxide **27** in moderate yield (42% over two steps) [125, 119, 126]. Oxidative cleavage of **27** produced aldehyde **28** in high yield (75%) [126, 127].

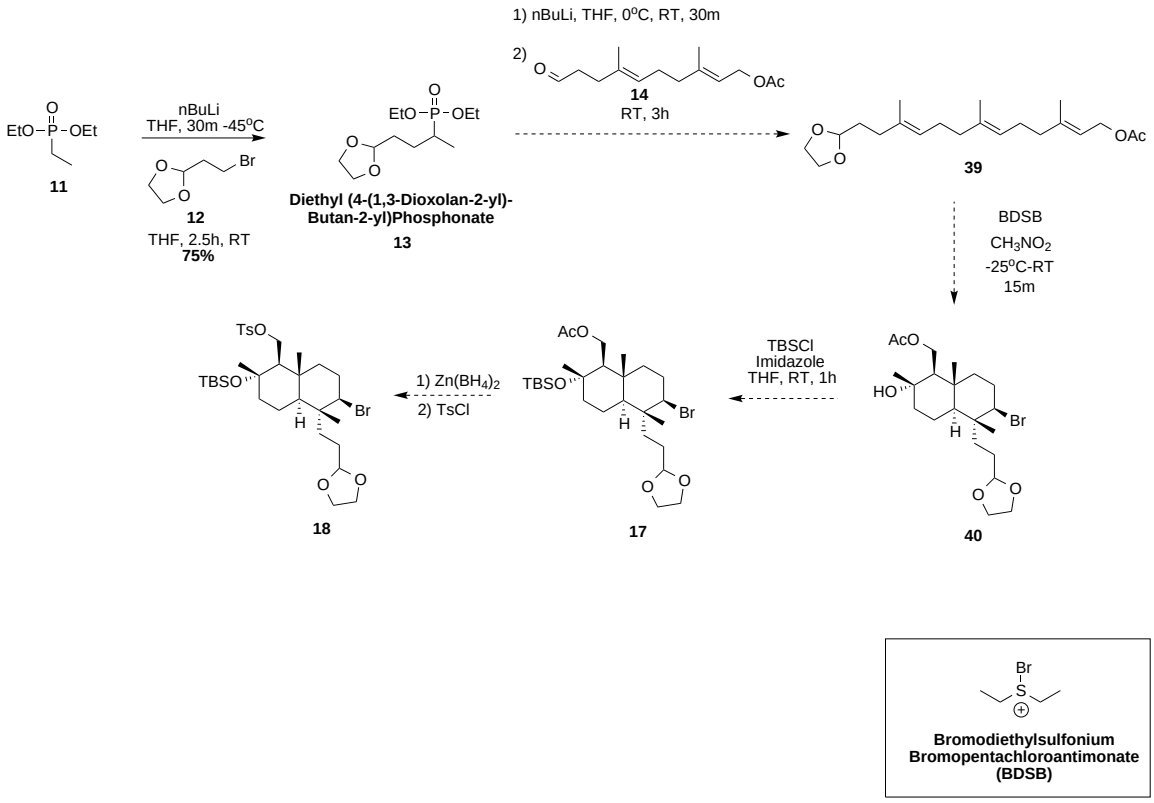

Figure 38: Synthesis of (2*E*,6*E*,10*E*)-13-(1,3-dioxolan-2-yl)-3,7,11-trimethyltrideca-2,6,10-trien-1-yl acetate **18** [114, 115, 59, 116, 117, 118].

Aldehyde **28** was originally going to be protected with a dioxolane group (compound **39**) prior to the cascade cyclization reaction (Figure 41) [124, 125, 119, 126, 127, 130, 59]. However, subjecting dioxolane **39** did not result in the formation of compound **40**; instead, the BDSB activated the dioxolane, which resulted in deprotection to give aldehyde **28** (Figure 42), as is reflected in the ^{1}H NMR spectra. Therefore, other protecting groups were sought that would be more stable under the reaction conditions, such as a silyl group. Thus, reduction of aldehyde **28** (producing alcohol **29**, 71% yield), followed by the protection of the alcohol, thus forming a TBDPS-protected ether, gave compound **30** in high yield (79%) (Figure 43) [124, 125, 119, 126, 127, 128, 129].

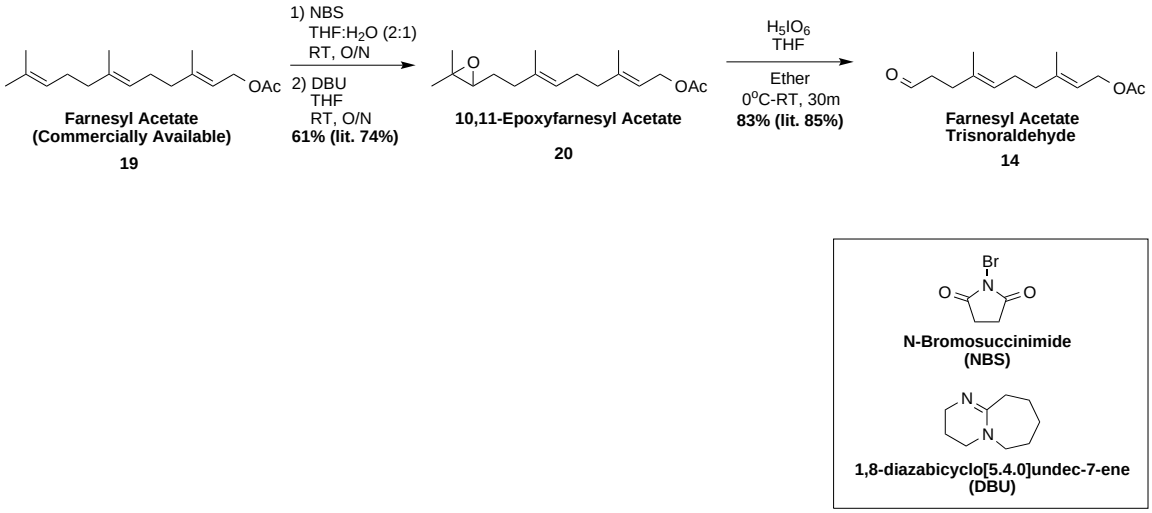

Figure 39: Synthesis of farnesyl acetate trisnoraldehyde **14** [119, 120].

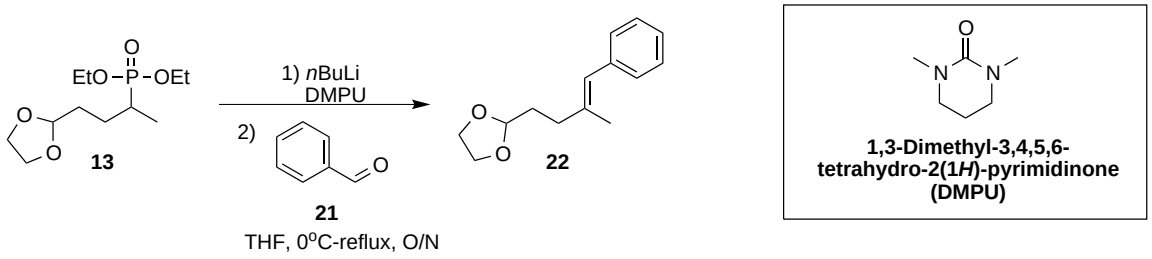

Figure 40: Model system for determination of the conditions for the Horner-Wadsworth-Emmons step of the synthetic pathway [121].

4.3.3 Synthesis of (1*R*,4a*S*,5*R*,6*R*,8a*R*)-6-bromo-5-(3-((*tert*-butyldiphenylsilyl)oxy)propyl)-5,8a-dimethyl-2-methylenedecahydronaphthalene-1-carbaldehyde (32)

With compound **30** in hand, formation of the *trans*-decalin core was investigated. It was proposed that callophycoic acids G and H, as well as callophycols A and B, most likely underwent a sequence of hydride shifts, followed by addition and elimination reactions, which are charasterictic of the biosynthesis of isoprenoids [131]. The aforementioned series of reactions resulted in the halogenation of the compounds at their electrophillic sites that can be obtained via vanadium haloperoxidase-based biosynthetic enzymes that are commonly involved in the biosynthesis of terpenoids [58]. To

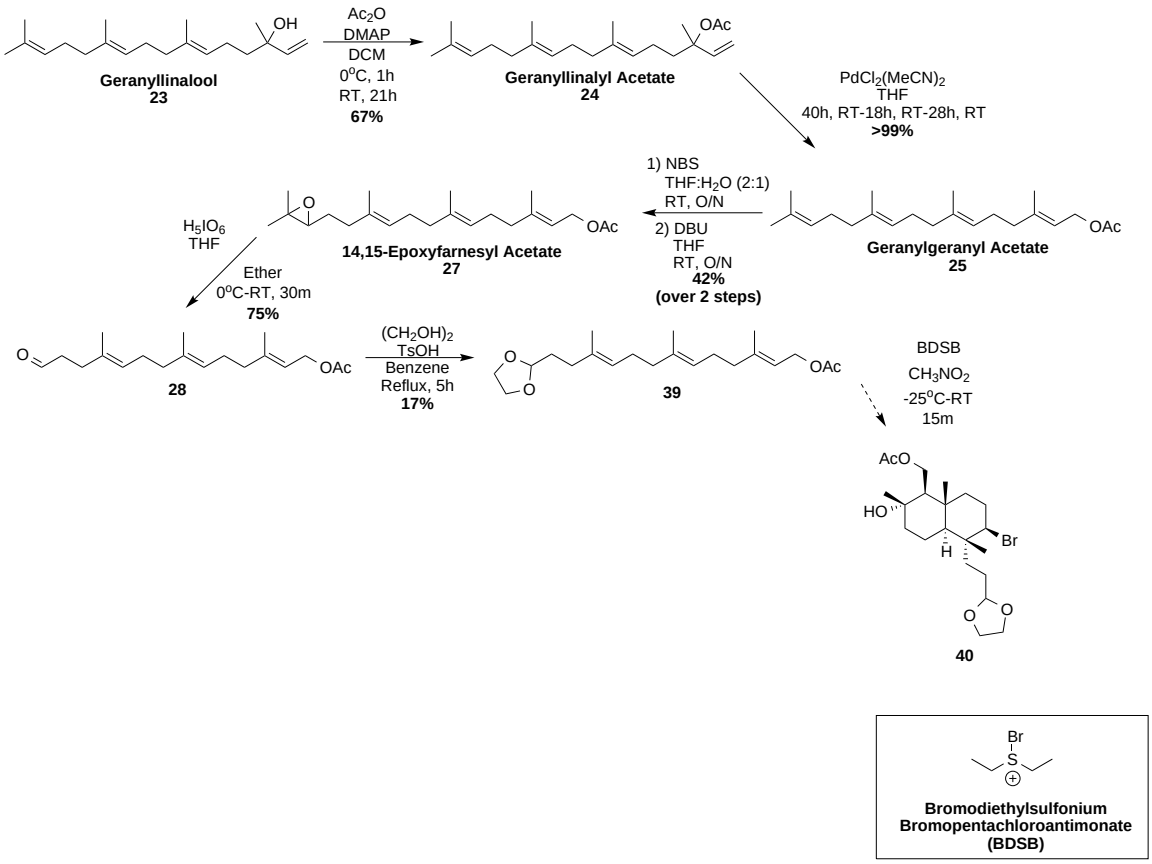

Figure 41: Synthesis of ((1*R*,2*S*,4a*S*,5*R*,6*R*,8a*R*)-5-(2-(1,3-dioxolan-2-yl)ethyl)-6-bromo-2-hydroxy-2,5,8a-trimethyldecahydronaphthalen-1-yl)methyl acetate (**40**) using dioxolane **39ald**, which was synthesized from geranyllinalool (**23**)[124, 125, 119, 126, 127, 130, 59].

circumvent the issue of poor stereoselectivity observed using vanadium haloperoxidases, bromodiethylsulfonium bromopentachloroantimonate(V) (BDSB), which has been used in the formation of stereospecific cation-pi cascade cyclizations, will be applied to the syntheses in the current study [59].

Specifically, the Snyder group had applied these cation-pi cascade cyclizations to the total syntheses of (both racemic and structurally revised) peyssonol A [132, 133], peyssonoic acid A [134], as well as a formal total synthesis of aplysin-20 [135, 136], all of which include the same or similar *trans*-decalin core [59] as callophycoic acids G and H and callophycols A and B (Figure 45) [59, 132, 133, 134, 135, 136].

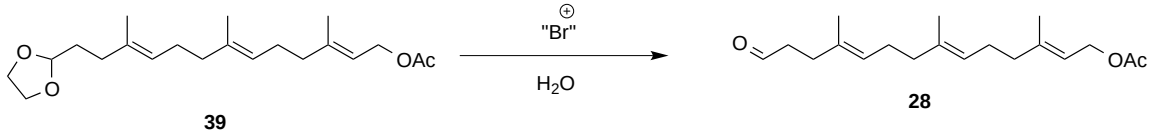

Figure 42: Depiction of the BDSB activation of dioxolane **39** to form aldehyde **28**.

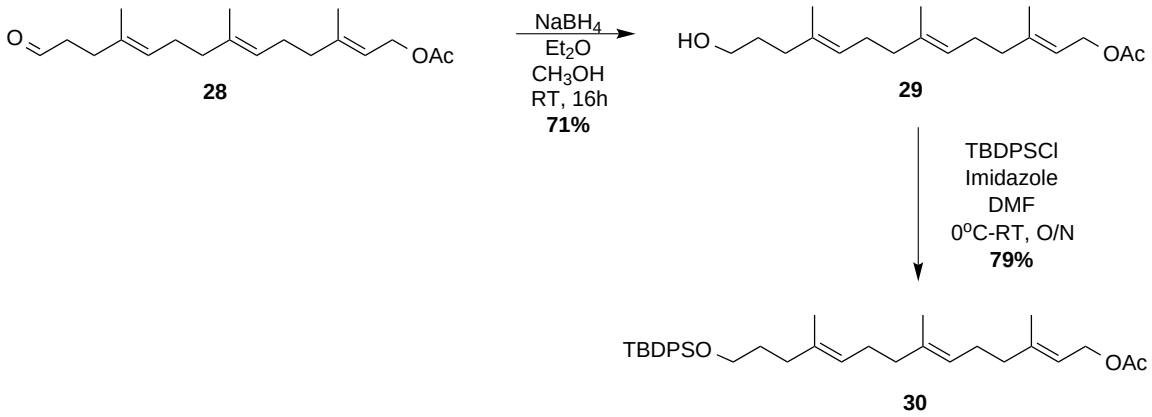

Figure 43: Synthesis of the *trans*-decalin precursor (2*E*,6*E*,10*E*)-14-((*tert*-butyldiphenylsilyl)oxy)-3,7,11-trimethyltetradeca-2,6,10-trien-1-yl acetate (**30**) [124, 125, 119, 126, 127, 128, 129].

Therefore, it was proposed that the *trans*-decalin core for callophycoic acids G and H (compound **32**) could also be synthesized via a bromonium-induced cation-pi cyclization using BDSB. Thus, compound **30** was subjected to BDSB in nitromethane and purified via preparative TLC (PTLC) to give crude compound **32** in low yield (Figure 44).

4.3.4 Proposed endgame of the total syntheses of callophycoic acids G (2) and H (3).

Upon the synthesis of compound **32**, approaches to the endgame of the synthesis of callophycoic acids G and H were investigated. Originally, it was proposed that upon formation of a *trans*-decalin core common to all four metabolites (compound **40**, Figure 38), protection of the tertiary alcohol using TBS (to form **17**), followed by deacetylation and subsequent tosylation of the resulting primary alcohol (forming **18**),

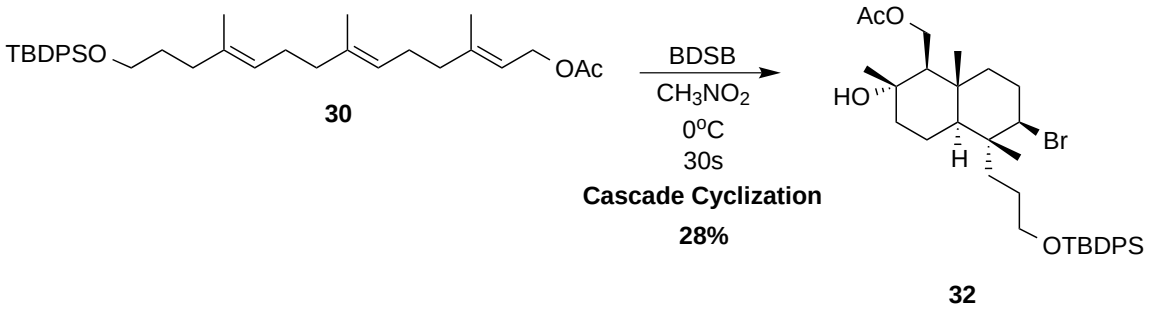

Figure 44: Cascade cyclization to form compound **32** [59].

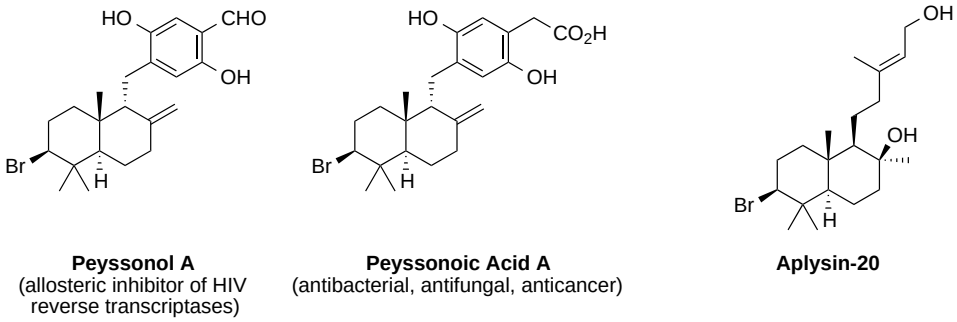

Figure 45: Natural products synthesized by Snyder's group, all containing a similar *trans*-decalin core [59, 132, 133, 134, 135, 136].

and organocuprate cross-couping would give the *trans*-decalin benzoate compounds **43** and **44**, as shown in Figures 38 [114, 115, 59, 116, 117, 118] and Figure 46 [59, 137, 120, 138, 139, 140].

Acid hydrolysis (forming **45** or **46**), followed by a Wittig reaction (forming **47** or **48**), silyl ether deprotection (forming **49** or **50**), and finally dehydration would provide the target molecules **2** and **3**.

However, upon further investigation of Snyder's syntheses of peyssonol A (Figure 45) [59, 132, 133, 134, 135, 136], it was proposed that this methodology to form peyssonol A could be applied to compounds **2** and **3**. To explore this possibility, a model system was established to optimize the endgame, as shown in Figure 47 [59].

Compounds **51 - 53** were synthesized according to previously published procedures [59]. With aldehyde **53** in hand, it was subjected to nucleophilic addition of lithiated

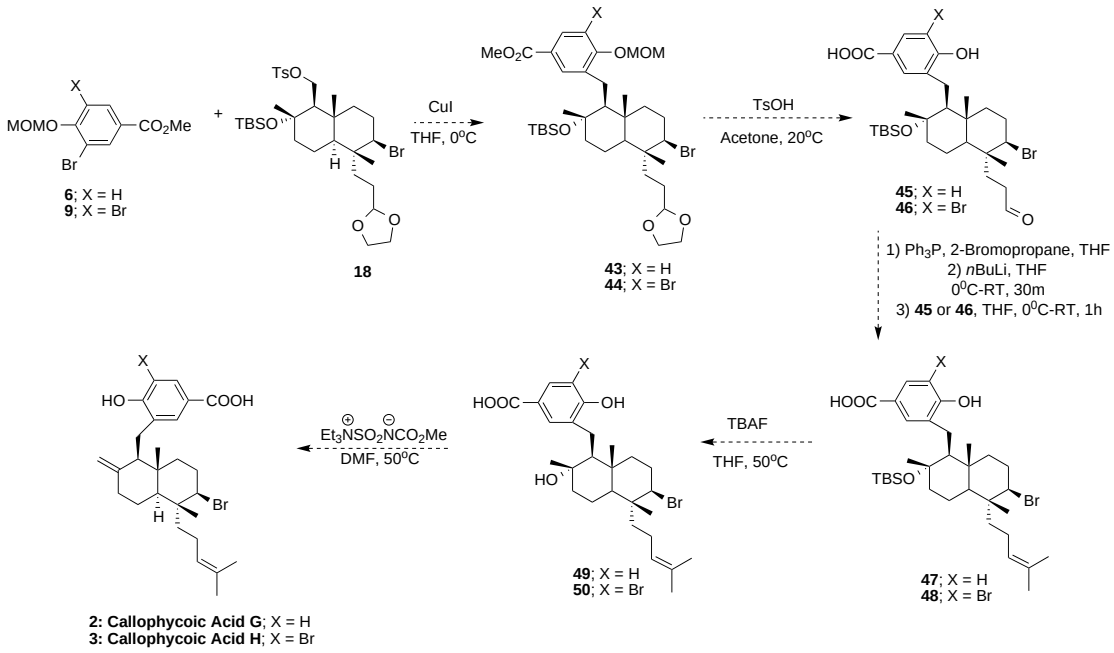

Figure 46: Initial proposed endgame for the syntheses of callophycoic acids G and H [59, 137, 120, 138, 139, 140].

arene **7** to potentially give compound **54**. Removal of the hydroxyl group should provide the model system target **56** for callophycoic acid G [59]. Note that aldehyde **53** can also undergo nucleophilic attack by lithiated arene **10** to provide the model system target for callophycoic acid H (**57**).

Specifically, optimization of coupling the benzoic acid moieties is in progress. The nucleophilic addition method used by Snyder et al. in the synthesis of peyssonol A, in which they used a 1,4-dibromo-2,5-bis(methoxymethoxy)benzene [59], could not be applied to our system with benzoic acid **7**, even with 2.1 equivalents of *n*-BuLi to circumvent the sole deprotonation of the benzoic acid; ^{1}H NMR analysis alluded to a symmetrical arene, which does not correspond to the desired product. Therefore, it

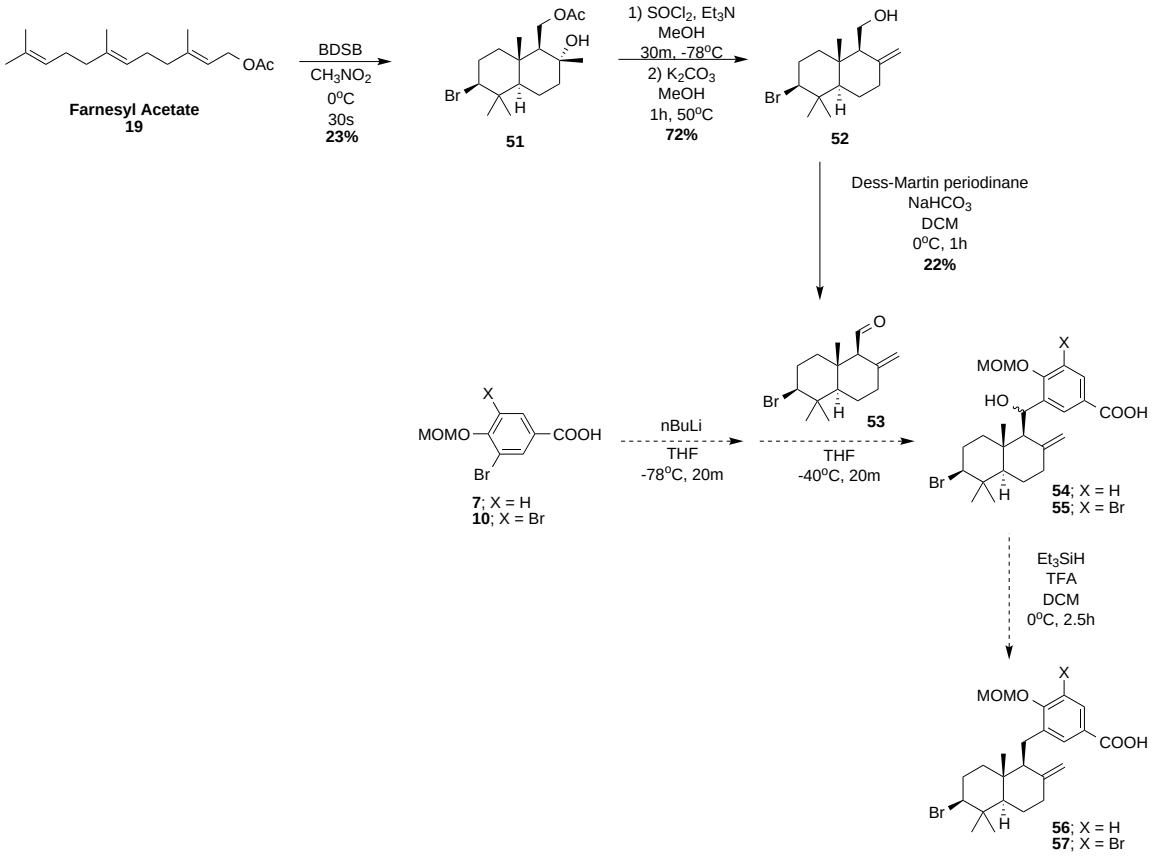

Figure 47: Model system for the endgame of the syntheses of callophycoic acids G and H [59].

is proposed that the methyl benzoate moiety (**6** or **9**) be reduced to a benzyl alcohol (**19** or **20**) [141], followed by subsequent protection by converting it to a TBS ether (**21** or **22**) (Figure 48) [**?**, 116]. Once these compound are synthesized, they can be utilized for the synthesis of the model targets (**37** and **38**) for callophycoic acids G and H (Figure 59) [59, 141]. Thus far, compounds **19** and **21** were synthesized in moderate to high yields (99% and 59%, respectively) [**?**, 116].

Once the model system is established and optimized, it can be applied to the target molecules **2** and **3** (Figures 44 and 50). Swern elimination of **32** followed by deacetylation should give compound **33**. Oxidation of **33** using Dess-Martin periodinane should give compound **34**; note that compound **34** can be used to synthesize

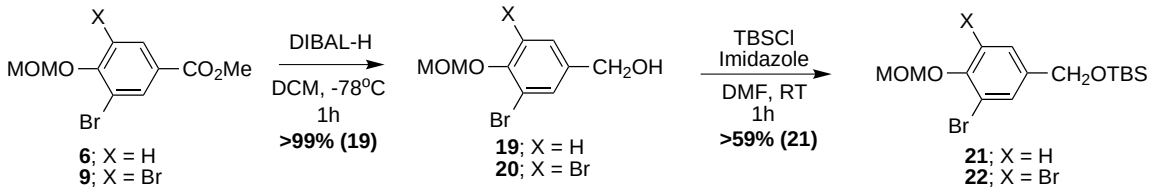

Figure 48: Alternative arene for the model system for the endgame of the syntheses of callophycoic acids G and H [**?**, 116].

callophycoic acids G and H and callophycols A and B. Nucleophilic addition to **34** using either **7** or **10** gives benzyl alcohol **35** or **36**, and hydroxyl removal should give compounds **37** or **38** (Figure 44) [59]. Deprotection (forming **39** or **40**), followed by a Swern oxidation (to form **41** or **42**), and a Wittig reaction, should provide target molecules **2** and **3** (Figures 49 and 50) [59, 120].

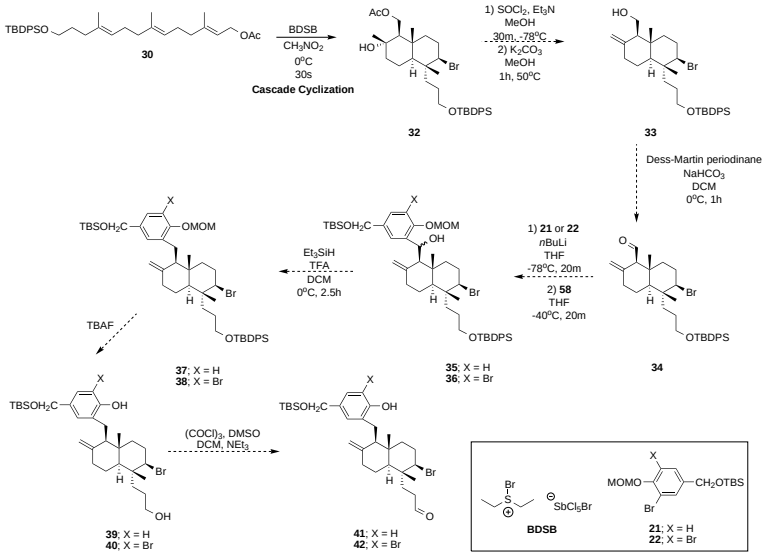

Figure 49: Synthesis of compounds **41** and **42** [59, 120].

4.4 Conclusions

Routes toward divergent, modular, total syntheses of callophycoic acids G and H, as well as callophycols A and B were sought in an effort to provide synthetic alternatives to obtaining these biologically active metabolites. Thus far, *trans*-decalin precursor

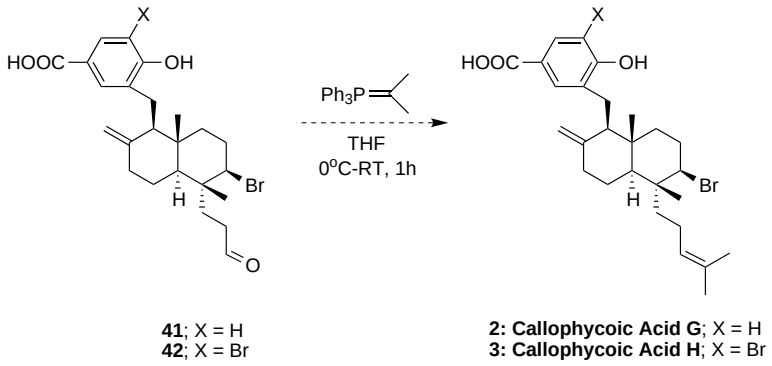

Figure 50: Endgame for callophycoic acids G and H [120].

30 has been effectively synthesized (Figure 44) [59]. Investigations are currently underway to purify *trans*-decalin precursor **32** (Figure 44) [59] in the progress toward obtaining these four metabolites. Studies are also underway regarding a model system for the endgame of these metabolites. Thus far, aldehyde **53** has been synthesized (Figure 47) [59]; further investigations are being conducted to determine a protocol to obtain compounds **54** and **55** to give the target models **56** and **57**, respectively (Figure 47) [59]. If the syntheses of these model systems, as well as the target molecules are successful, they can pave the way to accessing novel antibacterial agents and potential antimalarials. In addition, the target models **56** and **57**, if sythesized, could also provide additional biologically active models.

4.5 Experimental

4.5.1 General

Reagents were purchased from commercial vendors and used as received unless otherwise stated. All synthesized starting materials were dried under vacuum prior to use. Anhydrous DCM was distilled from CaH_2, and anhydrous THF was distilled from Na and benzophenone. NBS was recrystallized using water. Anhydrous nitromethane was dried using CaH_2, distilled under vacuum, and stored over 4 Å molecular sieves. K_2CO_3 and $NaHCO_3$ were dried in an oven overnight and then stored in a dessicator.

All other anhydrous solvents were purchased from commercial vendors and were sealed under nitrogen. *n*BuLi (2.5 M in hexanes) was purchased from Sigma-Aldrich (St. Louis, MO USA) and titrated against *N*-(3-benzylphenyl)pivalamide (recrystallized in hexanes) prior to use. All glassware was flame dried and placed under a nitrogen atmosphere prior to use. Purification via flash chromatography was performed using silica gel from Dynamic Adsorbents (32-65 μm) and technical grade eluents. Thin-layer chromatography (TLC) was conducted using EMD silica gel 60 F_{254} glass-backed plates. Preparative thin-layer chromatography (PTLC) was conducted using silica gel F_{254} glass-backed plates (1000 μm). For *N*,*N*-diisopropylethylamine (DIPEA)-treated silica, untreated silica was stirred in a solution of 5% DIPEA in DCM, stirred for 30 min at room temperature, and placed under reduced pressure until dry. DIPEA-treated silica plates were prepared by running the plates in 5% solution of DIPEA in DCM and allowed to dry overnight. Plate visualization was accomplished using UV light, iodine, and/or *para*-anisaldehyde (PAA) staining. ^{1}H NMR spectra were obtained using either a Varian Mercury Vx spectrometer (300 or 400 MHz) or a Bruker AVII (400 or 500 MHz) spectrometer; the chemical shifts were expressed in ppm and are referenced to the corresponding residual nuclei in the deuterated solvents. ESI-MS/accurate mass was performed using a ThermoFisher Scientific LTQ Orbitrap XL ETD, and EI/accurate mass analyses were performed using a Micromass AutoSpec M. Infrared (IR) spectroscopy was accomplished by attenuated total reflection (ATR) using a Bruker Optics Alpha-P FT-IR spectrometer.

4.5.2 Synthesis of the benzoic acid moieties of callophycoic acids G and H

Compounds **5**, **6**, **8** and **9** were synthesized according to previously published procedures, and the characterization data matched the data previously reported [111, 112].

4.5.2.1 Synthesis of 3-bromo-4-(methoxymethoxy)benzoic acid ***7***

To a round-bottom flask, compound **6** (0.5 g, 1.82 mmol) was dissolved in 200-proof ethanol (0.78 mL). A solution composed of potassium hydroxide (0.6119 g, 10.9 mmol) and 200-proof ethanol (2.6 mL) was added to the above methyl ester/ethanol solution, and the reaction mixture was allowed to stir at room temperature for 3 h. The solvent was then removed under reduced pressure, and the residue was poured into water, where the pH was adjusted to 5 using 10% aq. HCl. Next, the reaction mixture was extracted 4X with DCM, dried with Na_2SO_4, and concentrated under reduced pressure [113]. Purification of the crude mixture using silica gel and 5% EtOAc/hexanes afforded compound **7** as a white solid (42% yield). ^{1}H NMR (MeOD, 300 MHz) δ 8.34-8.24 (d, 1H), δ 7.86-7.81 (dd, 1H), δ 7.16-7.12 (d, 1H), δ5.23 (s, 2H), δ3.38 (s, 3H). ^{13}C NMR (MeOD, 400 MHz) δ 135.89, δ 131.60, δ 115.96, δ 95.98, δ 56.81. HRMS (EI) m/z $[M]^+$ Calcd. for $C_9H_9O_4Br$, 259.9684, found 259.9691.

4.5.3 Synthesis *trans*-decalin precursors

Compounds **14**, **20** and **24** - **28** were synthesized according to previously published procedures, and the characterization data matched the data previously reported [124, 125, 119, 126, 127, 120].

4.5.3.1 Synthesis of diethyl (4-(1,3-dioxolan-2-yl)-butan-2-yl)phosphonate ***13***

To a round-bottom flask was added diethyl ethylphosphonate (**11**) (0.100 g, 0.60 mmol) and THF (0.6 mL); the solution was then allowed to cool to -45°C. *n*BuLi (0.38 mL, 0.72 mmol, 1.9 M in hexanes) was added, and the reaction was allowed to stir for 30 min at -45°C. Then, 2-(2-bromoethyl)-1,3-dioxolane (**12**) was added to the flask in one shot, and the reaction was allowed to stir for 2.5 h at room temperature. Upon completion, the reaction was quenched with water, extracted with ethyl ether (3X), washed with brine, dried with $MgSO_4$, and concentrated under reduced pressure [114]. Purification using silica gel and 0-1% MeOH/DCM afforded phosphonate **13**

as a pale yellow, viscous oil (75% yield). ^{1}H NMR ($CDCl_3$, 300 MHz) δ 4.86-4.77 (t, 1H), δ 4.16-3.99 (q, 4H), δ 3.98-3.77 (m, 4H), δ 1.98-1.75 (m, 2H), δ 1.75-1.58 (m, 2H), δ 1.58-1.41 (m, 1H), δ 1.33-1.24 (t, 6H), δ 1.22-1.06 (dd, 3H).

*4.5.3.2 Synthesis of (2E,6E,10E)-13-(1,3-dioxolan-2-yl)-3,7,11-trimethyltrideca-2,6,10-trien-1-yl acetate **39***

To a round-bottom flask was added aldehyde **28** (0.4224 g, 1.38 mmol), ethylene glycol (0.12 mL, 2.07 mmol), *para*-toluenesulfonic acid monohydrate (5.33 mg, 0.028 mmol), and benzene. A Dean-Stark trap was added, and the reaction was allowed to reflux for 5 h or until the amount of water collected remained constant. Upon completion, the reaction was quenched with saturated aq. $NaHCO_3$ and concentrated under reduced pressure. The mixture was then extracted with EtOAc (3X), washed with saturated aq. brine (2X), dried over anhydrous $MgSO_4$, and concentrated under reduced pressure. Purification using DIPEA-treated silica gel and 5% DIPEA/hexanes-1% EtOAc/5% DIPEA/94% hexanes produced diooxolane **39** (17% yield). ^{1}H NMR ($CDCl_3$, 400 MHz), δ 5.37-5.29 (t, 1H), δ 5.18-5.04 (m, 2H), δ 4.86-4.81 (t, 1H), δ 4.61-4.54 (d, 2H), δ 3.98-3.81 (m, 4H), δ 2.16-1.93 (m, 13H), δ 1.77-1.70 (m, 2H), δ 1.70 (s, 3H), δ 1.68 (s, 3H), δ 1.62-1.54 (m, 3H). ^{13}C NMR ($CDCl_3$, 400 MHz) δ 171.06, δ 142.17, δ 135.48, δ 134.33, δ 124.36, δ 124.25, δ 118.19, δ 104.29, δ 64.82, δ 61.33, δ 39.78, δ 33.82, δ 32.41, δ 26.42, δ 26.01, δ 23.33, δ 21.00, δ 16.41, δ 15.95.

*4.5.3.3 Synthesis of (2E,6E,10E)-14-hydroxy-3,7,11-trimethyltetradeca-2,6,10-trien-1-yl acetate (**29**)*

In a round-bottom flask, aldehyde **28** (0.91 g, 2.97 mmol) was dissolved in ethyl ether (9 mL). Sodium borohydride (0.1888 g, 4.99 mmol) was added in portions, followed by methanol, and the reaction was stirred overnight at room temperature. Upon reaction completion, the reaction mixture was quenched at 0°C through the slow addition of water. Extraction using ethyl ether, followed by drying with anhydrous $MgSO_4$ and

then concentration under reduced pressure, afforded the crude product [128], which was then purified using silica gel and 10-20% EtOAc/hexanes to provide alcohol **29** as a clear, colorless oil (71% yield). ^{1}H NMR ($CDCl_3$, 300 MHz) δ 5.37-5.30 (t, 1H), δ 5.20-5.05 (m, 2H), δ 4.61-4.55 (d, 2H), δ 3.66-3.59 (m, 2H), δ 2.17-1.94 (m, 15H), δ 1.69 (s, 3H), δ 1.68 (s, 3H), δ 1.62 (s, 3H). ^{13}C NMR ($CDCl_3$, 300 MHz) δ 171.181, δ 142.253, δ135.471, δ 134.863, δ 125.387, δ 124.501, δ 118.188, δ 62.807, δ 61.401, δ 39.767, δ 39.481, δ 35.981, δ 30.708, δ 26.387, δ 26.050, δ 23.326, δ 21.063, δ 16.442, δ 15.841. HRMS (EI) m/z $[M]^+$ Calcd. for $C_{19}H_{32}O_3$, 308.2351, found 308.2355. IR: 3375 (w), 2931.32 (w), 1737.63 (m), 1444.69 (w), 1365.59 (w), 1229.21 (s), 1020.96 (m) cm^{-}1.

*4.5.3.4 Synthesis of (2E,6E,10E)-14-((tert-butyldiphenylsilyl)oxy)-3,7,11-trimethyltetradeca-2,6,10-trien-1-yl acetate (**30**)*

To a round-bottom flask, imidazole (48.3 mg, 0.71 mmol) was dissolved in anhydrous DMF (0.65 mL). Compound **29** was then added, and the mixture was cooled to 0°C. TBDPSCl (0.18 mL, 0.71 mmol) was then added dropwise, and the reaction was allowed to stir overnight at room temperature. Upon completion, the reaction was quenched with water, extracted with ethyl ether, washed with brine, dried with $MgSO_4$, and concentrated under reduced pressure [129]. Purification using silica gel and 0-1-2% EtOAc/hexanes afforded **30** as a clear, colorless oil (79% yield). ^{1}H NMR ($CDCl_3$, 300 MHz) δ 7.71-7.65 (dd, 4H), δ 7.46-7.34 (m, 6H), δ 5.38-5.30 (t, 1H), δ 5.14-5.06 (t, 2H), δ 4.62-4.56 (d, 2H), δ 3.68-3.61 (m, 2H), δ 2.16-1.92 (m, 15H), δ 1.70 (s, 3H), δ 1.65 (s, 3H), δ 1.57 (s, 3H) δ 1.05 (s, 9H). ^{13}C NMR ($CDCl_3$, 300 MHz) δ 171.137, δ 135.552, δ134.658, δ 134.094, δ 127.554, δ 124.252, δ 124.142, δ 123.563, δ 118.173, δ 63.803, δ 61.386, δ 45.685, δ 39.518, δ 35.805, δ 31.946, δ 30.989, δ 26.841, δ 26.028, δ 23.046, δ 21.063, δ 19.203, δ 16.478, δ 15.914. IR: 2930.79 (w), 2875 (w), 1738.09 (m), 1427.56 (m), 1229.14 (s), 1106.96 (m), 1020.80 (w), 700.71 (s), 503.81 (m) cm^{-1}.

4.5.4 Endgame for callophycoic acids G and H

*4.5.4.1 Synthesis of ((1R,2S,4aS,5R,6R,8aR)-6-bromo-5-(3-((tert-butyldiphenylsilyl)oxy)propyl)-2-hydroxy-2,5,8a-trimethyldecahydronaphthalen-1-yl)methyl acetate (**32**)*

To a round-bottom flask was added compound **30** (73.4 mg, 0.13 mmol) and nitromethane (13 mL). The mixture was allowed to cool to 0°C, and a solution of BDSB (81.1 mg, 0.15 mmol) in nitromethane (0.36 mL) was prepared and immediately added to the reaction flask. The reaction was stirred at 0°C for 30 s, followed by immediate quenching via the sequential addition of equal volumes of 5% aq. Na_2SO_3 and saturated aq. $NaHCO_3$ (20 mL each). After quenching, the reaction was stirred vigorously for 1 h at room temperature. The reaction mixture was then poured into brine (50 mL), extracted with EtOAc (3X), washed with brine, dried with anhydrous $MgSO_4$, and concentrated under reduced pressure [59] to give an orange oil that will be carried forward to the next step without further purification. Purification via preparative TLC (PTLC) of 20% EtOAc/hexanes (3X) provided an isomer of compound **45** as an off-white solid (potential mixture of diastereomers). ^{1}H NMR ($CDCl_3$, 400 MHz) δ 7.70-7.62 (m, 4H), δ 7.46-7.34 (m, 6H), δ 4.47-3.92 (m, 3H), δ 3.75-3.56 (m, 2H), δ 2.10-2.01 (m, 4H), δ 1.95-1.76 (m, 2H), δ 1.75-1.56 (m, 5H), δ 1.55-1.38 (m, 4H), δ 1.38-1.28 (m, 2H), δ 1.28-1.21 (m, 3H), δ 1.21-1.12 (m, 2H), δ 1.06 (s, 9H), δ 0.9 (s, 1H), δ 0.8 (s, 1H), δ 0.75-0.70 (m, 1H), δ 0.88 (s, 1H). ^{1}3C NMR ($CDCl_3$, 400 MHz) δ 168.00, δ135.53, δ 129.55, δ 127.59, δ72.1, δ 64.05, δ 63.21, δ 62.11, δ 59.91, δ 49.97, δ 43.57, δ 41.37, δ 40.84, δ 39.16, δ 37.87, δ 35.76, δ 30.85, δ 30.23, δ 26.81, δ 24.35, δ 21.23, δ 19.67, δ 19.13, δ 16.41.

4.5.5 Synthesis of the model system reflecting the endgame for callophycoic acids G and H

Compounds **51** - **53** were synthesized according to previously published procedures, and the characterization data matched the data previously reported [59].

4.5.5.1 Synthesis of 3-(((1S,4aR,6S,8aS)-6-bromo-5,5,8a-trimethyl-2-methylenedecahydronaphthalen-1-yl)(hydroxy)methyl)-4-(methoxymethoxy)benzoic acid

(**54**) Compound **7** (41.8 mg, 0.16 mmol) and THF (4 mL) were added to a round-bottom flask and cooled to -78°C. *n*BuLi (0.1 mL, 0.26 mmol, 2.2 M in hexanes) was added dropwise to the benzoic acid solution, and the clear, pale, yellow mixture was stirred for 20 min at -78°C. Then, this lithiated benzoic acid solution was syringed immediately into a solution of aldehyde **53** (37.7 mg, 0.12 mmol) at -40°C and stirred for 20 min and then quenched via the sequential addition of equal volumes of saturated aq. NH_4Cl and water (5.8 mL each). The reaction mixture was extracted with EtOAc (3X), washed with brine, dried using $MgSO_4$, concentrated under reduced pressure [59] and carried forward to the next step without further purification.

4.6 Acknowledgements

These studies were funded by the Blanchard Assistant Professor Fellowship and the Graduate Assistance in Areas of National Need (GAANN) fellowship. Mr. Kedar Perkins, Ms. Kymberlee Osborne, Mr. Angel Cobos, and Mr. Raynold Shenje are also acknowledged for experimental assistance.

CHAPTER V

CONCLUSIONS/FUTURE OUTLOOKS

5.1 Enantiopure and non-enantiopure Co(III)-salen catalysts and the effects of the counter-ion on hydrolytic kinetic resolution (HKR) reactions

The work involving the catalysis of the HKR of epichlorohydrin using 50% enantiopure ligand with a counter-ion constructed to make the salen complex nucleophile-delivering (e.g., $^{-}$OH) and 50% racemic ligand with a counter-ion constructed to make the salen complex a Lewis acidic, electrophilic complex (e.g., SbF_6^{-}) was conducted. The goal of these studies was to determine whether high activity and enantioselectivity could be achieved for HKR that is comparable to a catalyst system composed of both (*R,R*)-Co-salen-OH and (*R,R*)-Co-salen-SbF_6 complexes [84], thus lowering the cost of the reactions. It was shown that the catalysis systems containing only 50% enantiopure ligand did not lead to enantioselective catalysis, which was a result of the scrambling of the counter-ions between the Co-centers, as was reflected via kinetic studies, EA, and FT-IR [84].

In conducting the experiments to confirm the counter-ion exchange in the aforementioned catalytic systems, it was discovered that oxidation of a Co(II) on a polymer support can occur via exposure to a homogeneous Co(III) species [84]. This not only further exemplified the counter-ion exchange but it also exhibits potential to serve as a method for regenerating the Co(III)-salen catalysts that are deactivated throughout the course of HKR due to counter-ion loss [83]. To further investigate these observations, HKR reactions were performed using a 1:1 ratio of homogeneous (*R,R*)-Co(II)-salen (**1**) and homogeneous (*R,R*)-Co(III)-salen-SbF_6 (**2**) (Figure 51) to study the reaction kinetics [142]; this catalytic system provided high initial TOFs

(2.6 min^{-1}) as well as displayed high enantioselectivity, reaching 99% ee in 90 min [142]. When tested with a 1:1 ratio of polymer resin-supported Co(II)-salen and homogeneous (*R,R*)-Co(III)-salen-SbF_6 (**2**), though not as active or selective as the case using all homogeneous Co complexes, slightly higher initial TOFs (4.02 min^{-1}) were obtained, reaching >99% ee in 3 h (Figure 51) [142]; this is comparable to the kinetic data shown in Chapter 2 (Table 3, entry 3), where a 1:1 mixture of (*R,R*)-Co(III)-salen-Cl and (*R,R*)-Co(III)-salen-SbF_6 was used [142]. This further supports the fact that the Co(II) plays a role in the catalysis of HKR. Thus, future work pertaining to the Co-salen-catalyzed HKR studies described in Chapter 2 could involve determining the specific role and/or reaction order on the homogeneous and supported Co(II)-salen catalysts and whether the rate of HKR coincided with the overall Co content in the system.

Although the role of the Co(II) has yet to be determined (to our knowledge) in HKR, Feng et al. investigated the role of polymer resin-supported Co(II)-salens in the regioselective ring-opening of 1,2-epoxyhexane using methanol (Figure 52) [143].

In this study, a poly(styrene)-supported salen ligand with various Co loadings (**4a-4c**, as well as a varying SbF_6^- counter-ion content), was used (Figure 52 and Table 6) [143]. In the ring-opening reactions, polymer resin-supported catalysts that had the greatest overall Co content (e.g., Co(II) + Co(III)) exhibited faster activities than the polymer resin-supported catalyst that had a greater amount of Co(III) species present, as catalyst **4a-SbF_6** reacted twice as fast as catalyst **4b-SbF_6** (initial TOF = 0.9 min$^-$1) [143]. Thus, the overall Co composition does play a role in the alcohol ring-opening (ARO) catalysis, which is supported by the fact that the reaction order was found to be approximately 0.1 with respect to the Co(II) species [143]. Thus, as previously mentioned, using a similar approach in the catalyst design for applications in HKR to determine the role of the Co(II) species could shed further knowledge and understanding about the currently accepted route for catalysis.[72]

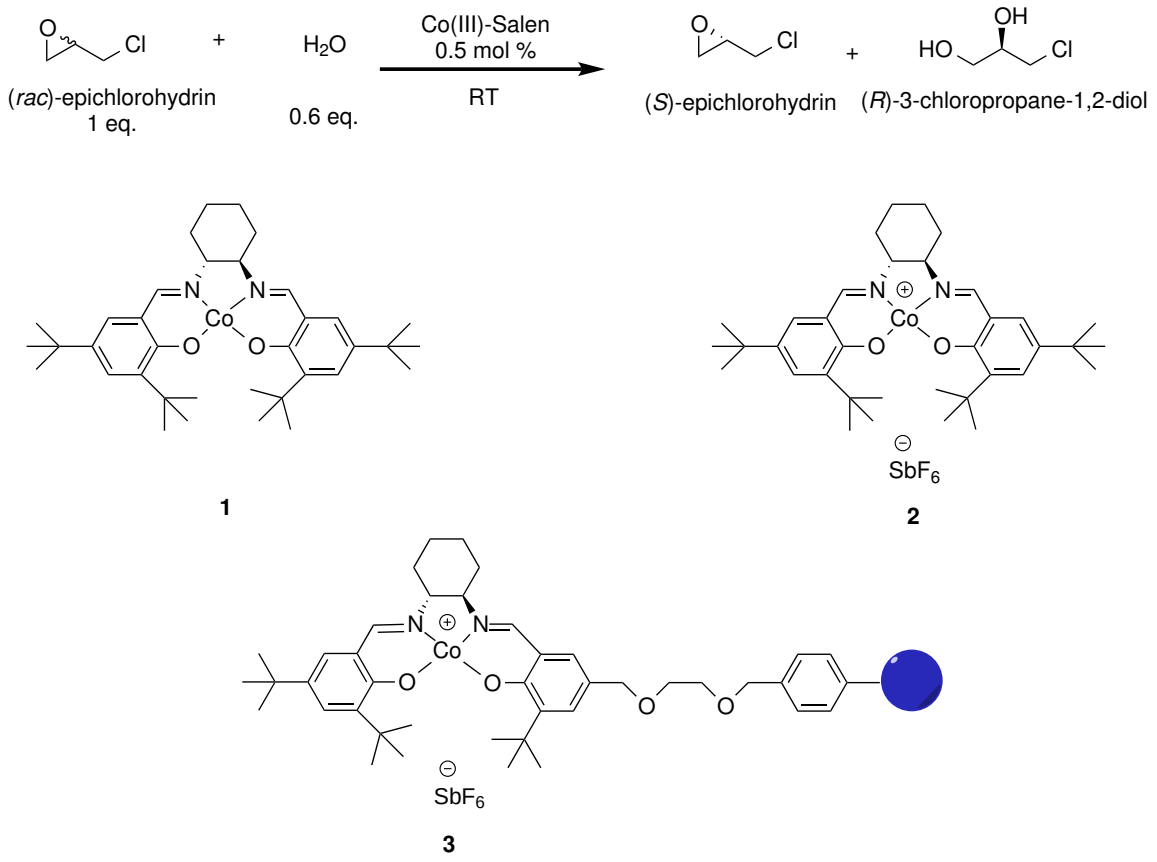

Figure 51: HKR of racemic ECH comprising a 1:1 ratio of homogeneous (***R,R***)-Co(III)-salen-SbF_6 and either homogeneous or polymer resin-supported (***R,R***)-Co(II)-salen [142].

The above-proposed investigations into HKR and ARO are regarding the more Lewis acidic salen, which has a non-coordinating SbF_6^- counter-ion. However, there have been no investigations thus far concerning the oxidation of polymer-supported Co-salens such that a nucleophile-delivering salen complex is formed. Therefore, reactions regarding HKR catalysis using supported Co(III)-salen-X (X = nucleophilic counter-ion, such as Cl, OAc) with varying degrees of oxidation could be conducted to determine whether catalysis using these Co-salens with a nucleophile-delivering complex are also dependent on the overall Co content. Studies investigating both types of counter-ions (nucleophilic and non-nucleophilic) could provide further insights into the bimetallic cooperative mechanism for HKR.[72]

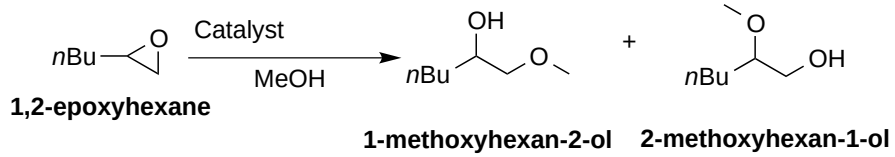

1,2-epoxyhexane **1-methoxyhexan-2-ol** **2-methoxyhexan-1-ol**

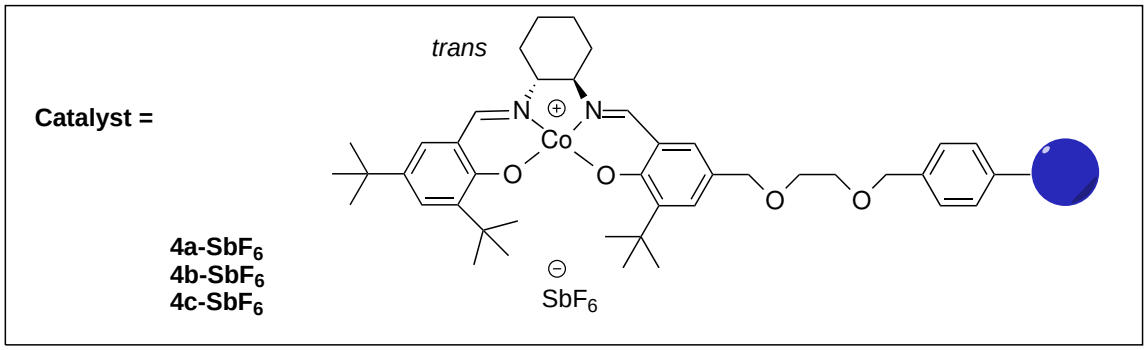

Figure 52: Regioselective ring opening of 1,2-epoxyhexane using methanol [143].

Table 6: Elemental analysis data from the catalysts used for the regioselective ring-opening of 1,2-epoxyhexane using methanol. Data from Ref. [143].

Entry	Catalyst	N (%)	Sb (%)	Co (%)	N/Co	Co loading (%)	Co/Sb	Co oxidized (%)
1	**4a-SbF$_6$**	1.8	0.25	0.53	2.4	83	2.1	48
2	**4b-SbF$_6$**	1.8	0.26	0.37	3.5	57	1.4	71
3	**4c-SbF$_6$**	1.7	0.15	0.17	7.1	28	1.1	91

Based on the findings in Chapter 2, it was suggested that this oxidation of a Co(II) species via a homogeneous Co(III) species could provide a method for catalyst regeneration after deactivation by counter-ion loss [83]. Venkatasubbaiah et al. investigated the recycling and regeneration of polymer resin-supported Co(III)-salen-X catalysts, where X = OAc (**5**), camphorsulfonate (CSA) (**6**), and BF_4^- (**7**) (Figure 53) [83]; it was determined that the deactivation of the catalyst was counter-ion dependent (e.g., the catalyst containing the BF_4^- counter-ion was stable over three cycles, with the initial TOF decreasing from 6.23 to 5.89 min^{-1}), and the regeneration of the polymer-supported Co(III)-salen-CSA using camphorsulfonic acid in toluene led to significant metal leaching due to possible ligand hydrolysis [83]. Thus, a method to regenerate

these catalysts while avoiding ligand hydrolysis would be ideal. The results obtained in Chapter 2 showed oxidation of a polymer-supported Co(II)-salen via contact of a homogeneous (*R,R*)-Co(III)-salen-SbF_6 [84], which is not a proton source. Although previous studies showed that regeneration of a polymer-supported Co(III)-salen-SbF_6 using lutidinium-SbF_6 ($LuSbF_6$) did result in further metal leaching in the recycled catalysts [143], using a lutidinium derivative, such as a lutidinium camphorsulfonate, could result in a smaller degree of metal leaching due to ligand hydrolysis because it is a weaker Bronsted acid relative to camphorsulfonic acid. If using a lutidinium source as an alternative to strong carboxylic acids, such as camphorsulfonic acid, leads to more effective catalyst regeneration, then this could provide and lead to more effective methods for catalyst regeneration, as there is a need for well-developed methods for supported catalyst regeneration because this is currently a drawback regarding their use in commercial-scale catalysis [90].

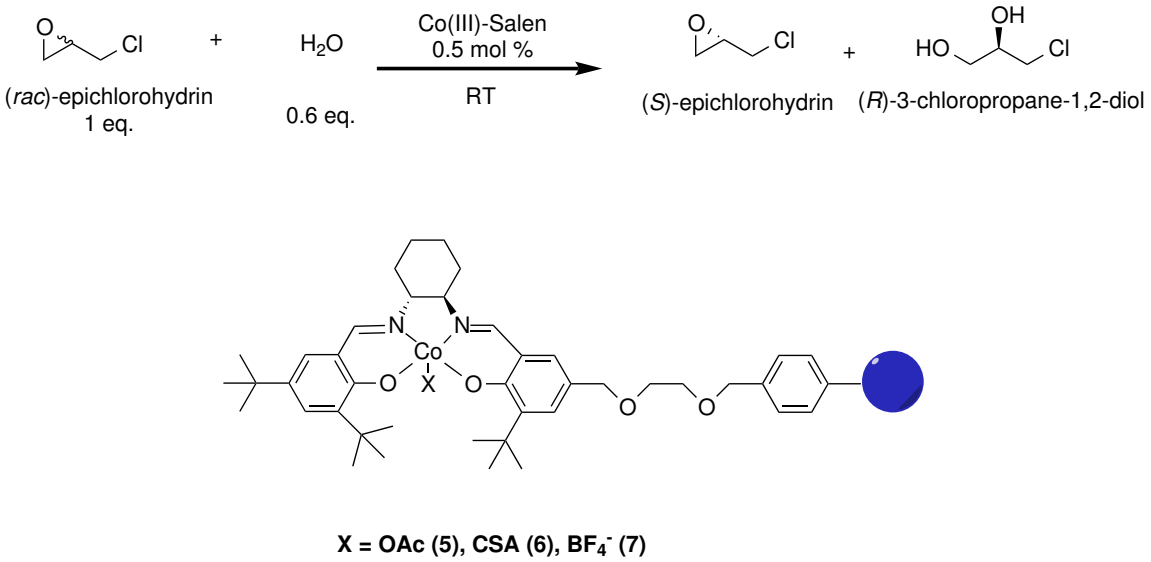

Figure 53: HKR of racemic epichlorohydrin using polymer resin-supported Co(III)-salen-X (X = OAc, CSA, BF_4^-) to investigate the recyclability of the catalysts, as well as the effectiveness of catalyst regeneration methods [83].

The aforementioned research regarding HKR involved studying it from a catalysis science perspective. As mentioned in the previous chapters, HKR can be used

as a method to synthesize chiral building blocks that might otherwise be inaccessible. In the following research involving the progress in the natural product total synthesis of metabolites isolated from *Callophycus serratus*, there is a need for chiral intermediates, where methods such as HKR can be utilized.

5.2 Callophycolide A

As previously described, of the 17 proposed steps required to accomplish the total synthesis of callophycolide A, eight of these steps were successfully completed. The major limiting factor for this synthesis regards the synthesis of compound **22**: the base-promoted ERO (Figure 54). Therefore, if this total synthesis was to be revisited, this step should be taken into consideration. First, the model system using ((2-methylallyl)sulfonyl)benzene **14** and styrene oxide to form **15** (Figure 55) [109, 110] should be performed in an atmosphere that is free of air and moisture. The reaction to form **16** was performed using Schlenk conditions; the *n*BuLi was titrated against a recrystallized indicator; the THF was freshly distilled; and the starting materials were confirmed to have no water contamination. However, this was not sufficient for obtaining a high yield of pure product. Thus, it is recommended that these reactions be performed in a glove box such that no air/moisture enter the system, thus potentially leading to a higher yield of pure product. Once this step is optimized, the ERO can be performed for the actual system, thus forming compound **22** (Figure 56) [57, 100, 102, 110, 109, 144, 145]. Subsequently, saponification, sulfone removal, Steglich esterification, and then global MOM deprotection should afford the desired callophycol A (**1**) (Figure 56) [57, 100, 102, 110, 109, 144, 145].

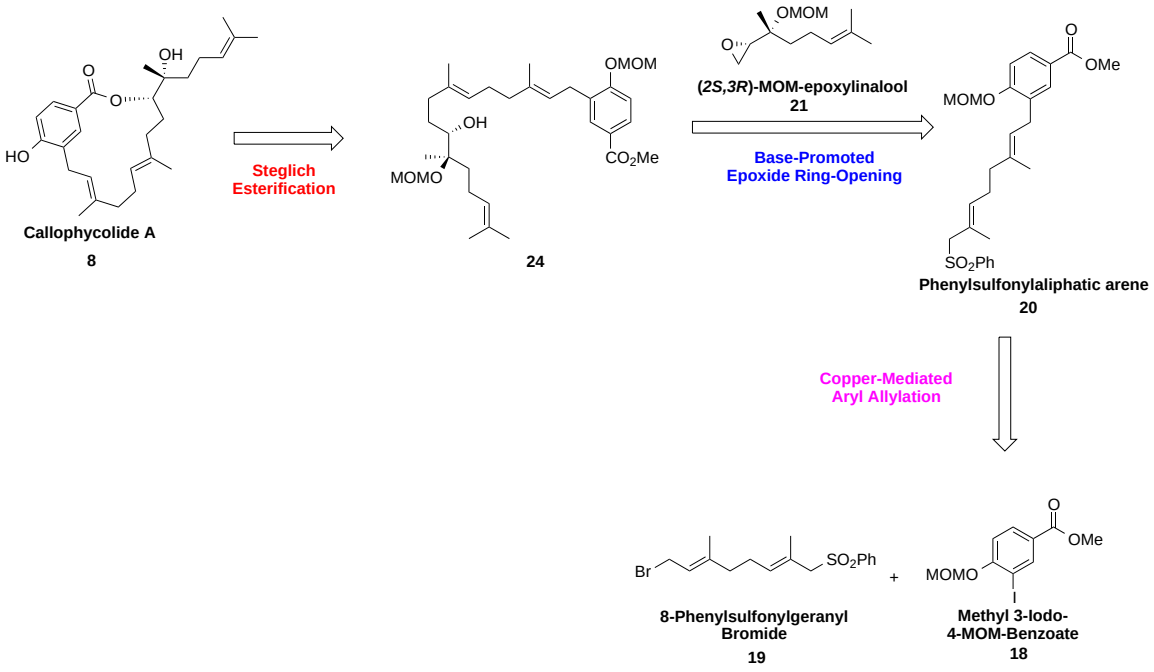

Figure 54: Retrosynthetic analysis of callophycolide A (**8**).

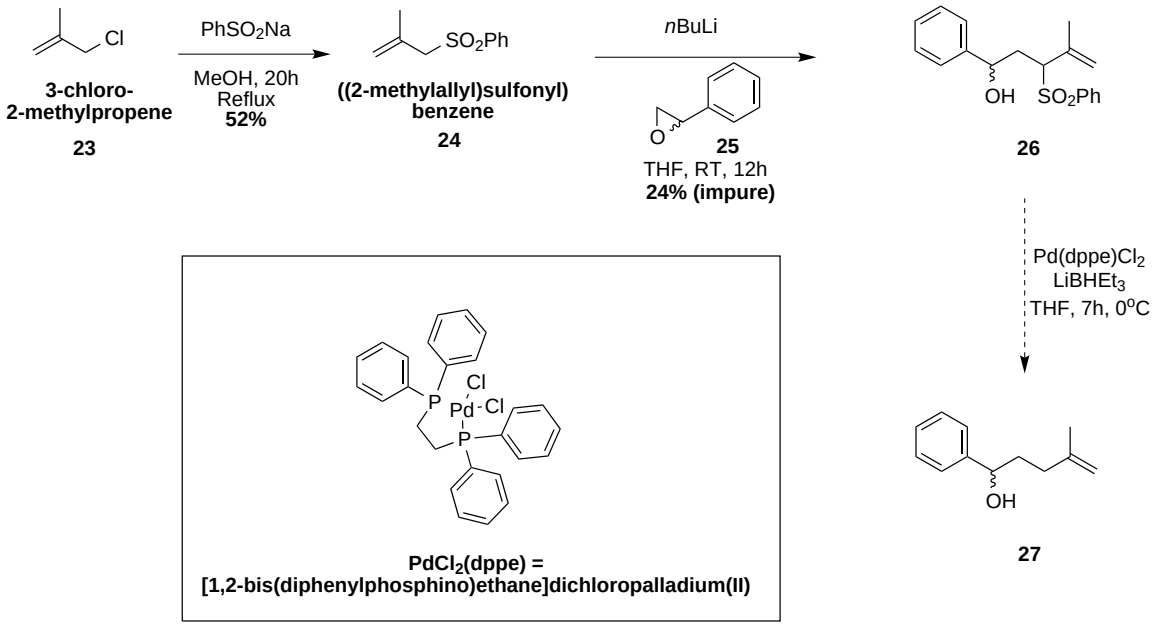

Figure 55: Scheme of the ERO model system, which should result in the formation of compound **17** [108, 109, 110].

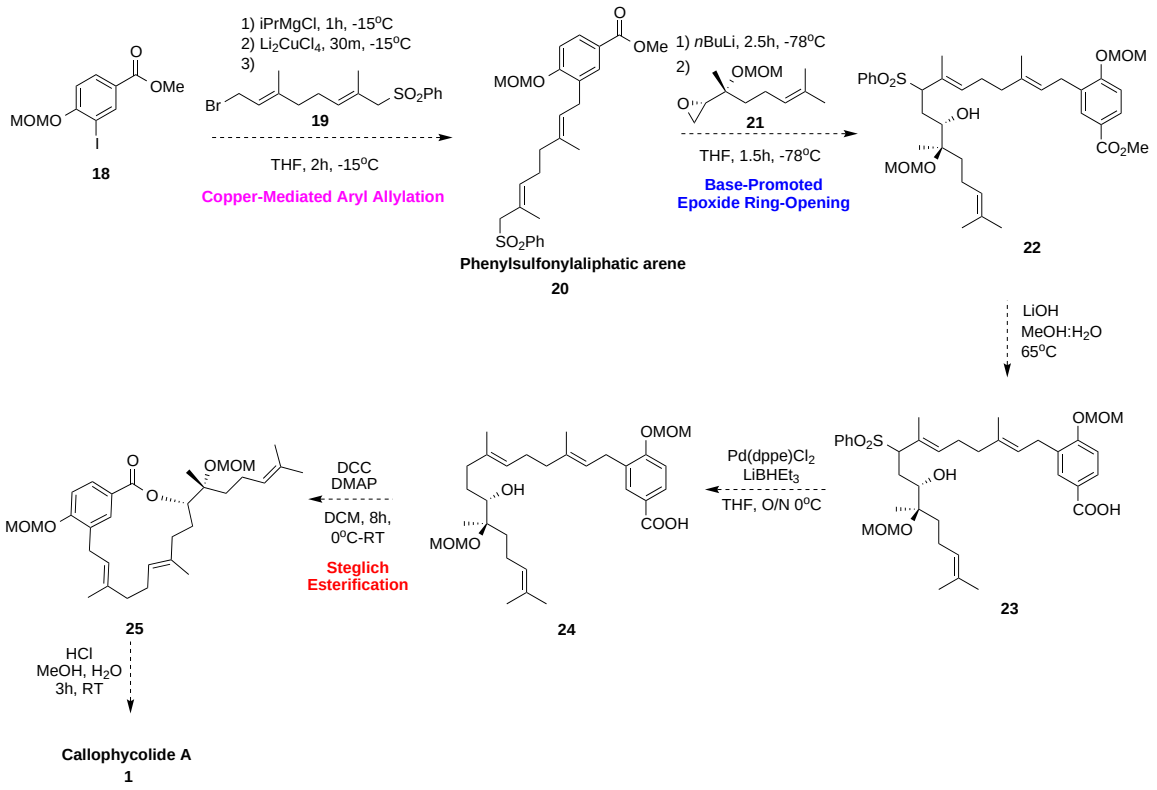

Figure 56: Proposed callophycolide A endgame [57, 100, 102, 110, 109, 144, 145].

As mentioned previously, concerning callophycolide A, there are two stereocenters present in the molecule. When Stout et al. first isolated callophycolide A, the absolute configuration of C-14 was confirmed as S by Mosher's ester analysis, ^{1}H NMR, HSQC-TOCSY, and $\Delta\delta_{S\text{-}R}$ calculations (Figure 57) [54, 146]. However, circular dichroism (CD) and NOE studies were only able to strongly suggest that the absolute configuration at C-15 was R (Figure 57) [54]. Therefore, not only will the total synthesis of callophycolide A serve as a template for the syntheses of more potent antimalarials but it can also lead to the synthesis of the diastereomers and enantiomers of the previously reported callophycolide A; an examination of the biological activities of these isomers will not only give rise to potentially potent synthetic derivatives of callophycolide A but the biological activity studies will also aid in the conformation of the actual compound isolated by Stout et al. [54].

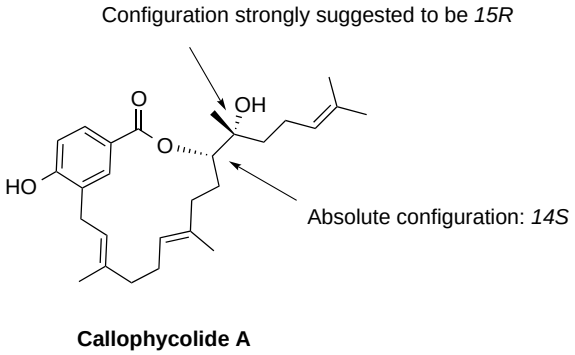

Figure 57: Figure depicting the configurations of the C-14 and C-15 stereocenters of callophycolide A [54].

5.3 Callophycoic Acids G and H

As mentioned in the previous chapter, efforts were made to develop a pathway to synthesize a common *trans*-decalin precursor, which can be used for the syntheses of callophycoic acids G and H and callophycols A and B. Although these metabolites display modest biological activities against bacteria, cancer, and malaria [55], this modular approach to access these compounds could serve as a template to synthesize the more potent metabolites of *C. serratus*.

5.3.1 *trans*-Decalin syntheses

5.3.1.1 Model system for the synthesis of callophycoic acids G and H

As mentioned previously, investigations are underway on a model system to determine the endgame of callophycoic acids G and H. These investigations involve forming the *trans*-decalin core and functionalizing this core with the appropriate benzoic acid moiety (Figure 58) [59].

Specifically, optimization of coupling the benzoic acid moieties is in progress. The nucleophilic addition method used by Snyder et al. in the synthesis of peyssonol A, in which they used a 1,4-dibromo-2,5-bis(methoxymethoxy)benzene [59], could not be applied to our system with benzoic acid **30**, even with 2.1 equivalents of *n*-BuLi to

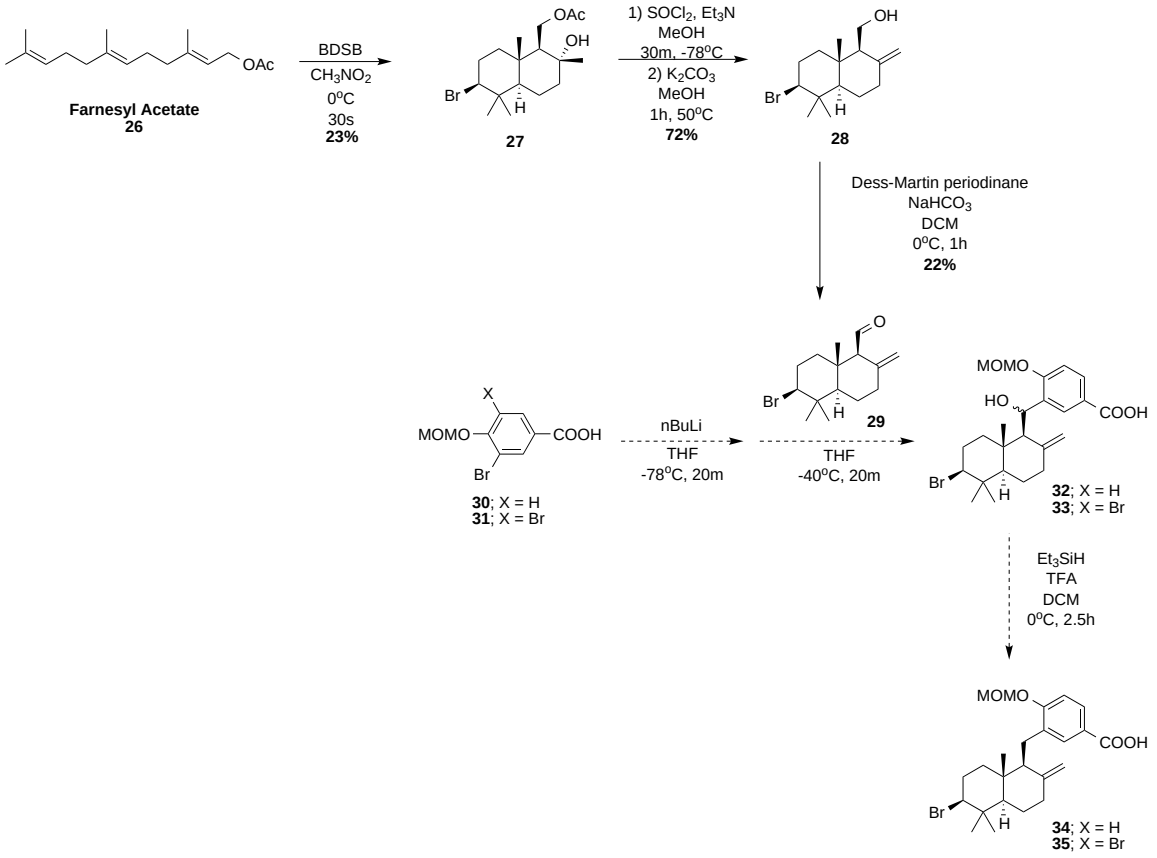

Figure 58: Model system for the endgame of the syntheses of callophycoic acids G and H [59].

circumvent the sole deprotonation of the benzoic acid; ^{1}H NMR analysis alluded to a symmetrical arene, which does not correspond to the desired product. Therefore, it is proposed that the methyl benzoate moiety (**36** or **37**) be reduced to a benzyl alcohol (**38** or **39**) [141], followed by subsequent protection by converting it to a TBS ether (**40** or **41**) (Figure 59) [59, 141]. Once these compound are synthesized, they can be subjected to lithiation, followed by nucleophilic addition to aldehyde **29**, to obtain the benzyl alcohol (**42** or **43**) ; removal of this benzyl alcohol (to form **44** or **45**), followed by removal of the TBS group using TBAF (to form **46** or **47**), and then oxidation to yield the model target (**37** or **38**) for callophycoic acids G and H (Figure 59) [59, 141].

If this pathway is successful in synthesizing the target models for both callophycoic

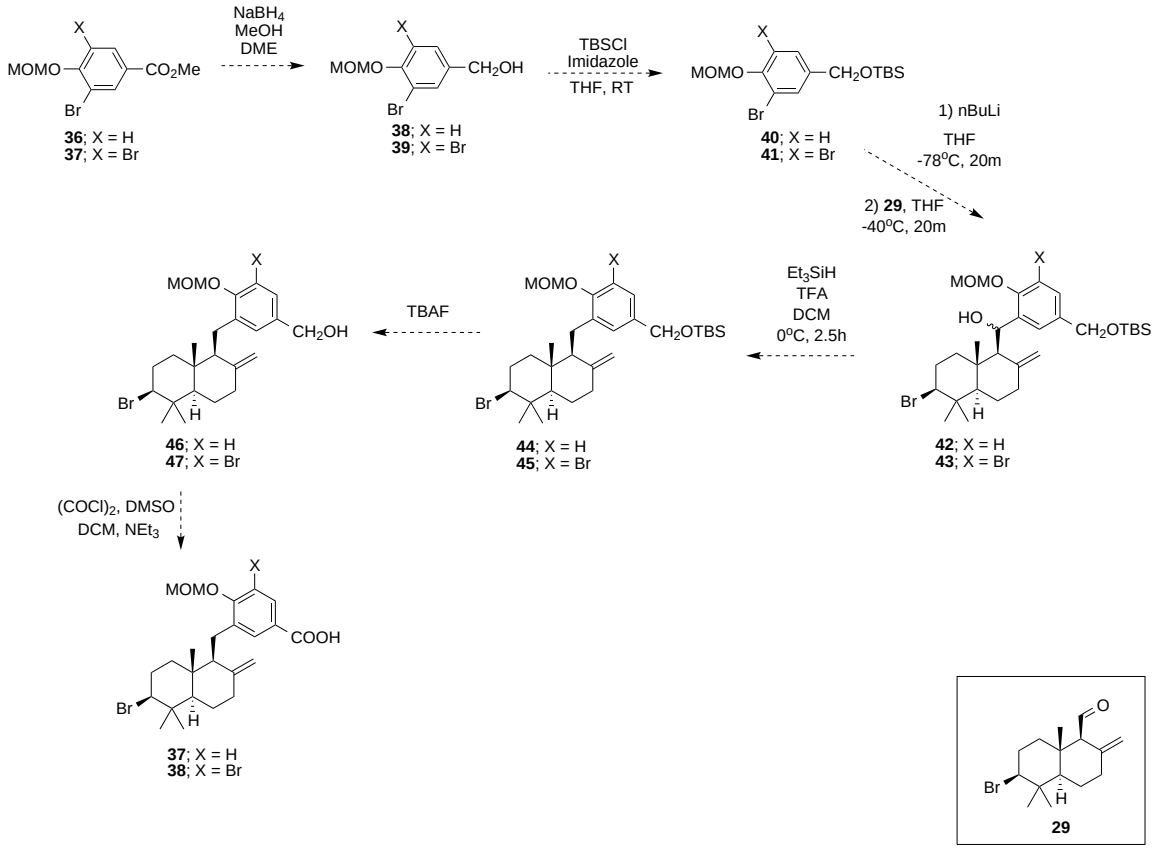

Figure 59: Revised model system for the endgame of the syntheses of callophycoic acids G and H [141, 59].

acids G and H, the MOM-protected tribromophenol (**50**) can also undergo lithiation, followed by nucleophilic attack to aldehyde **29**, which will correspond to the phenol head of callophycols A and B (Figure 60) [59]. The successful syntheses of these target models for callophycoic acids G and H and callophycols A and B will not only aid in the total syntheses of the desired target molecules; if effectively isolated and characterized, these molecules could also be tested for biological activity, thus leading to other pharmaceutical treatments via a natural product or derivatives. Because similar structures with the arene head groups and the *trans*-decalin cores exhibit activity against allosteric inhibitors of HIV transcriptase, such as peyssonol A [132, 133], and bacteria, such as peyssonoic acid A [134] and the callophycoic acids G and H [55], there is a strong likelihood that these models could have similar bioactivities

and biological targets.

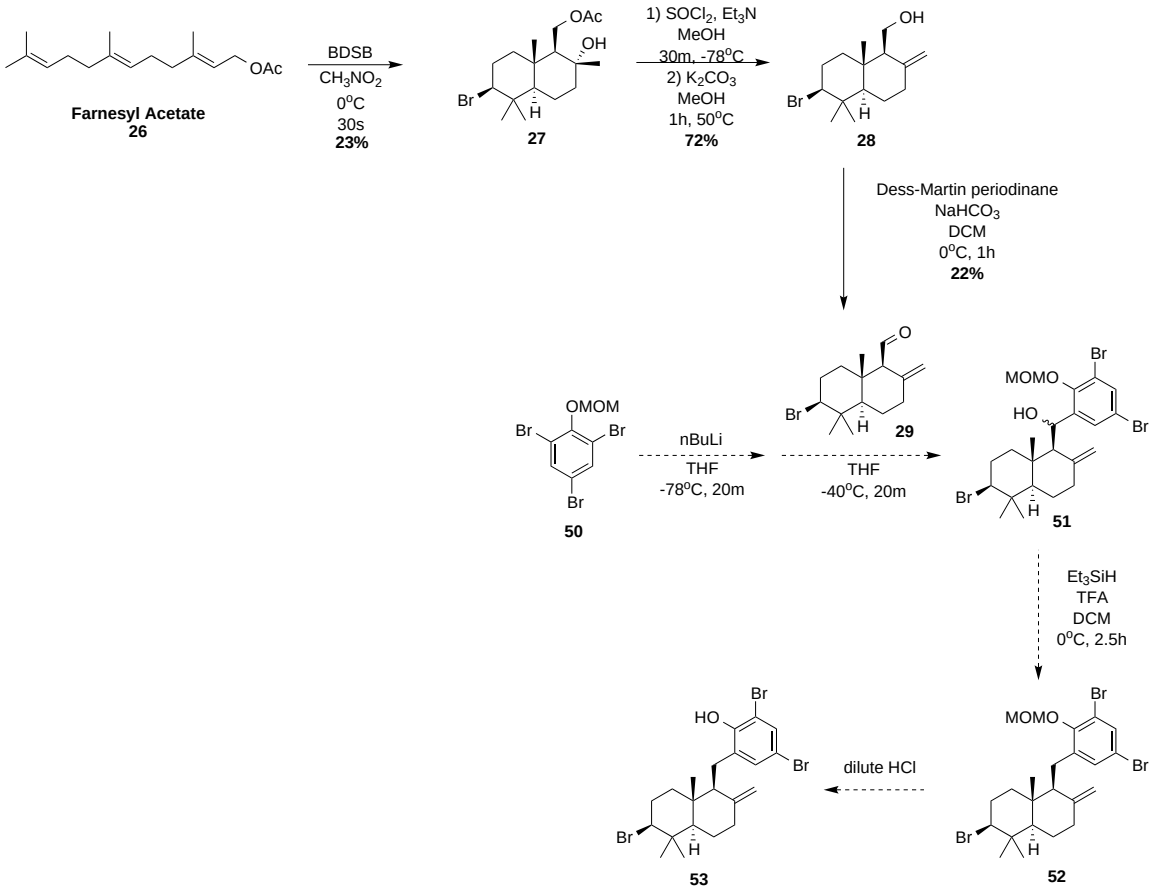

Figure 60: Model system for the endgame of the syntheses of callophycols A (**4**) and B (**5**) [59].

5.3.2 Syntheses of callophycoic acids G and H

Regarding compound **55**, efforts have been made to form this *trans*-decalin needed for callophycoic acids G and H according to the aforementioned procedures (Figure 61) [59]. In isolating the reaction components via flash column chromatography and PTLC, the preliminary conclusions drawn are that an isomer of **55** was synthesized; however, the product obtained via flash column chromatography and PTLC (at the upper limit) has been impure. To be able to effectively isolate compound **55**, optimization of the purification conditions, such as decreasing the sample loading of PTLC, or exploring recrystallization techniques, should result in a pure compound

55 or one of its pure isomers. Reactions are currently underway where the crude *trans*-decalin **55** will be carried forward to carry out the Swern elimination, followed by acetate removal to form compound **56** (Figure 61) [59]. Although the syntheses to form compound **56** will most likely result in a mixture of isomers, this approach does carry merit. First, if these isomers can be separated, then the callophycoic acids G and H could still be isolated. Second, syntheses and characterization of diastereomers would confirm that the chemistry is tolerant toward the functional groups present on the synthetic intermediates.

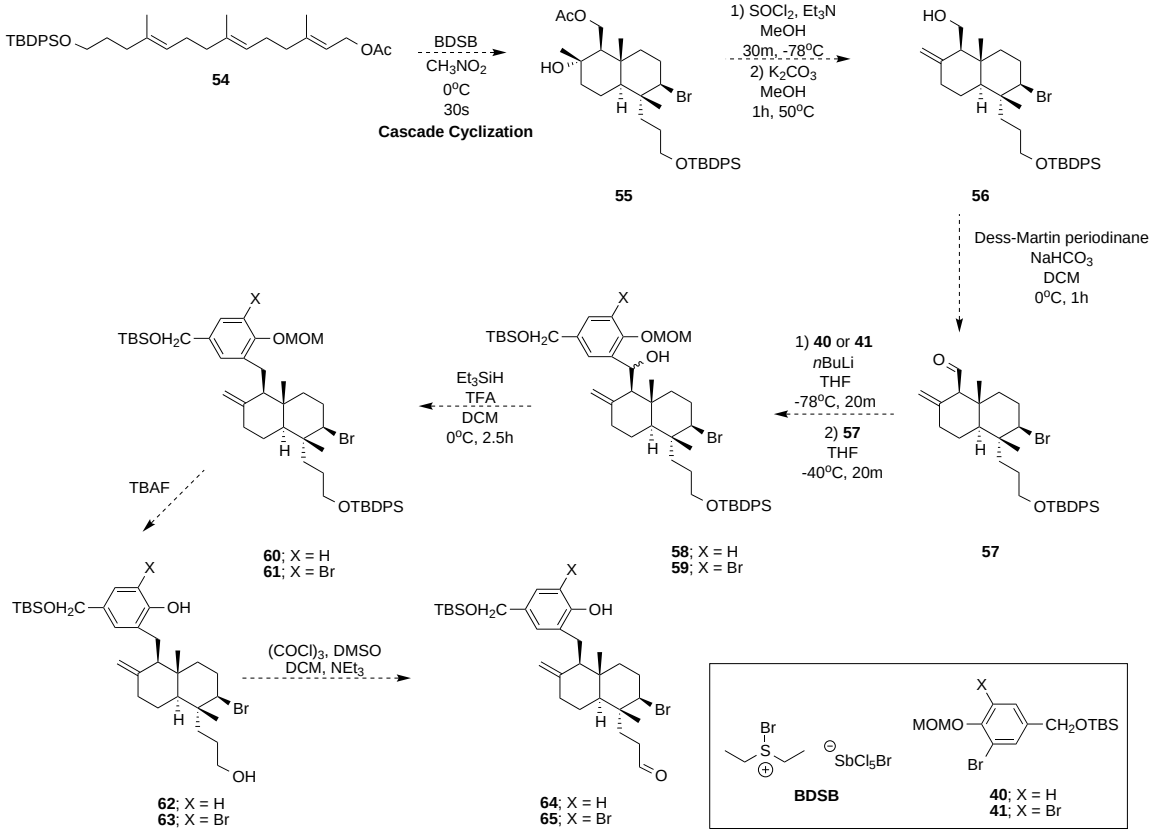

Figure 61: Progress toward the synthesis of compounds **64** and **65** [59].

With compound **56**, oxidation should give aldehyde **57**, which can be coupled to **40** or **41** to give **58** or **59**, respectively (Figure 61) [59]. Removal of the benzyl alcohol (to form **60** and **61**), followed by deprotection (to form **62** and **63**), oxidation (to form **64** and **65**) (Figure 61) [59], and finally, a Wittig reaction, should provide

callophycoic acids G or H (Figure 62) [120].

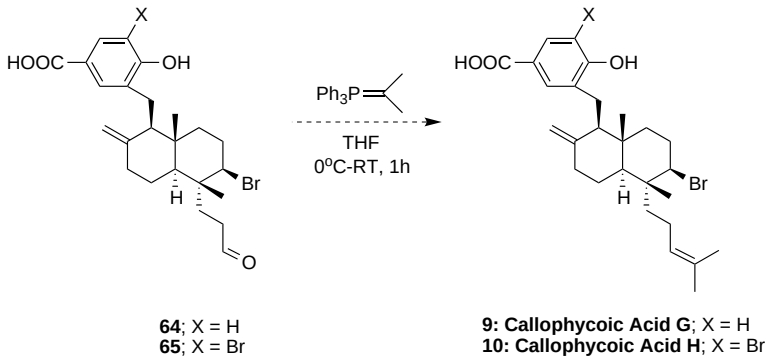

Figure 62: Endgame for callophycoic acids G and H [120].

5.3.3 Callophycols A and B

Callophycols A and B are halogenated diterpene-phenols, also isolated from *C. serratus*, as are the other natural products discussed in the current studies. Not only do they share the same *trans*-decalin core as the callophycoic acids G and H but they also exhibit modest antimalarial activity (IC_{50} = 35.7 μM (A) and 40.4 μM (B)) [55]. Due to this common identical core, if a divergent total synthesis of the callophycoic acids G and H can be established, it can serve as a template for callophycols A and B.

Evaluating the retrosynthetic analyses of callophycols A and B, both of the compounds can be synthesized via the appropriate vicinal dehydrohalogenation of trisubstituted olefin **66**, as shown in Figure 63. Olefin **66** can be synthesized via a Wittig reaction of compound **67**, which is formed via the nucleophilic addition of MOM-protected-2,4-6-tribromophenol (**50**) and the *trans*-decalin **57**, which was also used in the syntheses of callophycoic acids G and H; thus, the same synthetic steps can be used, starting with geranyllinalool **70**, as shown in Figure 64.

Regarding the current progress toward the syntheses of callophycols A and B, compound **54** has been synthesized (Figure 61) [59], as well as the MOM-protected

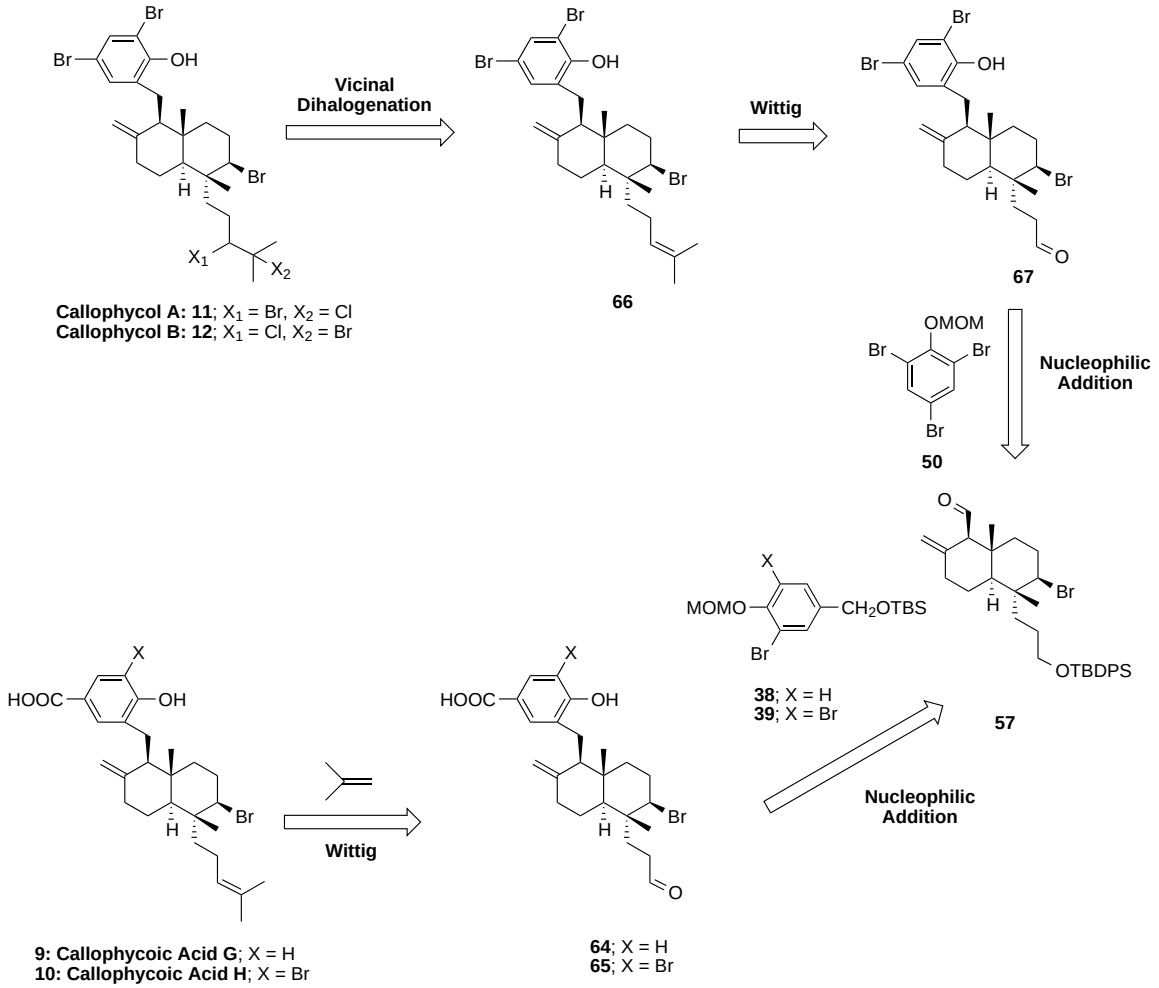

Figure 63: Retrosynthetic analyses of callophycols A and B and callophycoic acids G and H, part 1.

tribromophenol (**50**) (Figure 60) [59, 147]. Therefore, of the 20 steps needed to achieve each of these syntheses, 9 steps have already been completed. As mentioned, investigations of the model systems for callophycols A and B are currently underway, and compounds modeling structures **56** and **57** have been achieved (Figure 60) [59]. Moreover, in regards to the vicinal dihalogenation, a vicinal dihalide was previously synthesized in two steps from the commercially available 6-methyl-5-hepten-2-one (**71**) (Figure 65) [148, 149].

Based on ^{1}H NMR, ^{13}C NMR, and ESI-MS, the bromochloro compound **73** was produced. However, despite the low yields and isolation of both vicinal dihalides,

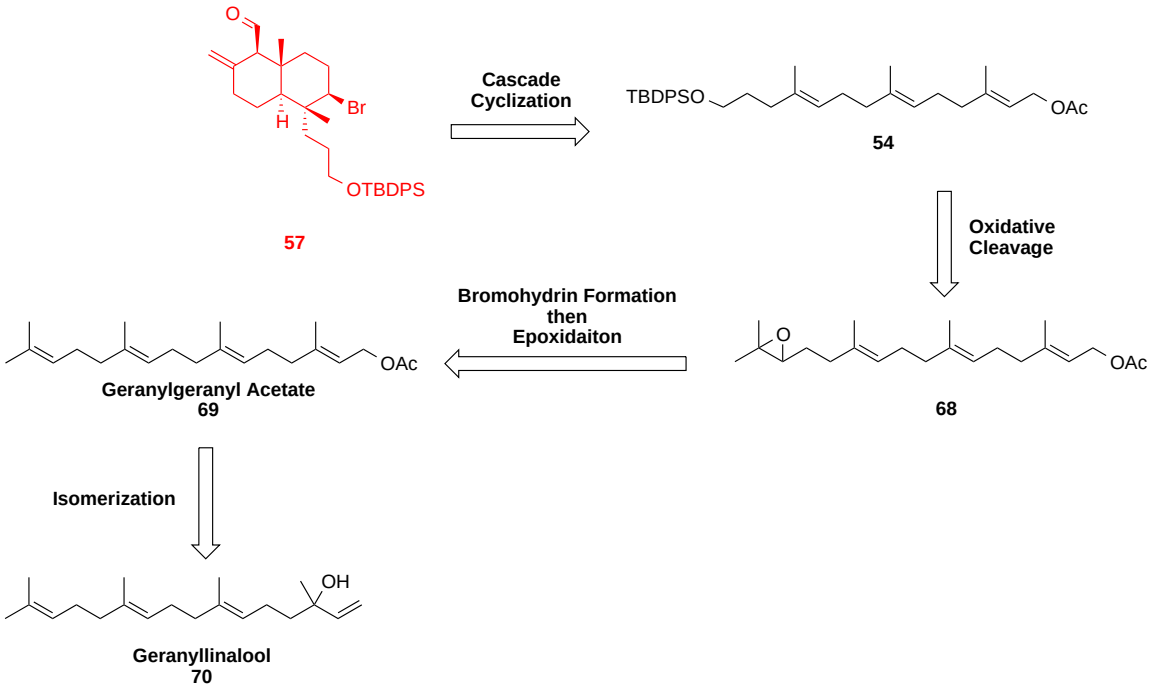

Figure 64: Retrosynthetic analyses of callophycols A and B and callophycoic acids G and H, part 2.

experiments for the vicinal dihalogenation of compound **69** will be conducted to first determine if the above conditions will provide the respective *trans*-decalin precursor for callophycols A and B. If this vicinal dihalogenation is successful, then this will open a pathway to synthesizing callophycols A and B with a fewer number of steps.

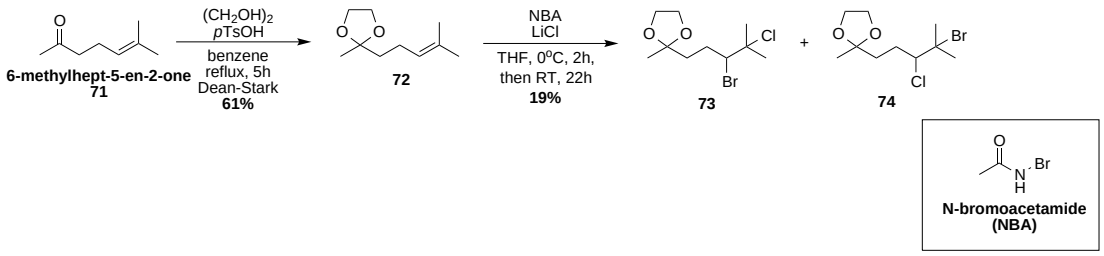

Figure 65: Synthesis of 2-(3-bromo-4-chloro-4-methylpentyl)-2-methyl-1,3-dioxolane [148, 149].

APPENDIX A

CHARACTERIZATION SPECTRA AND EXPERIMENTAL PROTOCOLS FOR COMPOUNDS IN CO(III)-SALEN-CATALYZED HKR AND THE SYNTHESES OF DITERPENES ISOLATED FROM *C. SERRATUS*

A.1 Co(III)-salen-catalyzed HKR (refer to Chapter 2 for the numbering of compounds)

Homogeneous catalysts **1** - **4** were prepared according to previously published procedures [72, 73]. Polymer resin-supported catalyst **8** was prepared according to previously published procedures [81, 82, 83]. Styrene/DVB resin was synthesized according to previously published procedures [82].

A.2 Callophycolide A (1) (refer to Chapter 3 for the numbering of compounds)

Compounds **5**, **6**, **8-12**, **20-22** and **24** were prepared according to previously published procedures [98, 100, 60, 101, 102, 103, 104, 105, 99, 106, 107, 108].

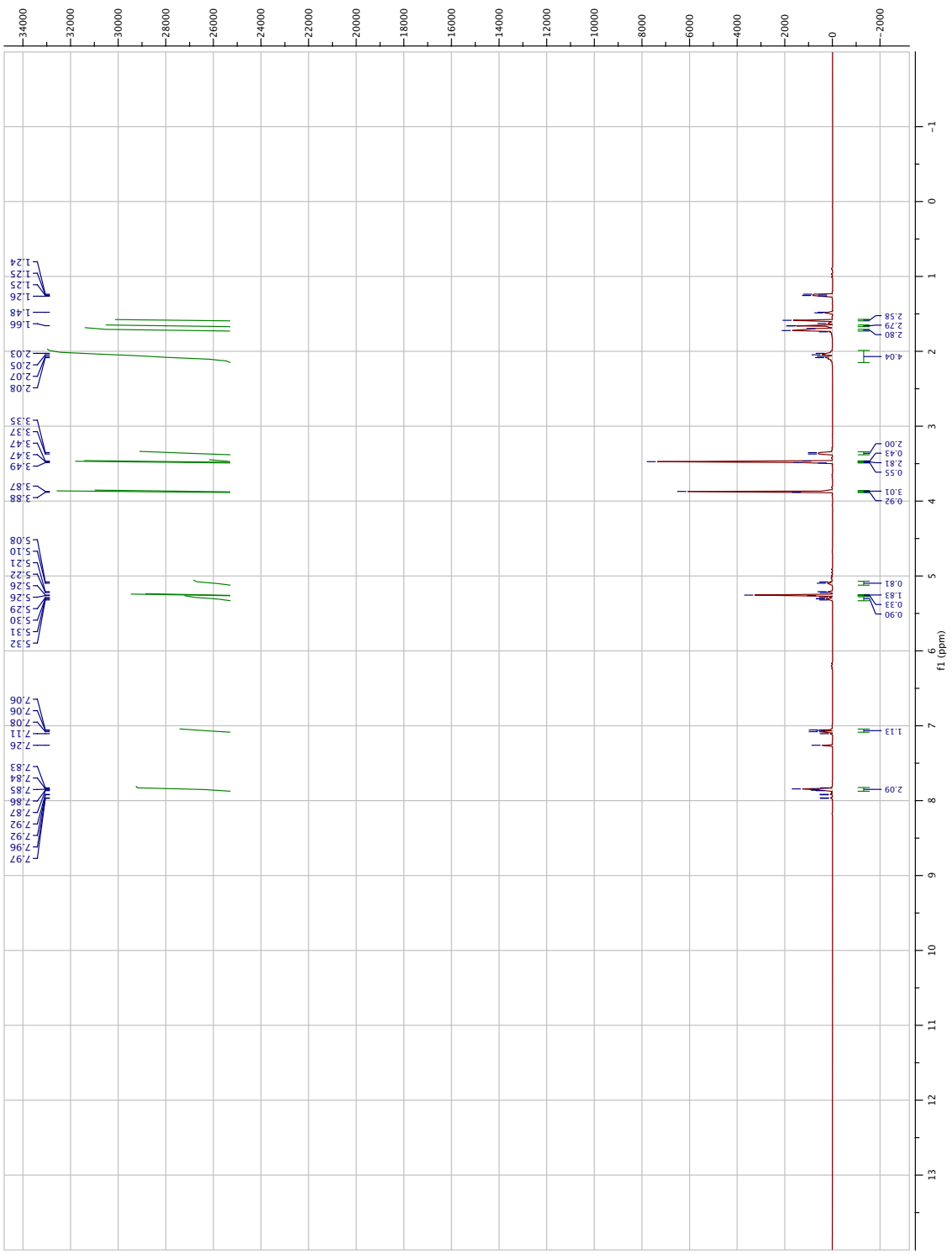

Figure 66: ^{1}H NMR spectrum of methyl (*E*)-3-(3,7-dimethylocta-2,6-dien-1-yl)-4-(methoxymethoxy)benzoate (**15**)

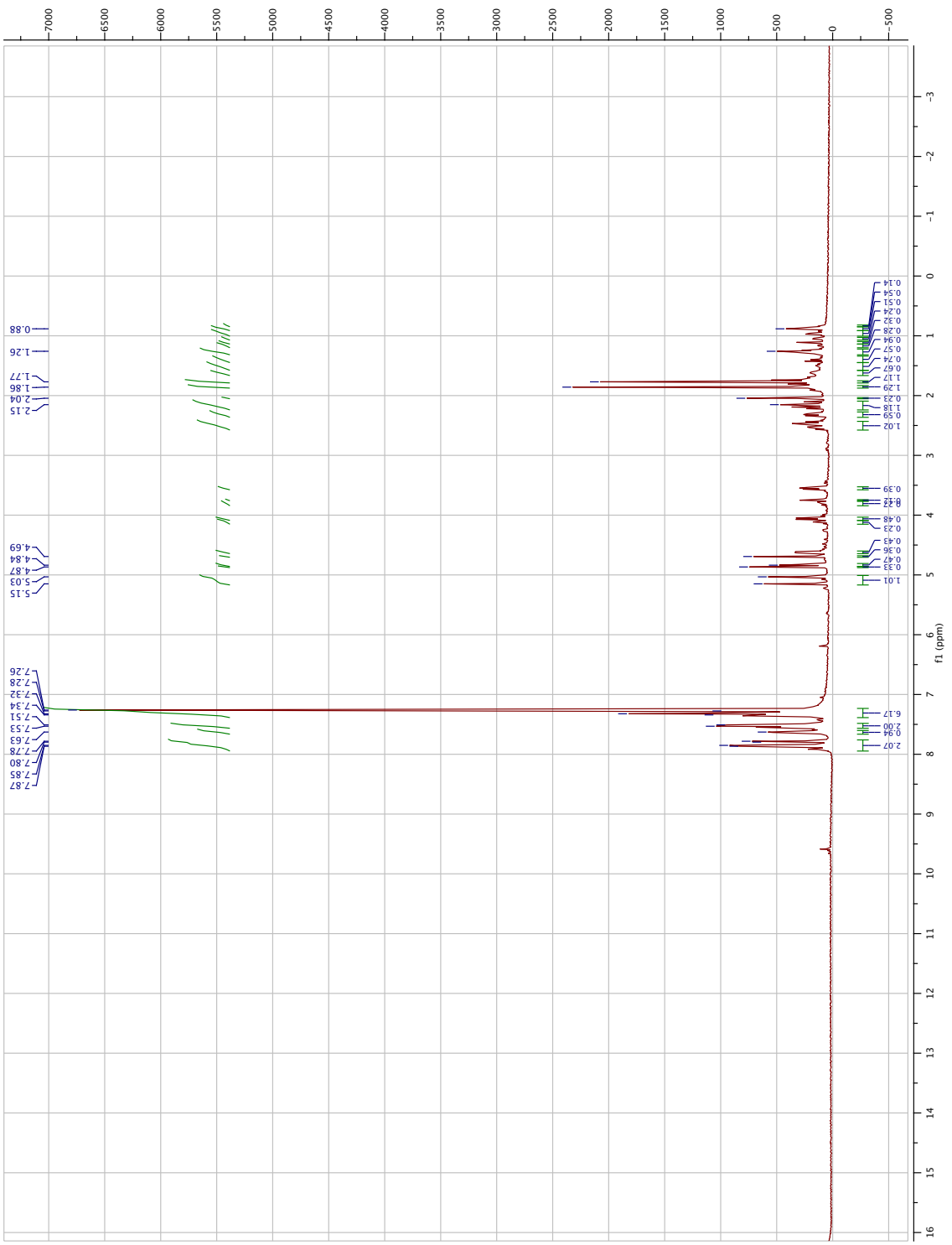

Figure 67: ^{1}H NMR spectrum of 4-methyl-1-phenyl-3-(phenylsulfonyl)pent-4-en-1-ol (**26**).

A.3 Callophycoic Acids G (2) and H (3), refer to Chapter 4 for the numbering of compounds

Compounds **5**, **6**, **8** and **9** were synthesized according to previously published procedures [111, 112].

Compounds **14**, **20** and **24** - **28** were synthesized according to previously published procedures [124, 125, 119, 126, 127, 120].

Compounds **51** - **53** were synthesized according to previously published procedures [59].

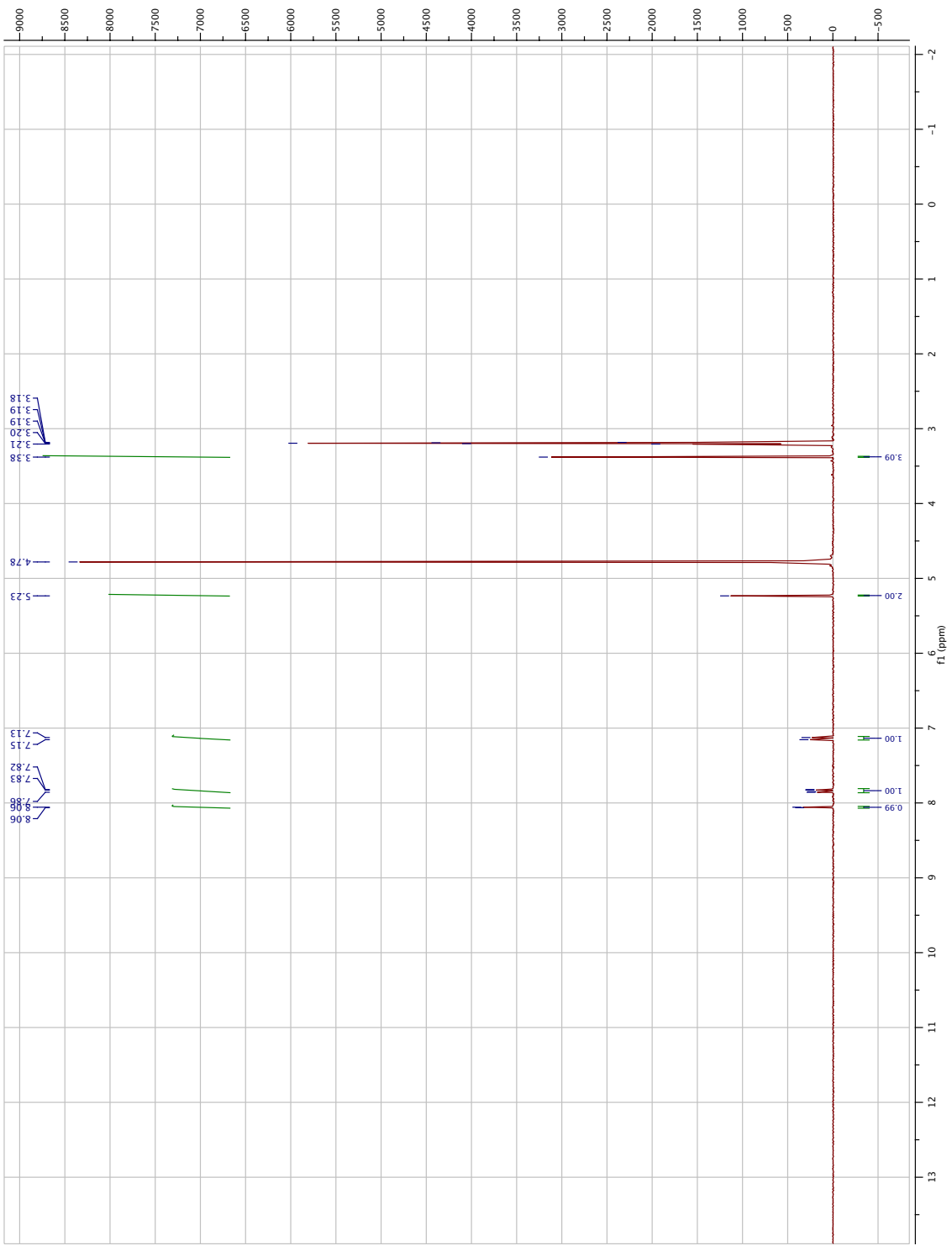

Figure 68: ^{1}H NMR spectrum of 3-bromo-4-methoxymethoxy)benzoic acid (**7**)

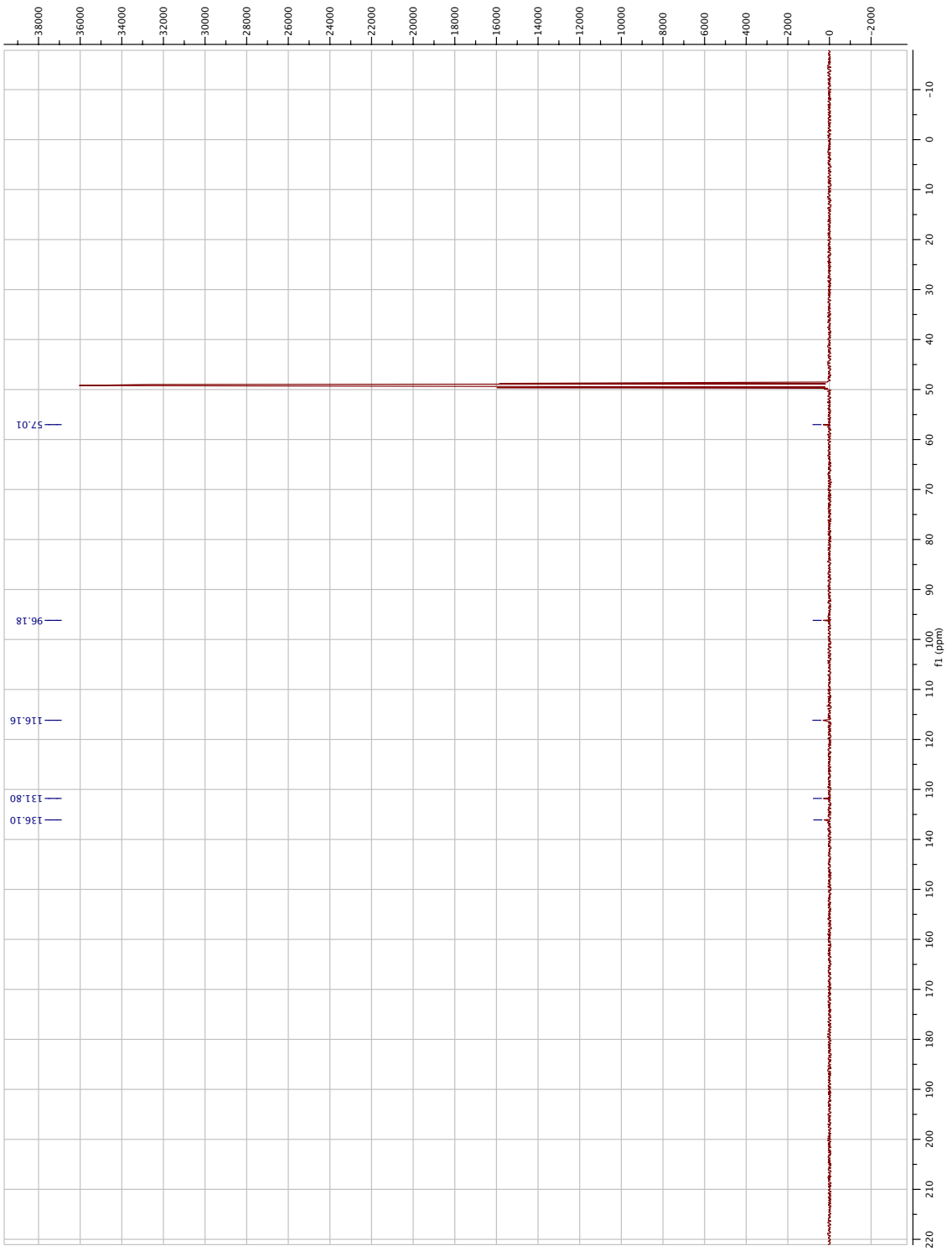

Figure 69: ^{13}C NMR spectrum of 3-bromo-4-methoxymethoxy)benzoic acid (**7**)

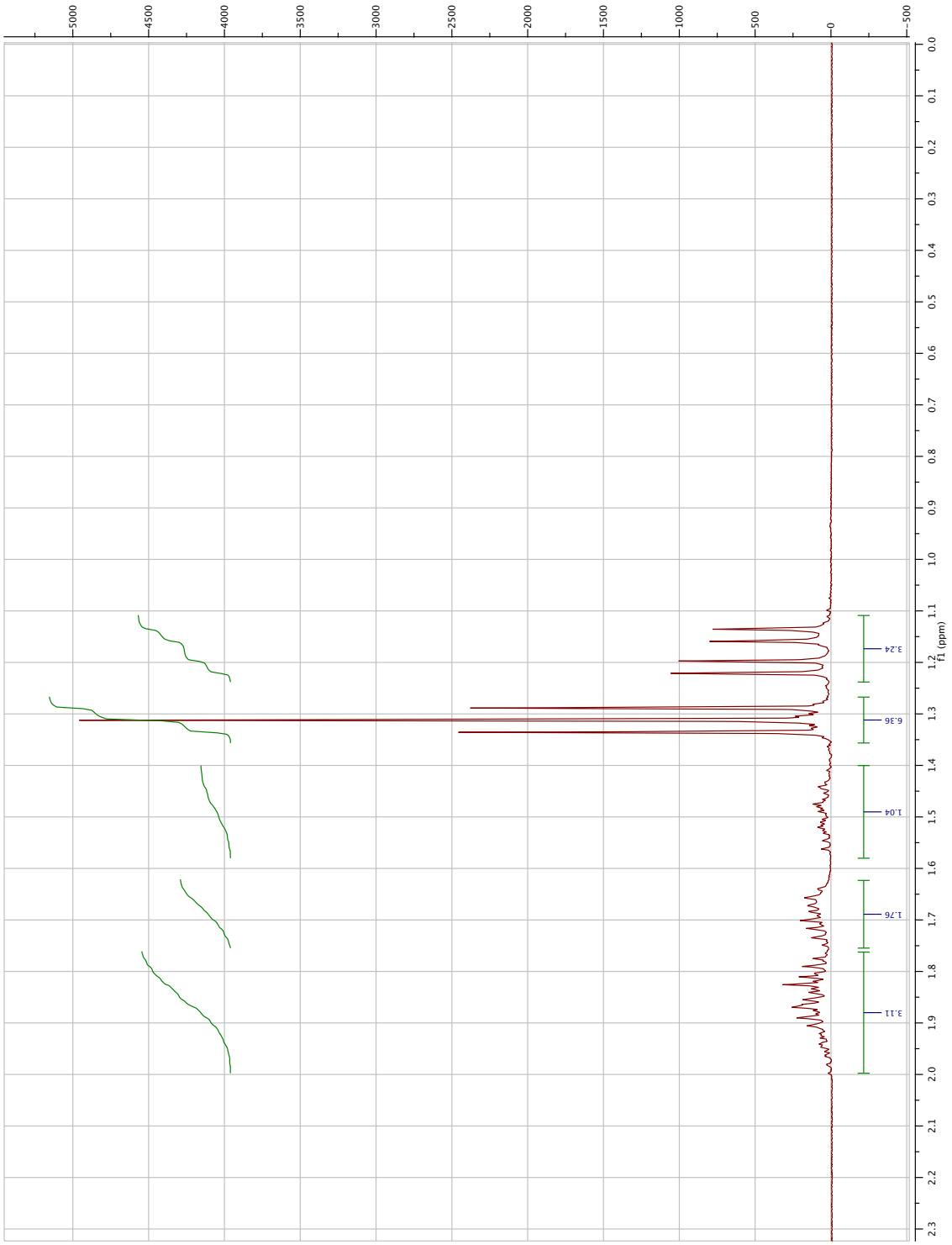

Figure 70: ^{1}H NMR spectrum of diethyl (4-(1,3-dioxolan-2-yl)-butan-2-yl)phosphonate (**37**)

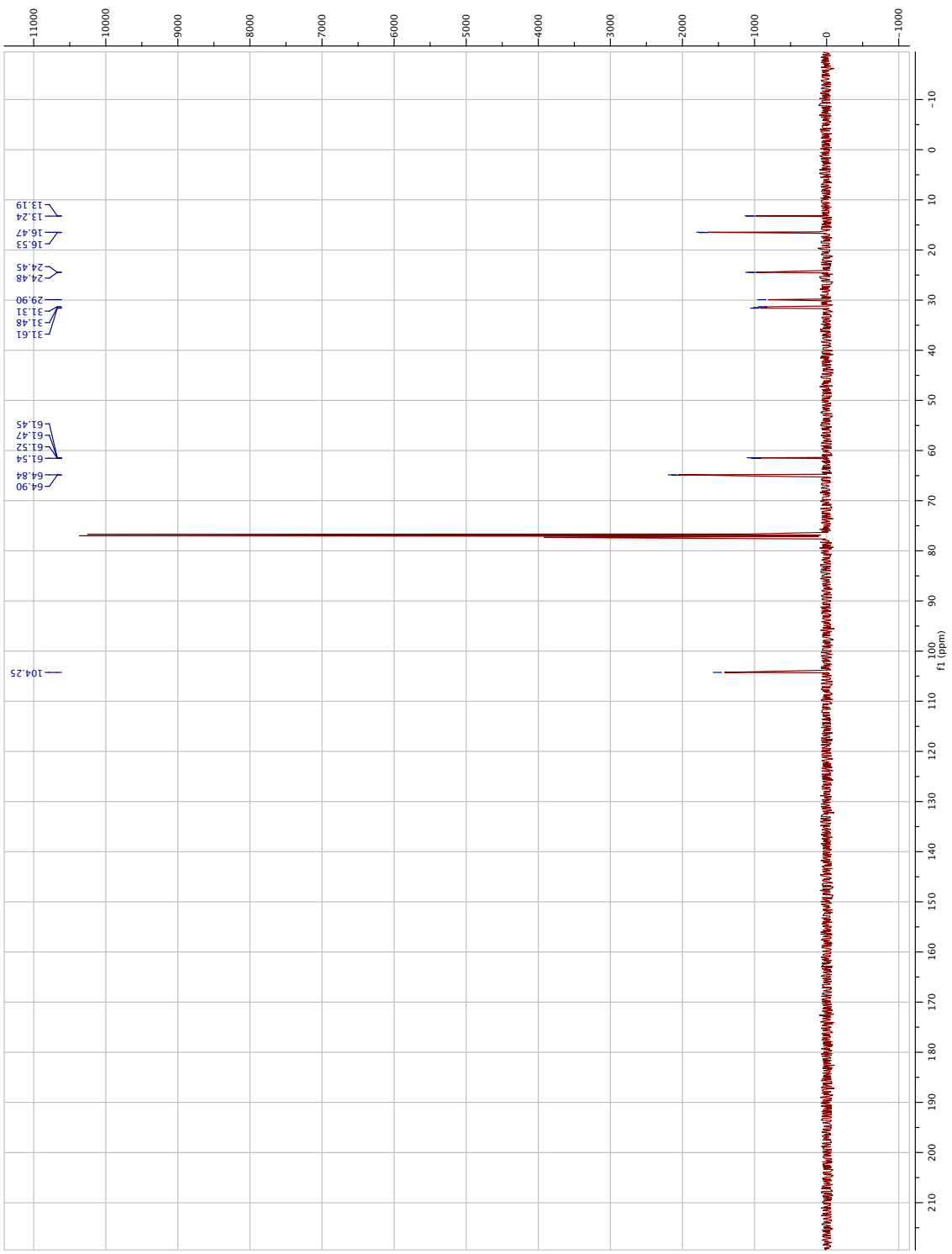

Figure 71: ^{13}C NMR spectrum of diethyl (4-(1,3-dioxolan-2-yl)-butan-2-yl)phosphonate (**37**)

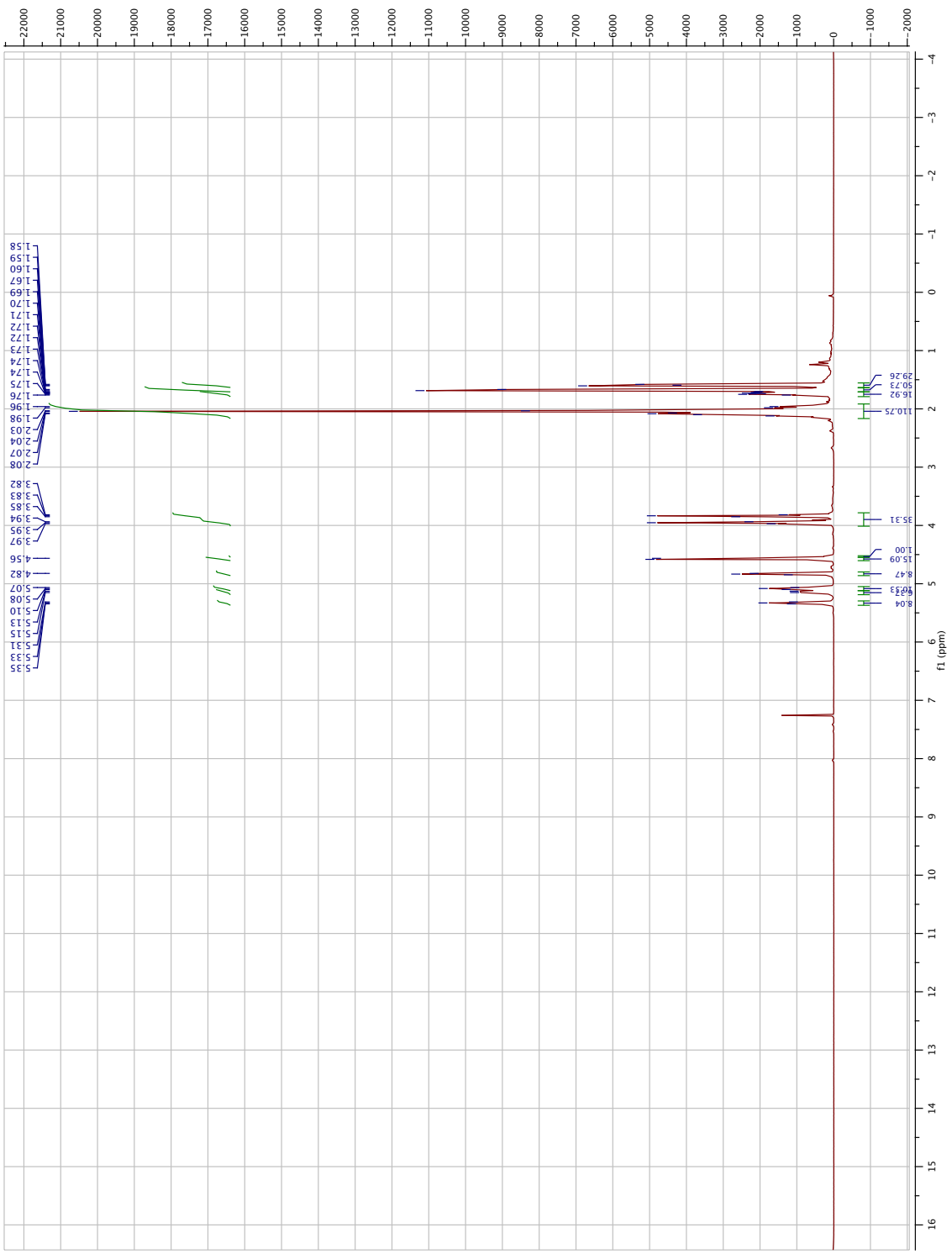

Figure 72: ^{1}H NMR spectrum of (2*E*,6*E*,10*E*)-13-(1,3-dioxolan-2-yl)-3,7,11-trimethyltrideca-2,6,10-trien-1-yl acetate (**39**)

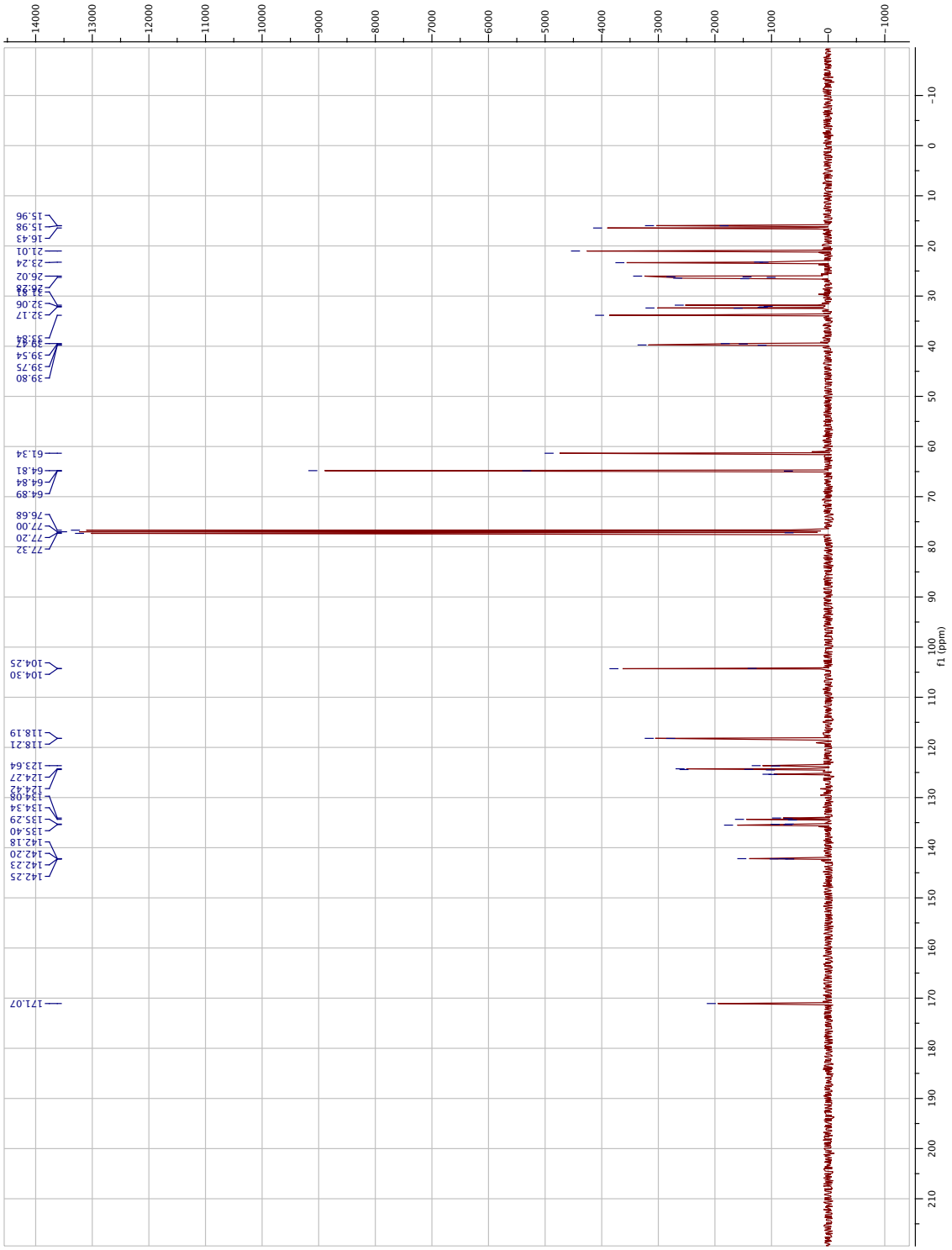

Figure 73: ^{13}C NMR spectrum of (2*E*,6*E*,10*E*)-13-(1,3-dioxolan-2-yl)-3,7,11-trimethyltrideca-2,6,10-trien-1-yl acetate (**39**)

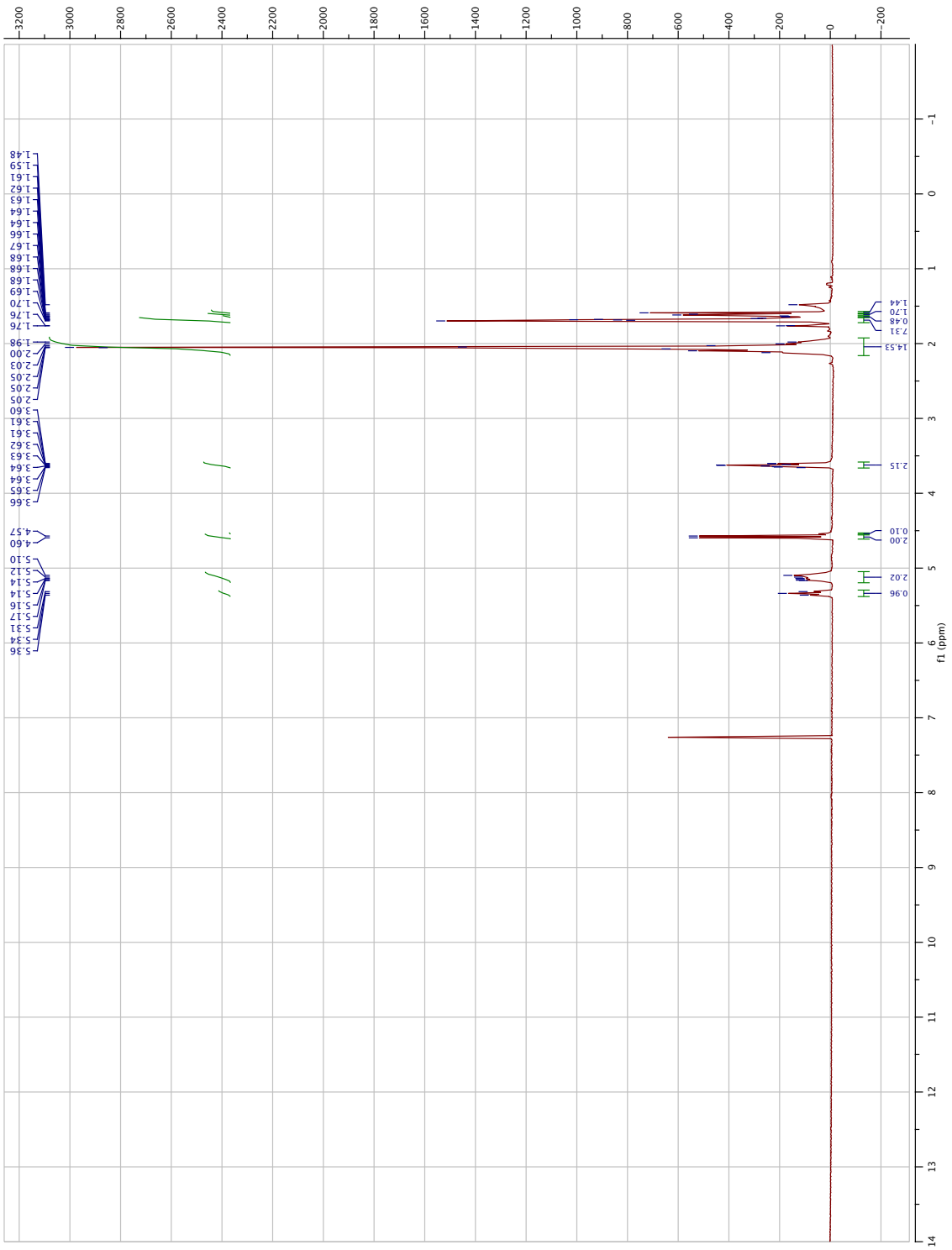

Figure 74: ^{1}H NMR spectrum of (2*E*,6*E*,10*E*)-14-hydroxy-3,7,11-trimethyltetradeca-2,6,10-trien-1-yl acetate (**29**)

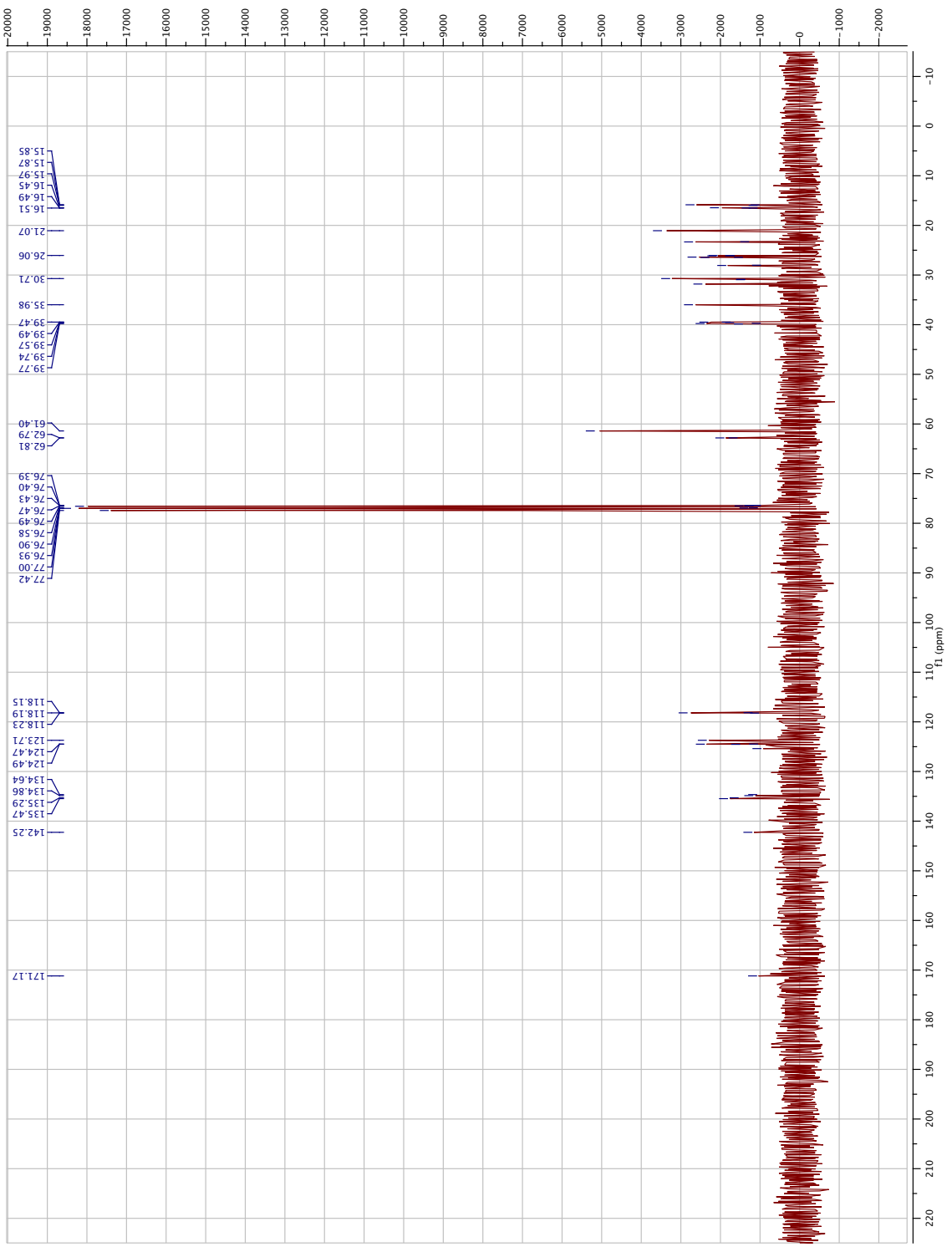

Figure 75: ^{13}C NMR spectrum of (2*E*,6*E*,10*E*)-14-hydroxy-3,7,11-trimethyltetradeca-2,6,10-trien-1-yl acetate (**29**)

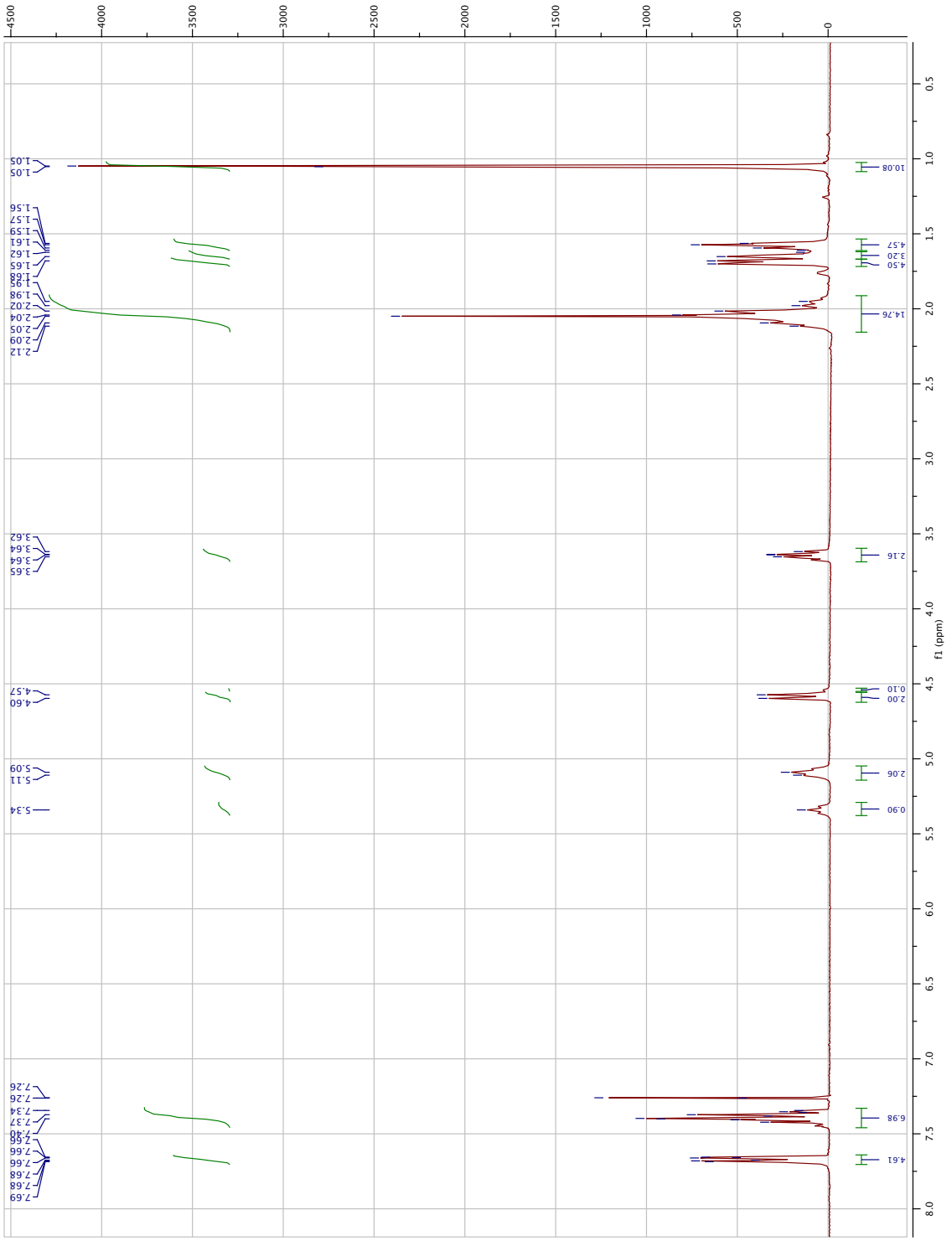

Figure 76: ^{1}H NMR spectrum of (2*E*,6*E*,10*E*)-14-(*tert*-butyldiphenylsilyl)oxy))-3,7,11-trimethyltetradeca-2,6,10-trien-1-yl acetate (**30**)

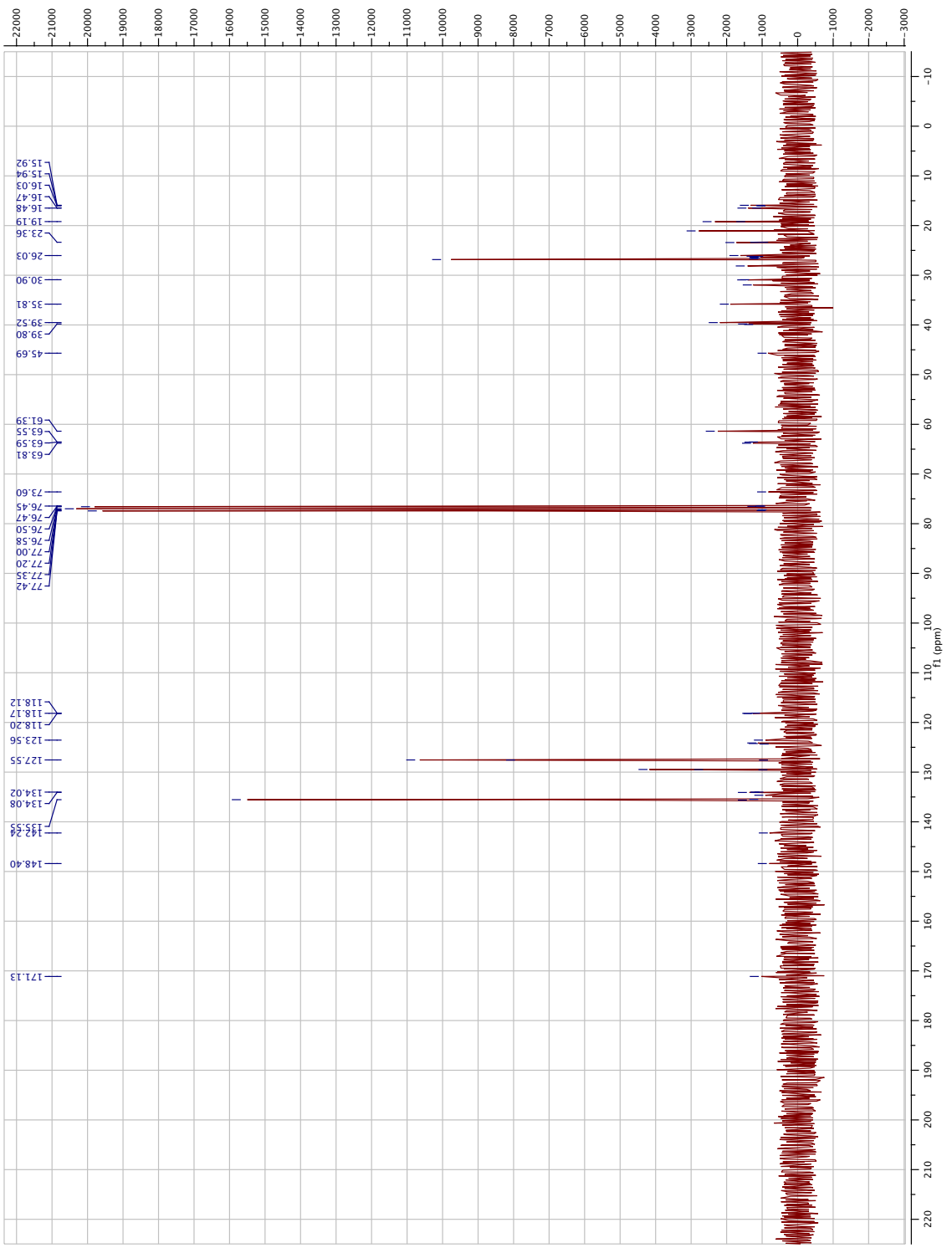

Figure 77: ^{13}C NMR spectrum of (2*E*,6*E*,10*E*)-14-(*tert*-butyldiphenylsilyl)oxy))-3,7,11-trimethyltetradeca-2,6,10-trien-1-yl acetate (**30**)

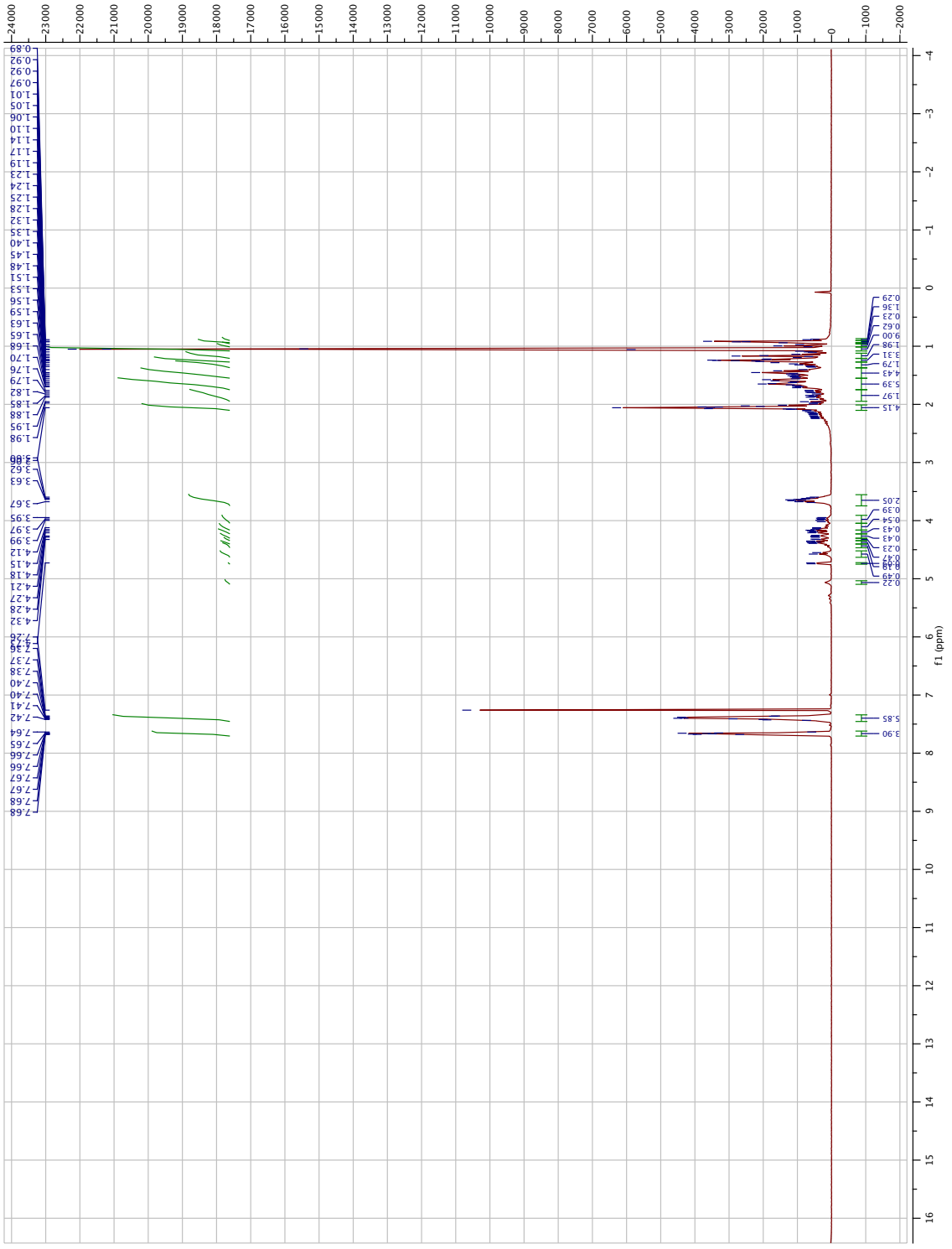

Figure 78: ^{1}H NMR spectrum of (1*R*,2*S*,4a*S*,5*R*,6*R*,8a*R*)-6-bromo-5-(3-((*tert*-butyldiphenylsilyl)oxy)propyl)-2-hydroxy-2,5,8a-trimethyldecahydronaphthalen-1-yl)methyl acetate (**30**)

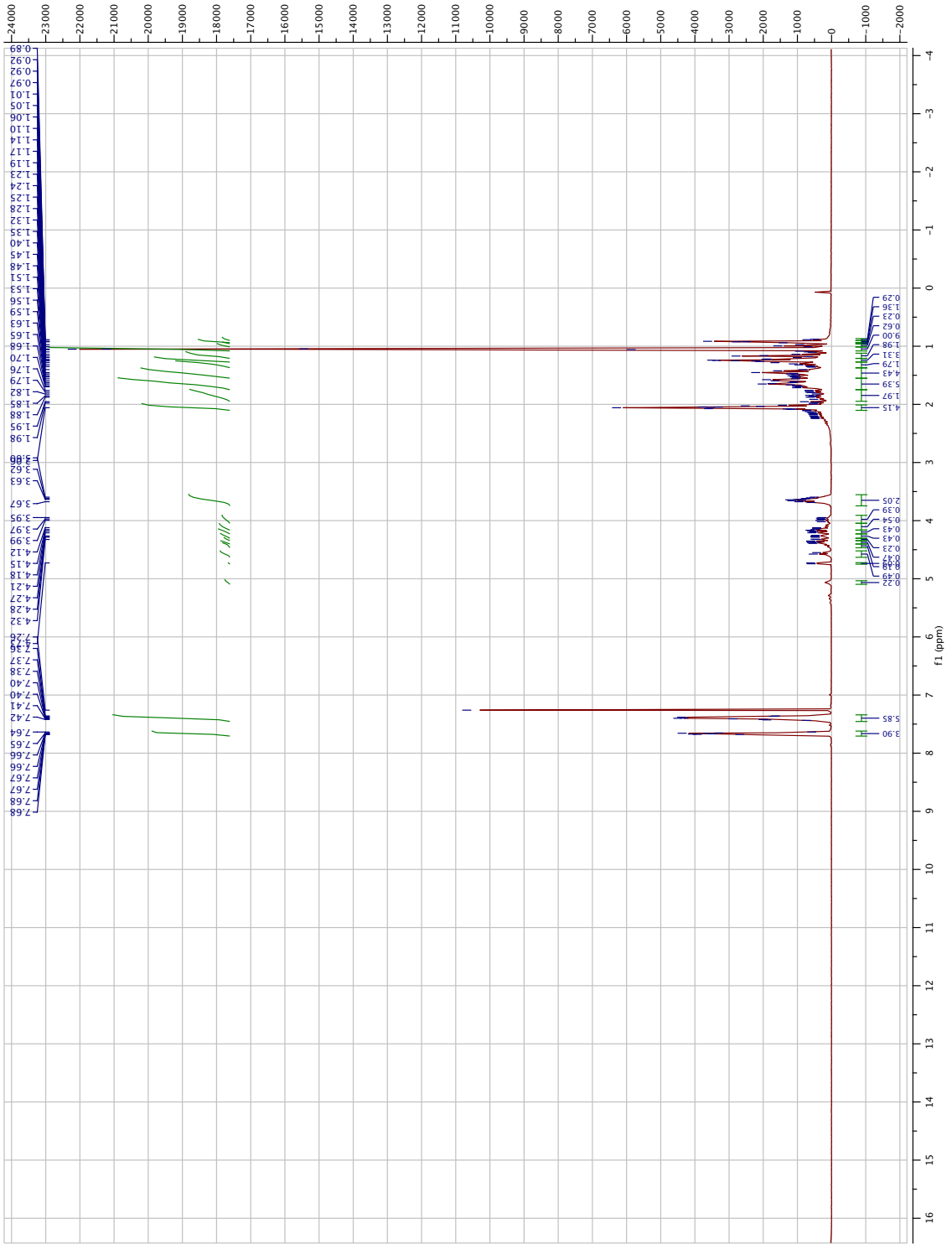

Figure 79: ^{1}H NMR spectrum of (1*R*,2*S*,4a*S*,5*R*,6*R*,8a*R*)-6-bromo-5-(3-((*tert*-butyldiphenylsilyl)oxy)propyl)-2-hydroxy-2,5,8a-trimethyldecahydronaphthalen-1-yl)methyl acetate (**32**).

A.4 Callophycols A (4) and B (5)

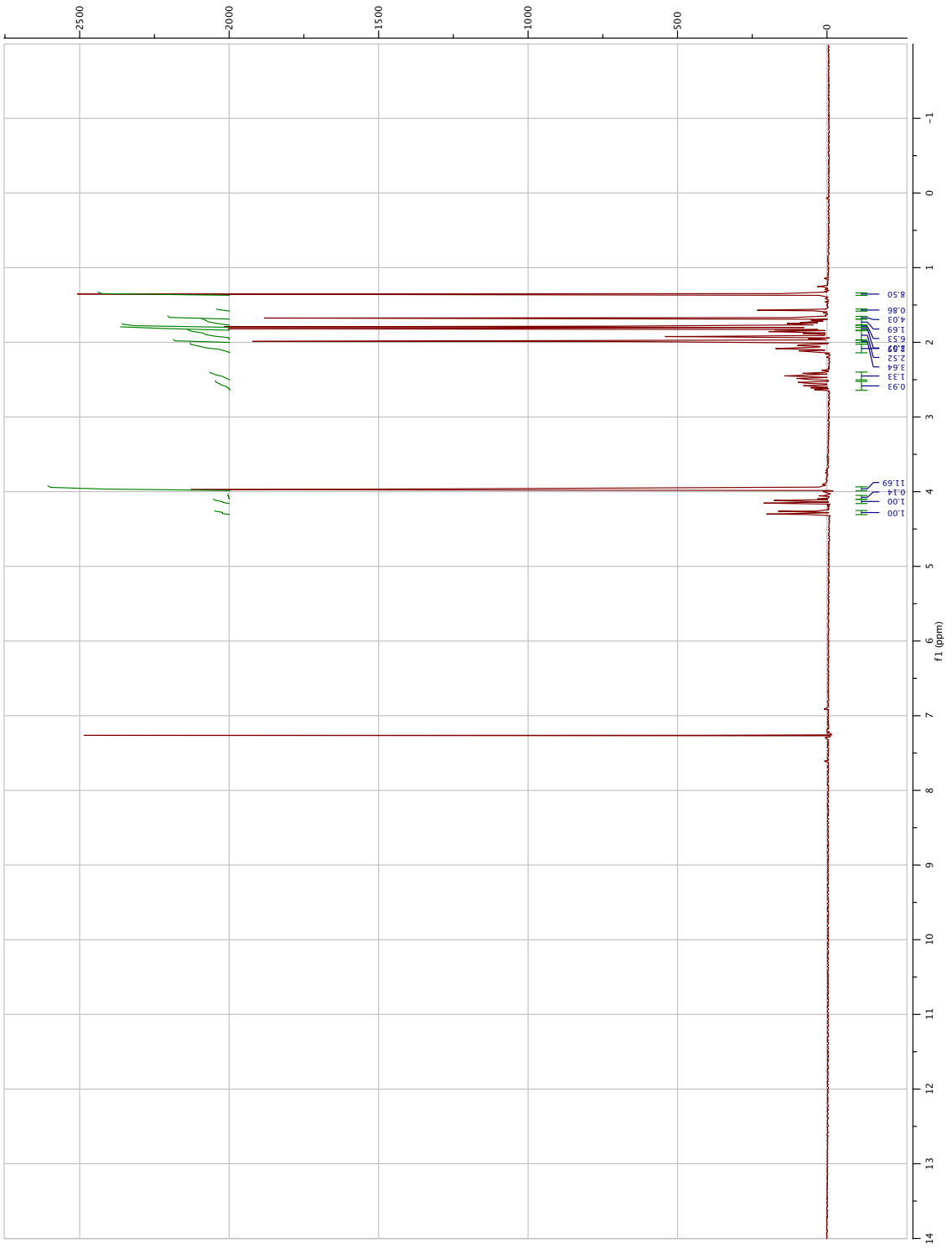

Figure 80: ^{1}H NMR spectrum of 2-(3-bromo-4-chloro-4-methylpentyl)-2-methyl-1,3-dioxolane (**73**)

.

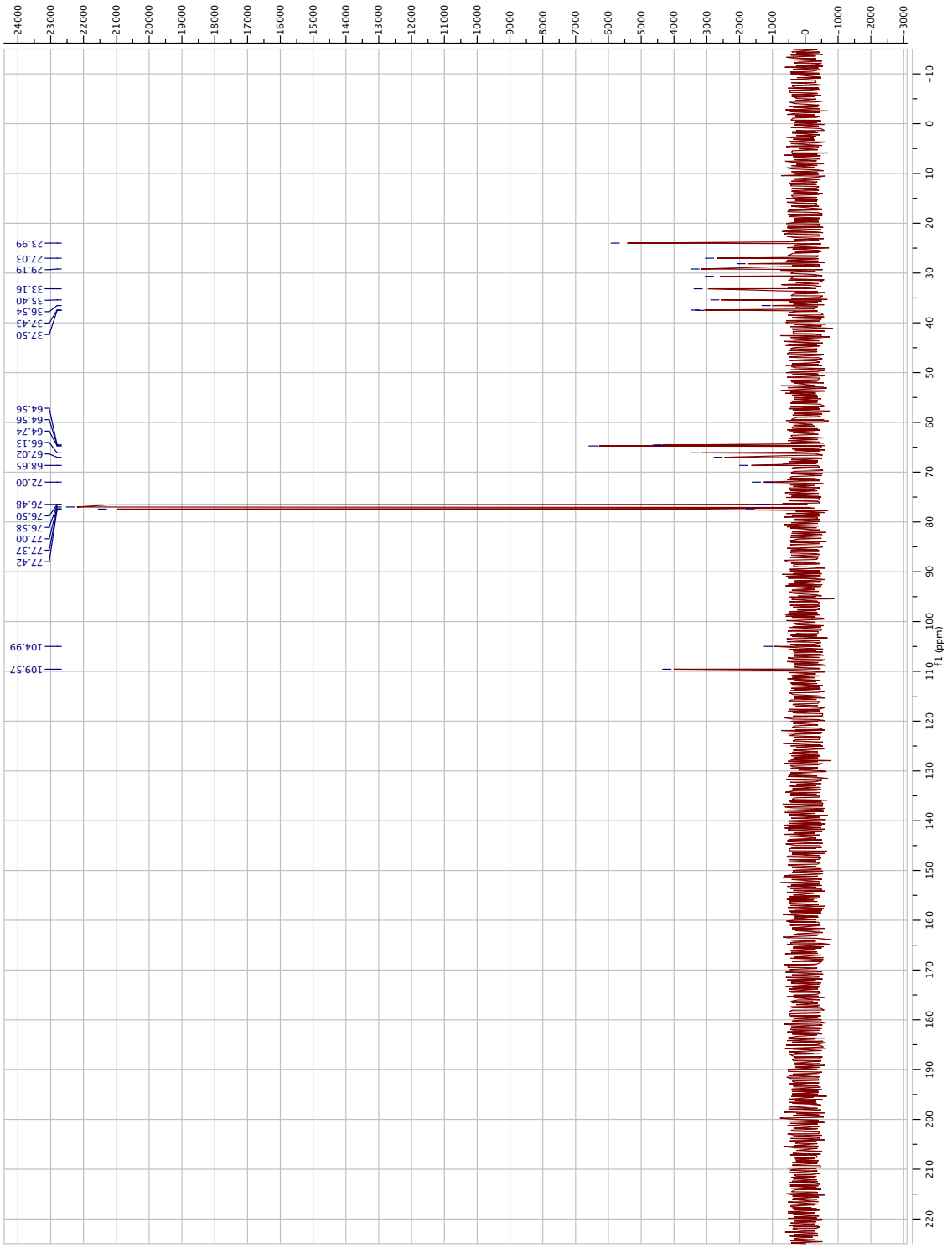

Figure 81: ^{13}C NMR spectrum of 2-(3-bromo-4-chloro-4-methylpentyl)-2-methyl-1,3-dioxolane (**73**)

.

A.5 Experimental Procedures

A.6 General

Reagents were purchased from commercial vendors and used as received unless otherwise stated. All synthesized starting materials were dried under vacuum before use. Anhydrous THF was distilled from Na and benzophenone. All glassware was flame dried and placed under a nitrogen atmosphere prior to use. Purification via flash chromatography was performed using silica gel from Dynamic Adsorbents (32-65μm) and technical grade eluents. Thin-layer chromatography (TLC) was conducted using EMD silica gel 60 F_{254} glass-backed plates. Plate visualization was accomplished using vanillin staining. NMR spectra were obtained using either a Varian Mercury Vx spectrometer (300 or 400 MHz) or a Bruker AVII (400 or 500 MHz) spectrometer; the chemical shifts were expressed in ppm and are referenced to the corresponding residual nuclei in the deuterated solvents. ESI-MS/accurate mass was performed using a ThermoFisher Scientific LTQ Orbitrap XL ETD, and EI/accurate mass analyses were performed using a Micromass AutoSpec M.

A.6.1 Synthesis of 2-(3-bromo-4-chloro-4-methylpentyl)-2-methyl-1,3-dioxolane (73).

To a round-bottom flask was added *N*-bromoacetamide (0.2028 g, 1.47 mmol), LiCl (62.3 mg, 1.47 mmol), and anhydrous THF (1.8 mL). The flask was cooled to 0°C, and the reaction was allowed to stir at 0°C for 2 h and then at room temperature for 22 h. Upon completion, the reaction mixture was concentrated under reduced pressure, and the residue was diluted with ether, extracted with ether, washed with brine, dried with anhydrous Na_2SO_4, and concentrated under reduced pressure. Purification using silica gel and 3-4% EtOAc/hexanes afforded impure compound **73** (19% yield). ^{1}H NMR ($CDCl_3$, 300 MHz) δ 4.32-4.26 (dd, 1H), δ 4.16-4.11 (dd, 1H), δ 3.98-3.94 (m, 8H), δ 2.63-2.52 (m, 1H), δ2.52-2.40 (m, 1H), δ 2.34-2.20 (m, 2H), δ 1.92 (s, 3H), δ

1.96-1.83 (m, 2H), δ 1.82 (m, 3H), δ 1.78 (s, 6H), δ 1.76-1.68 (m, 2H), δ 1.65 (s, 3H), δ 1.35 (d, 6H). ^{13}C NMR ($CDCl_3$, 300 MHz) δ 109.75 δ 72.042, δ 68.644, δ 67.018, δ 66.132, δ 64.740, δ 64.550, δ 37.497, δ 37.431, δ 33.161, δ 30.657, δ 29.185, δ 28.123, δ 27.024, δ 23.985. HRMS (ESI) $[M + H]^+$ Calc for $C_{10}H_{19}O_2BrCl$, 285.0251, found 285.0253.

REFERENCES

[1] Carter, R. and Mendis, K. N., "Evolutionary and historical aspects of the burden of malaria," *Clinical Microbiology Reviews*, vol. 15, p. 564, 2002.

[2] Varki, A. and Gagneux, P., "Human-specific evolution of sialic acid targets: Explaining the malignant malaria mystery?," *Proceedings of the National Academy of Sciences U.S.A.*, vol. 106, no. 35, pp. 14739–14740, 2009.

[3] Snow, R. W., Guerra, C. A., Noor, A. M., Myint, H. Y., and Hay, S. I., "The global distribution of clinical episodes of plasmodium falciparum malaria," *Nature*, vol. 434, no. 7030, pp. 214–217, 2005.

[4] Salas, P. F., Herrmann, C., and Orvig, C., "Metalloantimalarials," *Chemical Reviews*, vol. 113, no. 5, pp. 3450–3492, 2013.

[5] Stout, E. P., Cervantes, S., Prudhomme, J., France, S., La Clair, J. J., Le Roch, K., and Kubanek, J., "Bromophycolide a targets heme crystallization in the human malaria parasite plasmodium falciparum," *ChemMedChem*, vol. 6, no. 9, pp. 1572–1577, 2011.

[6] Kaur, K., Jain, M., Kaur, T., and Jain, R., "Antimalarials from nature," *Bioorganic & Medicinal Chemistry*, vol. 17, no. 9, pp. 3229–3256, 2009.

[7] "Malaria." http://www.cdc.gov/dpdx/malaria/. Accessed: 2015-07-01.

[8] Su, X., Hayton, K., and Wellems, T. E., "Genetic linkage and association analyses for trait mapping in plasmodium falciparum," *Nature Reviews Genetics*, vol. 8, pp. 497–506, 07 2007.

[9] Goldberg, D. E., Slater, A. F., Cerami, A., and Henderson, G. B., "Hemoglobin degradation in the malaria parasite plasmodium falciparum: an ordered process in a unique organelle," *Proceedings of the National Academy of Sciences*, vol. 87, no. 8, pp. 2931–2935, 1990.

[10] Rosenthal, P. J. and Meshnick, S. R., "Hemoglobin catabolism and iron utilization by malaria parasites," *Molecular and Biochemical Parasitology*, vol. 83, no. 2, pp. 131–139, 1996.

[11] Rosenthal, P., ed., *Antimalarial Chemotherapy. Mechanisms of Action, Resistance and New Directions in Drug Discovery*, vol. 51. Humana Press, 2001.

[12] Greenwood, B. and Mutabingwa, T., "Malaria in 2002," *Nature*, vol. 415, pp. 670–672, 02 2002.

[13] "Weekly epidemiological record-malaria, 1982-1997," Tech. Rep. 32. World Health Organization.

[14] "The Africa malaria report 2003," tech. rep. World Health Organization.

[15] Murray, C. J. L., Rosenfeld, L. C., Lim, S. S., Andrews, K. G., Foreman, K. J., Haring, D., Fullman, N., Naghavi, M., Lozano, R., and Lopez, A. D., "Global malaria mortality between 1980 and 2010: a systematic analysis," *Lancet*, vol. 379, no. 9814, pp. 413–431, 2012.

[16] "Malaria vector control and personal protection," tech. rep., 2006. World Health Organization.

[17] "World malaria report 2010," tech. rep., 2010. World Health Organization.

[18] Newman, D. J. and Cragg, G. M., "Natural products as sources of new drugs over the last 25 years," *Journal of Natural Products*, vol. 70, no. 3, pp. 461–477, 2007.

[19] Olliaro, P., "Mode of action and mechanisms of resistance for antimalarial drugs," *Pharmacology & Therapeutics*, vol. 89, no. 2, pp. 207 – 219, 2001.

[20] Hyde, J. E., "Drug-resistant malaria," *Trends in Parasitology*, vol. 21, no. 11, pp. 494–498, 2005.

[21] Meshnick, S. R. and Dobson, M. J., *The history of antimalarial drugs*. Humana Press, 2001.

[22] Winstanley, P. and Ward, S., "Malaria chemotherapy," in *Control of Human Parasitic Diseases* (Molyneux, D. H., ed.), vol. 61 of *Advances in Parasitology*, pp. 47 – 76, Academic Press, 2006.

[23] Egan, T. J., "Quinoline antimalarials," *Expert Opinion on Therapeutic Patents*, vol. 11, no. 2, pp. 185–209, 2001.

[24] Wiesner, J., Ortmann, R., Jomaa, H., and Schlitzer, M., "New antimalarial drugs," *Angewandte Chemie International Edition*, vol. 42, no. 43, pp. 5274–5293, 2003.

[25] Tilley, L., Loria, P., and Foley, M. Humana Press, 2001.

[26] Zarchin, S., Krugliak, M., and Ginsburg, H., "Digestion of the host erythrocyte by malaria parasites is the primary target for quinolinecontaining antimalarials," *Biochemical Pharmacology*, vol. 35, no. 14, pp. 2435 – 2442, 1986.

[27] Krugliak, M., Zhang, J., and Ginsburg, H., "Intraerythrocytic plasmodium falciparum utilizes only a fraction of the amino acids derived from the digestion of host cell cytosol for the biosynthesis of its proteins," *Molecular and Biochemical Parasitology*, vol. 119, no. 2, pp. 249 – 256, 2002.

[28] Srivastava, P. and Pandey, V. C., "Heme oxygenase and related indices in chloroquine-resistant and -sensitive strains of plasmodium berghei," *International Journal for Parasitology*, vol. 25, no. 9, pp. 1061 – 1064, 1995.

[29] Pagola, S., Stephens, P. W., Bohle, D. S., Kosar, A. D., and Madsen, S. K., "The structure of malaria pigment [beta]-haematin," *Nature*, vol. 404, pp. 307–310, March 2000.

[30] Bohle, D. S., Kosar, A. D., and Madsen, S. K., "Propionic acid side chain hydrogen bonding in the malaria pigment -hematin," *Biochemical and Biophysical Research Communications*, vol. 294, no. 1, pp. 132 – 135, 2002.

[31] Bohle, D. S., Kosar, A. D., and Stephens, P. W., "Phase homogeneity and crystal morphology of the malaria pigment β-hematin," *Acta Crystallographica Section D*, vol. 58, pp. 1752–1756, Oct 2002.

[32] Rangarajan, P. N. and Padmanaban, G., "Emerging targets for antimalarial drugs," *Expert Opinion on Therapeutic Targets*, vol. 5, no. 4, pp. 423–441, 2001. PMID: 12540258.

[33] Dorn, A., Vippagunta, S. R., Matile, H., Bubendorf, A., Vennerstrom, J. L., and Ridley, R. G., "A comparison and analysis of several ways to promote haematin (haem) polymerisation and an assessment of its initiation in vitro," *Biochemical Pharmacology*, vol. 55, no. 6, pp. 737 – 747, 1998.

[34] Sullivan Jr., D. J., Matile, H., Ridley, R. G., and Goldberg, D. E., "A common mechanism for blockade of heme polymerization by antimalarial quinolines," *J. Biol. Chem.*, vol. 273, p. 31103, 1998.

[35] Weissbuch, I. and Leiserowitz, L., "Interplay between malaria, crystalline hemozoin formation, and antimalarial drug action and design," *Chemical Reviews*, vol. 108, no. 11, pp. 4899–4914, 2008. PMID: 19006402.

[36] Mita, T., Tanabe, K., and Kita, K., "Spread and evolution of plasmodium falciparum drug resistance," *Parasitology International*, vol. 58, no. 3, pp. 201 – 209, 2009.

[37] Hien, T. T., White, N. J., and White, "Qinghaosu," *The Lancet*, vol. 341, no. 8845, pp. 603 – 608, 1993. Originally published as Volume 1, Issue 8845.

[38] Schlitzer, M., "Antimalarial drugs – what is in use and what is in the pipeline," *Archiv der Pharmazie*, vol. 341, no. 3, pp. 149–163, 2008.

[39] Basco, L. K. and Bras, J. L., "In vitro activity of artemisinin derivatives against African isolates and clones of plasmodium falciparum," *The American Journal of Tropical Medicine and Hygiene*, vol. 49, no. 3, pp. 301–307, 1993.

[40] "Guidelines for the treatment of malaria," tech. rep., 2010. World Health Organization.

[41] Price, R. N., "Artemisinin drugs: novel antimalarial agents," *Expert Opinion on Investigational Drugs*, vol. 9, no. 8, pp. 1815–1827, 2000. PMID: 11060779.

[42] "Global report on antimalarial drug efficacy and drug resistance: 2000-2010," tech. rep., 2010. World Health Organization.

[43] "Malaria and travelers." www.cdc.gov/malaria/travelers/. Accessed: 2015-07-01.

[44] Bhisutthiban, J., Pan, X.-Q., Hossler, P. A., Walker, D. J., Yowell, C. A., Carlton, J., Dame, J. B., and Meshnick, S. R., "The plasmodium falciparum translationally controlled tumor protein homolog and its reaction with the antimalarial drug artemisinin," *J. Biol. Chem.*, vol. 273, no. 16192, 1998.

[45] Meshnick, S. R., "Artemisinin: mechanisms of action, resistance and toxicity," *International Journal for Parasitology*, vol. 32, no. 13, pp. 1655 – 1660, 2002. Malaria Progress, Problems and Plans in the Genomic Era.

[46] Enserink, M., "Malaria's drug miracle in danger," *Science*, vol. 328, pp. 844–846, 2010.

[47] "Global plan for artemisinin resistance containment (gparc)," tech. rep., 2010. World Health Organization.

[48] Uys, A. C. U., Malan, S. F., van Dyk, S., and van Zyl, R. L., "Antimalarial compounds from parinari capensis," *Bioorganic & Medicinal Chemistry Letters*, vol. 12, no. 16, pp. 2167 – 2169, 2002.

[49] Ospina, C. A., Rodríguez, A. D., Ortega-Barria, E., and Capson, T. L., "Briarellins jp and polyanthellin a: new eunicellin-based diterpenes from the gorgonian coral briareum polyanthes and their antimalarial activity," *Journal of Natural Products*, vol. 66, no. 3, pp. 357–363, 2003. PMID: 12662092.

[50] Kubanek, J., Prusak, A. C., Snell, T. W., Giese, R. A., Hardcastle, K. I., Fairchild, C. R., Aalbersberg, W., Raventos-Suarez, C., and Hay, M. E., "Antineoplastic diterpenebenzoate macrolides from the fijian red alga callophycus serratus," *Organic Letters*, vol. 7, no. 23, pp. 5261–5264, 2005.

[51] Kubanek, J., Prusak, A. C., Snell, T. W., Giese, R. A., Fairchild, C. R., Aalbersberg, W., and Hay, M. E., "Bromophycolides ci from the fijian red alga callophycus serratus," *Journal of Natural Products*, vol. 69, no. 5, pp. 731–735, 2006.

[52] Lane, A. L., Stout, E. P., Lin, A.-S., Prudhomme, J., Le Roch, K., Fairchild, C. R., Franzblau, S. G., Hay, M. E., Aalbersberg, W., and Kubanek, J., "Antimalarial bromophycolides jq from the fijian red alga callophycus serratus," *The Journal of Organic Chemistry*, vol. 74, no. 7, pp. 2736–2742, 2009.

[53] Lin, A.-S., Stout, E. P., Prudhomme, J., Roch, K. L., Fairchild, C. R., Franzblau, S. G., Aalbersberg, W., Hay, M. E., and Kubanek, J., "Bioactive bromophycolides ru from the fijian red alga callophycus serratus," *Journal of Natural Products*, vol. 73, no. 2, pp. 275–278, 2010.

[54] Stout, E. P., Prudhomme, J., Roch, K. L., Fairchild, C. R., Franzblau, S. G., Aalbersberg, W., Hay, M. E., and Kubanek, J., "Unusual antimalarial meroditerpenes from tropical red macroalgae," *Bioorganic & Medicinal Chemistry Letters*, vol. 20, no. 19, pp. 5662–5665, 2010.

[55] Lane, A. L., Stout, E. P., Hay, M. E., Prusak, A. C., Hardcastle, K., Fairchild, C. R., Franzblau, S. G., Le Roch, K., Prudhomme, J., Aalbersberg, W., and Kubanek, J., "Callophycoic acids and callophycols from the fijian red alga callophycus serratus," *The Journal of Organic Chemistry*, vol. 72, no. 19, pp. 7343–7351, 2007.

[56] Teasdale, M. E., Shearer, T. L., Engel, S., Alexander, T. S., Fairchild, C. R., Prudhomme, J., Torres, M., Le Roch, K., Aalbersberg, W., Hay, M. E., and Kubanek, J., "Bromophycoic acids: Bioactive natural products from a fijian red alga callophycus sp," *The Journal of Organic Chemistry*, vol. 77, no. 18, pp. 8000–8006, 2012.

[57] Lin, H., Pochapsky, S. S., and Krauss, I. J., "A short asymmetric route to the bromophycolide a and d skeleton," *Organic Letters*, vol. 13, no. 5, pp. 1222–1225, 2011.

[58] Butler, A. and Carter-Franklin, J. N., "The role of vanadium bromoperoxidase in the biosynthesis of halogenated marine natural products," *Natural Product Reports*, vol. 21, pp. 180–188, 2004.

[59] Snyder, S. A., Treitler, D. S., and Brucks, A. P., "Simple reagents for direct halonium-induced polyene cyclizations," *Journal of the American Chemical Society*, vol. 132, no. 40, pp. 14303–14314, 2010.

[60] Snyder, S. A. and Treitler, D. S., "Et2sbrsbcl5br: An effective reagent for direct bromonium-induced polyene cyclizations," *Angewandte Chemie International Edition*, vol. 48, no. 42, pp. 7899–7903, 2009.

[61] Tokunaga, M., Larrow, J. F., Kakiuchi, F., and Jacobsen, E. N., "Asymmetric catalysis with water: Efficient kinetic resolution of terminal epoxides by means of catalytic hydrolysis," *Science*, vol. 277, no. 5328, pp. 936–938, 1997.

[62] Schaus, S. E., Brandes, B. D., Larrow, J. F., Tokunaga, M., Hansen, K. B., Gould, A. E., Furrow, M. E., and Jacobsen, E. N., "Highly selective hydrolytic kinetic resolution of terminal epoxides catalyzed by chiral (salen)coiii complexes. practical synthesis of enantioenriched terminal epoxides and 1,2-diols," *Journal of the American Chemical Society*, vol. 124, no. 7, pp. 1307–1315, 2002.

[63] Kumar, P., Naidu, V., and Gupta, P., "Application of hydrolytic kinetic resolution (hkr) in the synthesis of bioactive compounds," *Tetrahedron*, vol. 63, no. 13, pp. 2745–2785, 2007.

[64] Carey, F. A. and Sundberg, R. J., *Stereochemistry, Conformation, and Stereoselectivity*. Springer Science+Business Media, LLC, 2007.

[65] Jacobsen, E. N., Kakiuchi, F., Konsler, R. G., Larrow, J. F., and Tokunaga, M., "Enantioselective catalytic ring opening of epoxides with carboxylic acids," *Tetrahedron Letters*, vol. 38, no. 5, pp. 773 – 776, 1997.

[66] Jacobsen, E. N., "Asymmetric catalysis of epoxide ring-opening reactions," *Accounts of Chemical Research*, vol. 33, no. 6, pp. 421–431, 2000.

[67] Kagan, H. B. and Fiaud, J. C., *Kinetic Resolution*, pp. 249–330. John Wiley & Sons, Inc., 2007.

[68] Shi, G., Kozlowski, J. F., Schwedler, J. T., Wood, K. V., MacDougal, J. M., and McLaughlin, J. L., "Muconin and mucoxin: additional nonclassical bioactive acetogenins from rollinia mucosa," *The Journal of Organic Chemistry*, vol. 61, no. 23, pp. 7988–7989, 1996.

[69] Schaus, S. E., Brånalt, J., and Jacobsen, E. N., "Total synthesis of muconin by efficient assembly of chiral building blocks," *The Journal of Organic Chemistry*, vol. 63, no. 15, pp. 4876–4877, 1998.

[70] Sadhukhan, A., Khan, N.-u. H., Roy, T., Kureshy, R. I., Abdi, S. H. R., and Bajaj, H. C., "Asymmetric hydrolytic kinetic resolution with recyclable macrocyclic coiii–salen complexes: A practical strategy in the preparation of (r)-mexiletine and (s)-propranolol," *Chemistry – A European Journal*, vol. 18, no. 17, pp. 5256–5260, 2012.

[71] Madhavan, N., Jones, C. W., and Weck, M., "Rational approach to polymer-supported catalysts: Synergy between catalytic reaction mechanism and polymer design," *Accounts of Chemical Research*, vol. 41, no. 9, pp. 1153–1165, 2008.

[72] Nielsen, L. P. C., Stevenson, C. P., Blackmond, D. G., and Jacobsen, E. N., "Mechanistic investigation leads to a synthetic improvement in the hydrolytic kinetic resolution of terminal epoxides," *Journal of the American Chemical Society*, vol. 126, no. 5, pp. 1360–1362, 2004.

[73] Jain, S., Venkatasubbaiah, K., Jones, C. W., and Davis, R. J., "Factors influencing recyclability of co(iii)-salen catalysts in the hydrolytic kinetic resolution of epichlorohydrin," *Journal of Molecular Catalysis A: Chemical*, vol. 316, no. 1-2, pp. 8–15, 2010.

[74] Cozzi, P. G., "Metal-salen schiff base complexes in catalysis: practical aspects," *Chemical Society Reviews*, vol. 33, no. 7, pp. 410–421, 2004.

[75] Jain, S., Zheng, X., Jones, C. W., Weck, M., and Davis, R. J., "Importance of counterion reactivity on the deactivation of cosalen catalysts in the hydrolytic kinetic resolution of epichlorohydrin," *Inorganic Chemistry*, vol. 46, no. 21, pp. 8887–8896, 2007.

[76] Kemper, S., Hrobárik, P., Kaupp, M., and Schlörer, N. E., "Jacobsen's catalyst for hydrolytic kinetic resolution: Structure elucidation of paramagnetic co(iii) salen complexes in solution via combined nmr and quantum chemical studies," *Journal of the American Chemical Society*, vol. 131, no. 12, pp. 4172–4173, 2009.

[77] Vinck, E., Murphy, D. M., Fallis, I. A., Strevens, R. R., and Van Doorslaer, S., "Formation of a cobalt(iii)phenoxyl radical complex by acetic acid promoted aerobic oxidation of a co(ii)salen complex," *Inorganic Chemistry*, vol. 49, no. 5, pp. 2083–2092, 2010.

[78] Ready, J. M. and Jacobsen, E. N., "A practical oligomeric [(salen)co] catalyst for asymmetric epoxide ring-opening reactions," *Angewandte Chemie International Edition*, vol. 41, no. 8, pp. 1374–1377, 2002.

[79] Nielsen, L. P. C., Zuend, S. J., Ford, D. D., and Jacobsen, E. N., "Mechanistic basis for high reactivity of (salen)co–ots in the hydrolytic kinetic resolution of terminal epoxides," *The Journal of Organic Chemistry*, vol. 77, no. 5, pp. 2486–2495, 2012.

[80] Kim, G. J., Lee, H., and Kim, S. J., "Catalytic activity and recyclability of new enantioselective chiral co-salen complexes in the hydrolytic kinetic resolution of epichlorohydrine," *Tetrahedron Letters*, vol. 44, no. 27, pp. 5005–5008, 2003.

[81] Zheng, X., Jones, C. W., and Weck, M., "Engineering polymer-enhanced bimetallic cooperative interactions in the hydrolytic kinetic resolution of epoxides," *Advanced Synthesis & Catalysis*, vol. 350, no. 2, pp. 255–261, 2008.

[82] Venkatasubbaiah, K., Gill, C. S., Takatani, T., Sherrill, C. D., and Jones, C. W., "A versatile co(bisalen) unit for homogeneous and heterogeneous cooperative catalysis in the hydrolytic kinetic resolution of epoxides," *Chemistry – A European Journal*, vol. 15, no. 16, pp. 3951–3955, 2009.

[83] Venkatasubbaiah, K., Zhu, X.-J., and Jones, C., "Effect of counter-ion on recycle of polymer resin supported co(iii)-salen catalysts in the hydrolytic kinetic resolution of epichlorohydrin," *Topics in Catalysis*, vol. 53, no. 15, pp. 1063–1065, 2010.

[84] Key, R. E., Venkatasubbaiah, K., and Jones, C. W., "Evaluation of enantiopure and non-enantiopure co(iii)-salen catalysts and their counter-ion effects in the hydrolytic kinetic resolution (hkr) of racemic epichlorohydrin," *Journal of Molecular Catalysis A: Chemical*, vol. 366, no. 0, pp. 1–7, 2013.

[85] Belser, T. and Jacobsen, E. N., "Cooperative catalysis in the hydrolytic kinetic resolution of epoxides by chiral [(salen)co(iii)] complexes immobilized on gold colloids," *Advanced Synthesis & Catalysis*, vol. 350, no. 7-8, pp. 967–971, 2008.

[86] Gill, C. S., Venkatasubbaiah, K., and Jones, C. W., "Recyclable polymer- and silica-supported ruthenium(ii)-salen bis-pyridine catalysts for the asymmetric cyclopropanation of olefins," *Advanced Synthesis & Catalysis*, vol. 351, no. 9, pp. 1344–1354, 2009.

[87] Zheng, X., Jones, C. W., and Weck, M., "Poly(styrene)-suppoted co-salen complexes as efficient recyclable catalysts for the hydrolytic kinetic resolution of epichlorohydrin," *Chemistry – A European Journal*, vol. 12, pp. 576–583, 2006.

[88] Gill, C. S., Venkatasubbaiah, K., Phan, N. T. S., Weck, M., and Jones, C. W., "Enhanced cooperativity through design: Pendant coiii-salen polymer brush catalysts for the hydrolytic kinetic resolution of epichlorohydrin (salen=n,n-bis(salicylidene)ethylenediamine dianion)," *Chemistry – A European Journal*, vol. 14, no. 24, pp. 7306–7313, 2008.

[89] Munro, O. Q., Shabalala, S. C., and Brown, N. J., "Structural, computational, and 59co nmr studies of primary and secondary amine complexes of co(iii) porphyrins," *Inorganic Chemistry*, vol. 40, no. 14, pp. 3303–3317, 2001.

[90] Jones, C. W., "On the stability and recyclability of supported metal–ligand complex catalysts: Myths, misconceptions and critical research needs," *Topics in Catalysis*, vol. 53, pp. 942–952, August 2010.

[91] Klayman, D. L., Lin, A. J., Acton, N., Scovill, J. P., Hoch, J. M., Milhous, W. K., Theoharides, A. D., and Dobek, A. S., "Isolation of artemisinin (qinghaosu) from artemisia annua growing in the united states," *Journal of Natural Products*, vol. 47, no. 4, pp. 715–717, 1984.

[92] Klayman, D., "Qinghaosu (artemisinin): an antimalarial drug from china," *Science*, vol. 228, no. 4703, pp. 1049–1055, 1985.

[93] Noedl, H., Se, Y., Schaecher, K., Smith, B. L., Socheat, D., and Fukuda, M. M., "Evidence of artemisinin-resistant malaria in western cambodia," *The New England Journal of Medicine*, vol. 359, no. 24, pp. 2619–2620, 2008.

[94] Dondorp, A. M., Nosten, F., Yi, P., Das, D., Phyo, A. P., Tarning, J., Lwin, K. M., Ariey, F., Hanpithakpong, W., Lee, S. J., Ringwald, P., Silamut, K., Imwong, M., Chotivanich, K., Lim, P., Herdman, T., An, S. S., Yeung, S., Singhasivanon, P., Day, N. P., Lindegardh, N., Socheat, D., and White, N. J., "Artemisinin resistance in plasmodium falciparum malaria," *New England Journal of Medicine*, vol. 361, no. 5, pp. 455–467, 2009.

[95] Smilkstein, M., Sriwilaijaroen, N., Kelly, J. X., Wilairat, P., and Riscoe, M., "Simple and inexpensive fluorescence-based technique for high-throughput antimalarial drug screening," *Antimicrobial Agents and Chemotherapy*, vol. 48, no. 5, pp. 1803–1806, 2004.

[96] Bennett, T. N., Paguio, M., Gligorijevic, B., Seudieu, C., Kosar, A. D., Davidson, E., and Roepe, P. D., "Novel, rapid, and inexpensive cell-based quantification of antimalarial drug efficacy," *Antimicrobial Agents and Chemotherapy*, vol. 48, no. 5, pp. 1807–1810, 2004.

[97] Stout, E. P., *Discovery and synthesis of bioactive natural product probes from marine systems*, vol. Ph.D. Atlanta, GA: Georgia Institute of Technology, 2010.

[98] Qian, X., McDonald, A., Zhou, H., Ashcraft, L., Yao, B., Jiang, H., Huang, J., Wang, J., Morgans, D., Morgan, B., and others, "Imidazopyridinyl-benzamide anti-cancer agents," Nov. 17 2009. US Patent 7,618,981.

[99] "Acetals." http://www.faculty.virginia.edu/mcgarveylab/Carbsyn/Acetals.html. Accessed: 2015-06-13.

[100] Lang, M. and Steglich, W., "An effective method for the synthesis of 13c-labeled polyprenylhydroxybenzoic acids," *Synthesis*, no. 6, pp. 1019–1027, 2005.

[101] Paz, J. L. and Rodrigues, A. R., "Preparation of aromatic geraniol analogues via a cu(i)-mediated grignard coupling," *Journal of the Brazilian Chemical Society*, vol. 14, no. 6, pp. 975–981, 2003.

[102] Krajewski, K., Kutner, A., Dzikowska, J., Gutowska, J., Napiórkowski, M., Winiarski, J., Kubiszewski, M., Jedynak, Ł., Morzycki, J., and Witkowski, S., "Process for preparation of mk-7 type of vitamin k2," 2014.

[103] Miller, D. J., Gao, J., Truhlar, D. G., Young, N. J., Gonzalez, V., and Allemann, R. K., "Stereochemistry of eudesmane cation formation during catalysis by aristolochene synthase from penicillium roqueforti," *Organic & Biomolecular Chemistry*, vol. 6, no. 13, pp. 2346–2354, 2008.

[104] Rainier, J. D. and Smith III, A. B., "Polyene cyclizations to indole diterpenes. the first synthesis of (+)-emindole sa using a biomimetic approach," *Tetrahedron Letters*, vol. 41, no. 49, pp. 9419–9423, 2000.

[105] Hashimoto, M., Kan, T., Nozaki, K., Yanagiya, M., Shirahama, H., and Matsumoto, T., "Total syntheses of (+)-thyrsiferol, (+)-thyrsiferyl 23-acetate, and (+)-venustatriol," *The Journal of Organic Chemistry*, vol. 55, no. 17, pp. 5088–5107, 1990.

[106] Mori, K., Ebata, T., and Takechi, S., "Pheromone synthesis—63 synthesis of both the enantiomers of 2,3-dihydro-2- isopropyl-2,5-dimethylfuran, a sex specific compound in females of the beetle hylecoetus dermestoidesl," *Tetrahedron*, vol. 40, no. 10, pp. 1761 – 1766, 1984.

[107] Singh, S. and Guiry, P. J., "A short and efficient asymmetric synthesis of ()-frontalin, ()-exo-isobrevicomin and a volatile contributor of beer-aroma," *Tetrahedron*, vol. 66, no. 30, pp. 5701 – 5706, 2010.

[108] Demont, E., Martin, J., Redshaw, S., and Swallow, S., "Preparation d'inhibiteurs de la protease du vih," Apr. 10 2003. WO Patent App. PCT/EP2002/010,599.

[109] Trost, B. M. and Merlic, C. A., "Diastereoselectivity control elements. acyclic diastereocontrol in formation and reactions of γ-hydroxy sulfones," *Journal of the American Chemical Society*, vol. 110, no. 15, pp. 5216–5218, 1988.

[110] Skattebol, L. and Aukrust, I., "Process for the preparation of vitamin k2," 2010. Patent.

[111] Brown, S., Dransfield, P., Houze, J., Kohn, T., Liu, J., Medina, J., Pattaropong, V., Shen, W., Vimolratana, M., Wang, Y., and others, "Conformationally constrained carboxylic acid derivatives useful for treating metabolic disorders," Sept. 11 2009. WO Patent App. PCT/US2009/001,435.

[112] Esumi, T., Makado, G., Zhai, H., Shimizu, Y., Mitsumoto, Y., and Fukuyama, Y., "Efficient synthesis and structure–activity relationship of honokiol, a neurotrophic biphenyl-type neolignan," *Bioorganic & Medicinal Chemistry Letters*, vol. 14, no. 10, pp. 2621 – 2625, 2004.

[113] Inouye, M., Chiba, J., and Nakazumi, H., "Glucopyranoside recognition by polypyridine-macrocyclic receptors possessing a wide cavity with a flexible linkage," *The Journal of Organic Chemistry*, vol. 64, no. 22, pp. 8170–8176, 1999. PMID: 11674733.

[114] Douglass, M. R., Stern, C. L., and Marks, T. J., "Intramolecular hydrophosphination/cyclization of phosphinoalkenes and phosphinoalkynes catalyzed by organolanthanides: Scope, selectivity, and mechanism," *Journal of the American Chemical Society*, vol. 123, no. 42, pp. 10221–10238, 2001.

[115] Padwa, A. and Zhang, H., "Synthesis of some members of the hydroxylated phenanthridone subclass of the amaryllidaceae alkaloid family," *The Journal of Organic Chemistry*, vol. 72, no. 7, pp. 2570–2582, 2007.

[116] Akai, S., Ikawa, T., Takayanagi, S.-i., Morikawa, Y., Mohri, S., Tsubakiyama, M., Egi, M., Wada, Y., and Kita, Y., "Synthesis of biaryl

compounds through three-component assembly: Ambidentate effect of the tert-butyldimethylsilyl group for regioselective diels–alder and hiyama coupling reactions," *Angewandte Chemie International Edition*, vol. 47, no. 40, pp. 7673–7676, 2008.

[117] Narasimhan, S., Madhavan, S., and Prasad, K. G., "Facile reduction of carboxylic acids to alcohols by zinc borohydride," *The Journal of Organic Chemistry*, vol. 60, no. 16, pp. 5314–5315, 1995.

[118] Narasimhan, S. and Balakumar, R., "Synthetic applications of zinc borohydride," *Aldrichimica Acta*, vol. 31, no. 1, pp. 19–27, 1998.

[119] Berger, G. O. and Tius, M. A., "Total synthesis of (±)-terpestacin and (±)-11-epi-terpestacin," *The Journal of Organic Chemistry*, vol. 72, no. 17, pp. 6473–6480, 2007. PMID: 17630803.

[120] Fryszkowska, A., Fisher, K., Gardiner, J. M., and Stephens, G. M., "Highly enantioselective reduction of β,β-disubstituted aromatic nitroalkenes catalyzed by clostridium sporogenes," *The Journal of Organic Chemistry*, vol. 73, no. 11, pp. 4295–4298, 2008.

[121] Domínguez, B., Pazos, Y., and de Lera, A. R., "Stereocontrolled synthesis of 6-s-cis- and 6-s-trans-locked 9z-retinoids by hydroxyl-accelerated stille coupling of (z)-tri-n-butylstannylbut-2-en-1-ol and bicyclic dienyl triflates," *The Journal of Organic Chemistry*, vol. 65, no. 19, pp. 5917–5925, 2000. PMID: 10987922.

[122] "Sigma-aldrich: Geranylgeraniol ≥85%." http://www.sigmaaldrich.com/catalog/product/sigma/g3278?lang=en&region=US, 6. Accessed: 2015-06-24.

[123] "Vwr: Geranyl linalool ca. 95%." https://us.vwr.com/store/catalog/product.jsp?catalog_number=200037-518, 6. Accessed: 2015-06-24.

[124] Bakkestuen, A. K., Gundersen, L.-L., Petersen, D., Utenova, B. T., and Vik, A., "Synthesis and antimycobacterial activity of agelasine e and analogs," *Organic & Biomolecular Chemistry*, vol. 3, pp. 1025–1033, 2005.

[125] Grinco, M., Kulcitki, V., Ungur, N., Vlad, P., Gavagnin, M., Castelluccio, F., and Cimino, G., "A biomimetic synthesis of sacculatane diterpenoids," *Helvetica Chimica Acta*, vol. 91, no. 2, pp. 249–258, 2008.

[126] Cox, N. J. G., Mills, S. D., and Pattenden, G., "Macrocyclisations using allylic radical intermediates. a new synthetic approach to natural 14-membered cembranoids," *Journal of the Chemical Society, Perkin Transactions 1*, pp. 1313–1321, 1992.

[127] Takanashi, S.-I. and Mori, K., "Pheromone synthesis, clxxix. synthesis of lurlenic acid and lurlenol, the sex pheromones of the green flagellate chlamydomonas," *Liebigs Annalen*, vol. 1997, no. 5, pp. 825–838, 1997.

[128] Handa, S., Nair, P., and Pattenden, G., "Novel regio- and stereoselective cascade 6-endo-trig cyclisations from polyene acyl radical intermediates leading to steroid-like pentacycles and heptacycles," *Helvetica Chimica Acta*, vol. 83, no. 9, pp. 2629–2643, 2000.

[129] Uyanik, M., Ishihara, K., and Yamamoto, H., "Catalytic diastereoselective polycyclization of homo(polyprenyl)arene analogues bearing terminal siloxyvinyl groups," *Organic Letters*, vol. 8, no. 24, pp. 5649–5652, 2006. PMID: 17107094.

[130] Liang, D., Gao, N., Liu, W., and Dong, J., "Construction of the 1,2-dialkenylcyclohexane framework via ireland-claisen rearrangement and intramolecular barbier reaction: Application to the synthesis of (±)-geijerone and a diastereoisomeric mixture with its 5-epimer," *Molecules*, vol. 19, no. 1, p. 1238, 2014.

[131] Herbert, R. B., *The biosynthesis of secondary metabolites*. Springer Science & Business Media, March 1989.

[132] Talpir, R., Rudi, A., Kashman, Y., Loya, Y., and Hizi, A., "Three new sesquiterpene hydroquinones from marine origin," *Tetrahedron*, vol. 50, no. 14, pp. 4179 – 4184, 1994.

[133] Loya, S., Bakhanashvili, M., Kashman, Y., and Hizi, A., "Peyssonols a and b, two novel inhibitors of the reverse transcriptases of human immunodeficiency virus types 1 and 2," *Archives of Biochemistry and Biophysics*, vol. 316, no. 2, pp. 789 – 796, 1995.

[134] Lane, A. L., Mular, L., Drenkard, E. J., Shearer, T. L., Engel, S., Fredericq, S., Fairchild, C. R., Prudhomme, J., Roch, K. L., Hay, M. E., Aalbersberg, W., and Kubanek, J., "Ecological leads for natural product discovery: novel sesquiterpene hydroquinones from the red macroalga peyssonnelia sp.," *Tetrahedron*, vol. 66, no. 2, pp. 455 – 461, 2010.

[135] Matsuda, H., Tomiie, Y., Yamamura, S., and Hirata, Y., "The structure of aplysin-20," *Chemical Communications (London)*, pp. 898b–899, 1967.

[136] Yamamura, S. and Hirata, Y., "A naturally-occurring bromo-compound, aplysin-20 from aplysia kurodai," *Bulletin of the Chemical Society of Japan*, vol. 44, no. 9, pp. 2560–2562, 1971.

[137] Bauduin, G., Bondon, D., Pietrasanta, Y., and Pucci, B., "Reactions de transcetalisation—ii: Influence des facteurs steriques et electroniques sur les energies de cetalisation," *Tetrahedron*, vol. 34, no. 22, pp. 3269 – 3274, 1978.

[138] Lalonde, M. and Chan, T. H., "Use of organosilicon rweagents as protective groups in organic synthesis," *Synthesis*, no. 9, p. 817, 1985.

[139] Nelson, T. D. and Crouch, R. D., "Selective deprotection of silyl ethers," *Synthesis*, no. 9, p. 1031, 1996.

[140] Burgess, E. M., Penton, H. R., and Taylor, E. A., "Thermal reactions of alkyl n-carbomethoxysulfamate esters," *The Journal of Organic Chemistry*, vol. 38, no. 1, pp. 26–31, 1973.

[141] Zanka, A., Ohmori, H., and Okamoto, T., "Highly efficient conversion of benzoates to alcohols with sodium borohydride in dme-meoh," *Synlett*, vol. 1999, no. 10, pp. 1636–1638, 1999.

[142] Key, R. E., "Unpublished data.." 2012.

[143] Feng, Y., Lydon, M. E., and Jones, C. W., "Polymer resin supported cobalt–salen catalysts: Role of co(ii) salen species in the regioselective ring opening of 1,2-epoxyhexane with methanol," *ChemCatChem*, vol. 5, no. 12, pp. 3636–3643, 2013.

[144] Hossion, A. M. L., Otsuka, N., Kandahary, R. K., Tsuchiya, T., Ogawa, W., Iwado, A., Zamami, Y., and Sasaki, K., "Design, synthesis, and biological evaluation of a novel series of quercetin diacylglucosides as potent anti-mrsa and anti-vre agents," *Bioorganic & Medicinal Chemistry Letters*, vol. 20, no. 17, pp. 5349–5352, 2010.

[145] Bernet, B., Bishop, P. M., Caron, M., Kawamata, T., Roy, B. L., Ruest, L., Sauve, G., Soucy, P., and Deslongchamps, P., "Formal total synthesis of erythromycin a. part i. total synthesis of a 1,7-dioxaspiro[5.5]undecane derivative of erythronolide a," *Canadian Journal of Chemistry*, vol. 63, no. 10, pp. 2810–2814, 1985.

[146] Ohtani, I., Kusumi, T., Kashman, Y., and Kakisawa, H., "High-field ft nmr application of mosher's method. the absolute configurations of marine terpenoids," *Journal of the American Chemical Society*, vol. 113, no. 11, pp. 4092–4096, 1991.

[147] "MOM protection." http://www.faculty.virginia/edu/mcgarveylab/. Accessed: 2015-06-27.

[148] Xing, Y., Cen, W., Lan, J., Li, Y., and Li, Y., "First total synthesis of (±)-13-hydroxyneocembrene," *Journal of the Chinese Chemical Society*, vol. 46, no. 4, pp. 595–600, 1999.

[149] Faulkner, D. J. and Stallard, M. O., "7-chloro-3,7-dimethyl-1,4,6-tribromo-1-octen-3-ol, a novel monoterpene alcohol from aplysia californica," *Tetrahedron Letters*, vol. 14, no. 14, pp. 1171 – 1174, 1973.